



universität
wien

MASTERARBEIT

Titel der Masterarbeit

Dissecting the role of PBRM1 in ccRCC
tumourigenesis and the search for synthetic lethal
interactions

verfasst von

David Hoffmann, BSc

angestrebter akademischer Grad

Master of Science (MSc)

Wien, 2015

Studienkennzahl lt. Studienblatt: A 066 834

Studienrichtung lt. Studienblatt: Masterstudium Molekulare Biologie

Betreut von: Ao. Univ.-Prof. Dr. Christian Seiser

Acknowledgements

First I would like to thank Sakari Vanharanta for giving me the opportunity to independently work on the PBRM1 project in his lab in Cambridge. It was great having the possibility to drop by in your office whenever I felt the need to ask something. I could learn a lot about the work in a lab and how difficult it can be to start a project. I could experience the ups and downs of scientific work and it helped me a lot to decide on my future plans.

Next I would like to thank the whole lab for the great atmosphere each day. You guys made the lab a special place and you were always helpful. Also without you, my weekends would have been a lot less eventful.

The biggest reward goes to Lisa, I think without you I wouldn't have undertaken the adventure of going to the UK and I was so glad that you were on my side. You of all people made it an awesome year and one I will miss too.

A special thanks goes to my family, who gave me the opportunity to life and work in England for a year and who supported me throughout all my studies.

Abstract

PBRM1 has recently been identified to be mutated in up to 40% of ccRCCs. The mechanisms through which PBRM1 loss contributes to renal tumorigenesis remain unknown. Previously published data by others, acquired by transient PBRM1 knockdown in PBRM1 wildtype ccRCC cell lines suggest a strong tumour suppressive role for PBRM1 in proliferation and colony formation. However, these studies did not interrogate ccRCCs that had developed in the PBRM1 mutant background. Here, I show that in PBRM1 mutant ccRCC, proliferation in standard and stress conditions and resistance to ROS and DNA damaging agents remained unchanged upon PBRM1 restoration. Colony formation was even elevated upon PBRM1 expression in metastatic cells. Furthermore the CRISPR-Cas9 system was applied to repair the small PBRM1 mutation in the OS-RC2 cell line and an indirect evidence for successful repair could be found. PBRM1 loss may have synthetic lethal interactions with other bromodomain containing proteins, SWI/SNF complex or PRC members. These hypotheses were tested by setting up a synthetic lethality screen using shRNA-mediated knockdown.

Contents

1. Introduction	9
1.1 <i>The hallmarks of cancer</i>	9
1.2 <i>Renal cell carcinoma</i>	12
1.3 <i>Genetics of ccRCC</i>	12
1.4 <i>The SWI/SNF complex</i>	13
1.5 <i>The SWI/SNF complex and cancer</i>	14
1.6 <i>PBRM1</i>	16
1.7 <i>The tumour suppressive function of PBRM1</i>	17
1.8 <i>Objective</i>	17
2. Results	18
2.1 <i>Tumour suppressive phenotype of PBRM1 knockdown</i>	18
2.1.1 <i>Knockdown of PBRM1</i>	18
2.1.2 <i>PBRM1 knockdown did not enhance in vitro proliferation</i>	19
2.2 <i>Effects of PBRM1 expression in PBRM1 mutant cell lines</i>	20
2.2.1 <i>PBRM1 expression is inducible by Dox</i>	20
2.2.2 <i>The expressed PBRM1 incorporates into the PBAF complex</i>	25
2.2.3 <i>In vitro proliferation is not PBRM1 dependent</i>	29
2.2.4 <i>PBRM1 has no effect on proliferation in stress conditions</i>	32
2.2.5 <i>Resistance to reactive oxygen species is not PBRM1 dependent</i>	37
2.2.6 <i>Resistance to induced DNA double strand breaks is not dependent on PBRM1</i>	39
2.2.7 <i>Anchorage independent growth is enhanced by PBRM1</i>	41
2.3 <i>Endogenous expression of PBRM1 in mutant cell lines by CRISPR-Cas9 mediated repair</i>	43
2.3.1 <i>Strategy 1 – Using HDR for repair of small mutation</i>	44
2.3.2 <i>Strategy 2 – Using HDR to repair small mutation and incorporate a Puromycin resistance gene</i>	48
2.4 <i>Screen for components that are synthetic lethal with PBRM1</i>	55
3. Discussion	60
3.1 <i>Tumour suppressive phenotype of PBRM1</i>	60
3.2 <i>Repair of small PBRM1 mutation</i>	63
3.3 <i>Synthetic Lethality</i>	65
4. Materials and Methods	67
4.1 <i>General methods</i>	67

4.1.1 Polymerase chain reaction (PCR)	67
4.1.2 Cloning	69
4.1.3 Miniprep and maxiprep	70
4.1.4 Protein extraction	70
4.1.5 Western Blot	71
4.1.6 Cell culture	72
4.1.7 Lentiviral transduction	73
4.2 <i>Knockdown of PBRM1</i>	74
4.3 <i>PBRM1 expression and assays</i>	74
4.3.1 PBRM1 expression	74
4.3.2 Immunoprecipitation	74
4.3.3 In vitro proliferation assay	75
4.3.4 High cell dilution assay	75
4.3.5 Proliferation in stress conditions	76
4.3.6 Cell survival	76
4.3.7 Soft agar assay	77
4.4 <i>Endogenous Reintroduction – Strategy 1</i>	78
4.4.1 sgRNA design and cloning	78
4.4.2 Transfection and cell sorting	79
4.4.3 Screening	79
4.5 <i>Endogenous Reintroduction – Strategy 2</i>	80
4.5.1 Cloning of template plasmid	80
4.5.2 Site directed mutagenesis	80
4.5.3 Transfection	80
4.5.4 Genomic DNA extraction and PCR	81
4.6 <i>Synthetic Lethality Screen</i>	81
4.6.1 shRNA plasmid library cloning	81
4.6.2 shRNA library lentivirus generation and infection	83
5. References	88
6. Internet References	96
7. Appendix	97
7.1 <i>Zusammenfassung</i>	97
7.2 <i>Curriculum vitae</i>	98

1. Introduction

1.1 The hallmarks of cancer

The growth of normal cells is usually strictly monitored and if a cell manages to bypass these control mechanisms the arising disease is called cancer. Uncontrolled proliferation is the phenotype that unites all the different kinds of cancers yet there are a sheer uncountable number of reasons for cancer development. Hanahan and Weinberg provided a list of capabilities that are accumulated in incipient cancer cells on their way to tumourigenesis. Different types of tumours acquire these functions via distinct mechanisms and at different time points during tumour formation [1].

As mentioned above the most important feature of cancer cells is that they acquire the capability to sustain chronic proliferation, either by altering the availability of extracellular growth signals, the hypersensitivity to normal levels of growth signals or by becoming independent from extracellular stimulation of downstream pathways.

For tumour cells it is not only important to maintain proliferative signals but also to avoid control mechanisms blocking proliferation. These pathways are often regulated by tumour suppressor genes, which are usually inactivated in cancer cells, either by somatic mutation or transcriptional repression.

Uncontrolled proliferation induces several different physiological stresses like DNA damage, which usually triggers programmed cell death. This mechanism presents a barrier to tumour formation and so cancer cells need to inactivate key players in these pathways.

Normal cells can only go through a limited number of cell divisions before they become senescent, a state that supports cell viability but irreversibly prohibits proliferation. This is controlled by a shortening of telomeres after each cell division. When a critical length is reached the telomeres fail to protect the chromosomal DNA from end-to-end fusion. Fused chromosomes cannot be separated properly in mitosis and are thus a threat to cell viability. Cancer cells circumvent this by activating the telomerase, a specialized polymerase that amplifies telomere ends.

Hypoxia and insufficient supply of nutrients limit tumour growth above a certain size. This is why the tumour cells induce an angiogenic switch that activates the normally quiescent vasculature causing a continuous sprouting of new vessels.

Ultimately tumour cells migrate to and invade into blood vessels and travel throughout the body to find new colonies at distant sites to the primary tumour, a process called metastasis. Both processes need a change in physical coupling of cells to their microenvironment by altering cell-cell adhesion proteins or cell-matrix proteins (Figure 1).

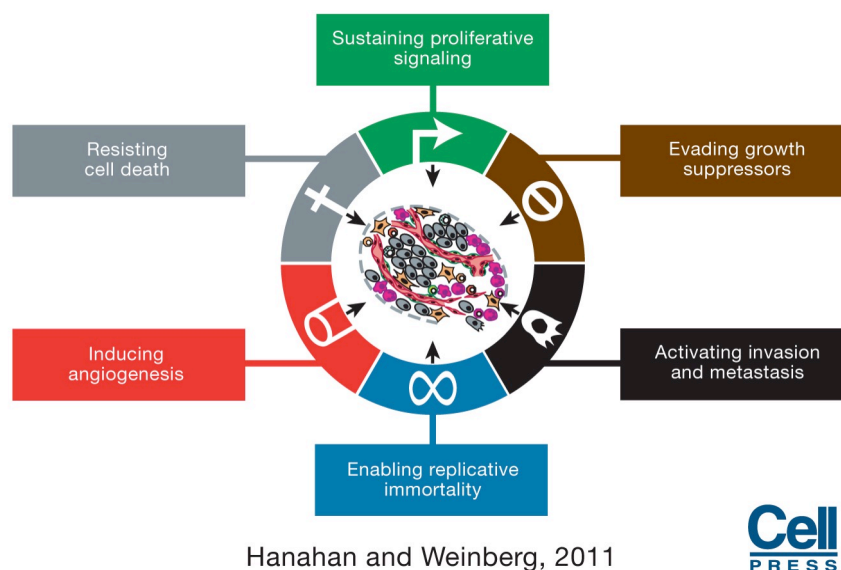


Figure 1 | The hallmarks of cancer

The six hallmarks of cancer are sustaining proliferative signalling, evading growth suppressors, activating invasion and metastasis, enabling replicative immortality, inducing angiogenesis and resisting cell death. Picture acquired from [1].

The acquisition of the capabilities allowing cancer cells to grow, survive and disseminate are made possible by two enabling characteristics.

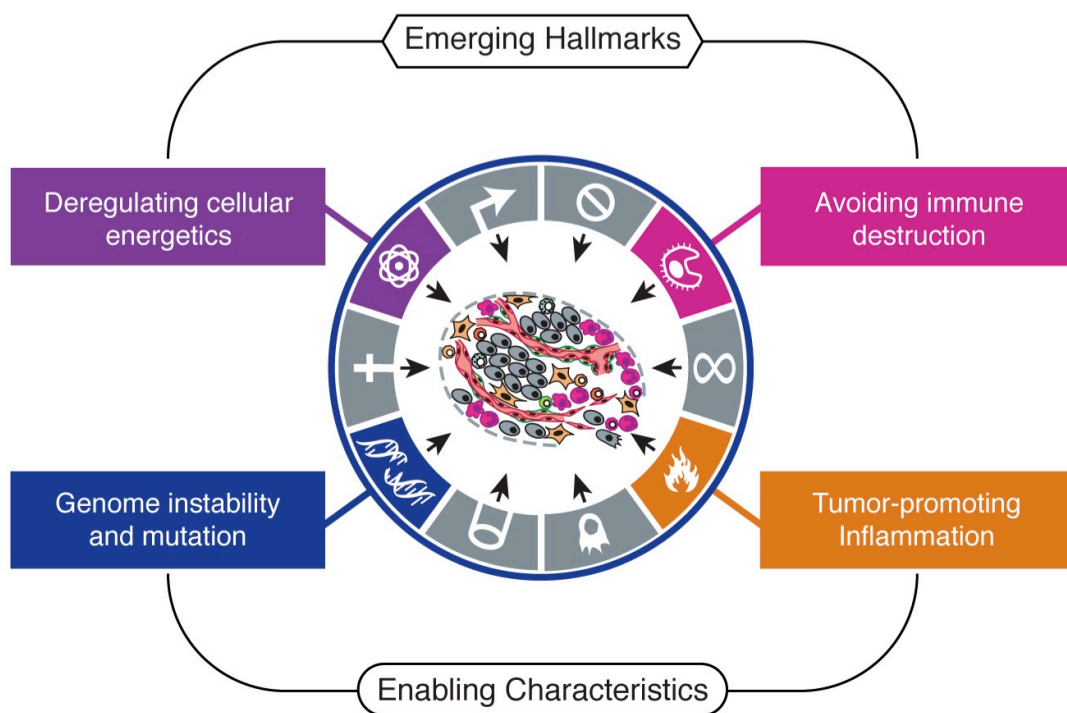
Genomic instability fuels cancer formation by introducing random mutations that can occasionally lead to e.g. tumour suppressor inactivation. Therefore cancer cells often increase their mutation rate.

Growing tumours are always invaded to a certain degree by immune cells. Yet these inflammations do not always try to eliminate tumour cells but in fact can support the acquirement of multiple hallmarks by supplying molecules like growth, survival or proangiogenic factors and enzymes modifying the extracellular matrix (Figure 2).

Two other hallmarks that may facilitate the development and progression of tumours are termed emerging hallmarks.

An adjustment in energy proliferation is needed in order to sustain uncontrolled proliferation. The Warburg effect describes the phenomenon that cancer cells can reprogram their glucose metabolism to glycolysis, a pathway that is usually used in anaerobic conditions, even if oxygen is present. The loss of energy by lower efficiency in ATP production is in part compensated by the increased uptake of glucose. Increased glycolysis might be required to produce glycolytic intermediates, which are needed for the biosynthesis of macromolecules and organelles for new cells.

The immune system constantly monitors cells and tissues and it is hypothesized that this immune surveillance recognizes and eliminates the majority of nascent tumours. Thus the immune system would act as barrier to tumour formation and progression (Figure 2).



Hanahan and Weinberg, 2011



Figure 2 | Emerging hallmarks and enabling characteristics

Genome instability and mutation as well as tumour promoting inflammation present enabling characteristics for tumour formation and growth. Deregulation cellular energetic and avoiding immune destruction are hallmarks that are emerging. Picture acquired from [1].

1.2 Renal cell carcinoma

61 500 new cases of kidney cancer are estimated to occur in the US in 2015. Over 90% of these and thus by far the most common type of kidney cancer is renal cell carcinoma (RCC) [2]. RCCs are classified into 3 main histopathological subtypes: Clear cell RCC (ccRCC), papillary RCC and chromophobe RCC of which ccRCC is by far the most common subtype with about 70% [3].

Upon diagnosis the initial treatment is either partial or complete removal of the kidney (nephrectomy) [4]. ccRCCs are not responsive to traditional chemotherapies and they are highly radiation resistant [5].

One third of all the patients develop metastatic disease and the median survival time after first distant metastases is less than 2 years. Metastases are most frequent in the lung, followed by bone and liver [6].

In RCC, as in most other cancer types, genomic mutations are the cause of the disease. These mutations activate specific pathways and investigating the dependencies of cancer cells on these pathways might lead to finding new vulnerabilities. Especially attractive as therapeutic targets are mutations that are acquired early in the evolutionary path the tumour takes, as they are present in each and every tumour cell, opening a possibility to fight even metastatic cancer.

1.3 Genetics of ccRCC

ccRCCs lack features of other solid tumours and so mutations in tumour protein 53 (*TP53*) and Kirsten rat sarcoma viral oncogene homolog (*KRAS*) mutation are extremely rare [7]. Its most prevalent feature is loss of heterozygosity (LOH) on the p arm of chromosome 3, which occurs in 94% of all cases [8]. Loss of the 3p arm effectively deletes one allele of every gene in this region, leaving the cells vulnerable to somatic mutations, which, in inherited cancer syndromes, were shown to occur before LOH.

The 4 genes with the highest mutation rates, von Hippel-Lindau tumour suppressor (*VHL*), Polybromo 1 (*PBRM1*), SET domain containing 2 (*SETD2*) and BRCA1 associated protein-1 (*BAP1*), are all located between the 3p21

and the 3p25 segment of chromosome 3. Predisposition of hereditary RCC, which accounts for 4% of all cases, is often caused by VHL germline mutations [7]. A recent finding of a predisposition to RCC by an inherited PBRM1 mutation, suggest that this might also be true for PBRM1 [9].

In the far more common sporadic disease, somatic VHL mutation and promoter methylation combine to a VHL inactivation frequency of over 90%. Inactivation of the other genes occurs exclusively by mutation [8]. *PBRM1* is mutated in 41% [10] and *SETD2* and *BAP1* are mutated in 10-15% of all ccRCCs [11]. The vast majority of *PBRM1*, *SETD2* and *BAP1* mutations are found in a subset of *VHL* inactivation cases [8]. Mutations in *PBRM1* and *BAP1* are mutually exclusive [12]. Furthermore it is of note that apart from VHL, all these genes are contributing to chromatin biology.

1.4 The SWI/SNF complex

The SWItch/Sucrose NonFermentable (SWI/SNF) complexes belong to the family of ATP dependent chromatin remodelling complexes. ATP dependent chromatin remodelling complexes utilize the energy provided by ATP hydrolysis to slide the DNA along the nucleosomes and thus are critical for the regulation of gene expression in a variety of cellular responses [13]. Human SWI/SNF complexes can be divided into two main types, the BAF (BRG1 associated factor) and PBAF (Polybromo associated BAF) complexes, depending on their subunit composition. THE BAF complex contains either the ATPase SMARCA2 (BRM) or SMARCA4 (BRG1) whereas the PBAF complex contains exclusively SMARCA4. The core subunits SMARCC1 (BAF155), SMARCC2 (BAF170), and SMARCB1 (BAF47) are shared between both complexes. Furthermore BAF complexes contain either ARID1A (BAF250a) or ARID1B (BAF250b) subunits whereas PBAF complexes comprise of ARID2 (BAF200) subunits. In addition to these core units, SWI/SNF complexes include 7 to 15 accessory subunits of which the PBAF specific unit PBRM1 (BAF180) is of note for this study (Figure 3) [14].

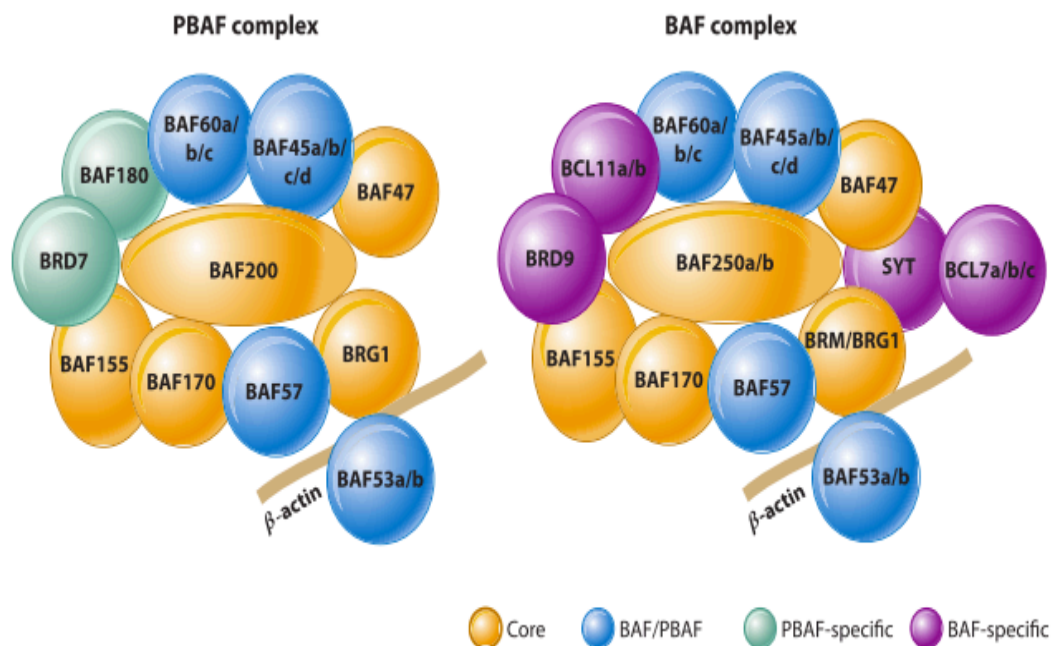


Figure 3 | The composition of the PBAF and BAF complex

The PBAF complex is exclusively composed of the ATPase BRG1, the core subunit BAF200 and additional PBAF specific unit BAF180. The BAF complex can either contain the ATPase BRM or BRG1 and the core subunits BAF250a or b. Picture was acquired from [14].

1.5 The SWI/SNF complex and cancer

In the last years the subunits of the SWI/SNF complexes were recognized as ubiquitously mutated throughout many human cancers. The average mutation rate of all subunits of the SWI/SNF complex in the TCGA studies is with 24.6% surprisingly close to the average mutation rate of TP53, the single most mutated gene in human cancers, which is 35.5% (Figure 4A and B) [15][16]. This further underlines the importance of SWI/SNF complex mutations in human cancer. Although mutations in some subunits are beneficial for human cancers, the SWI/SNF complex remains an important chromatin remodelling complex and complete loss of function might result in lethality. An example for this is the dependence of ARID1A mutant cancer cells on a functional ARID1B. Loss of both subunits impairs proliferation and destabilizes the SWI/SNF complex in general [17].

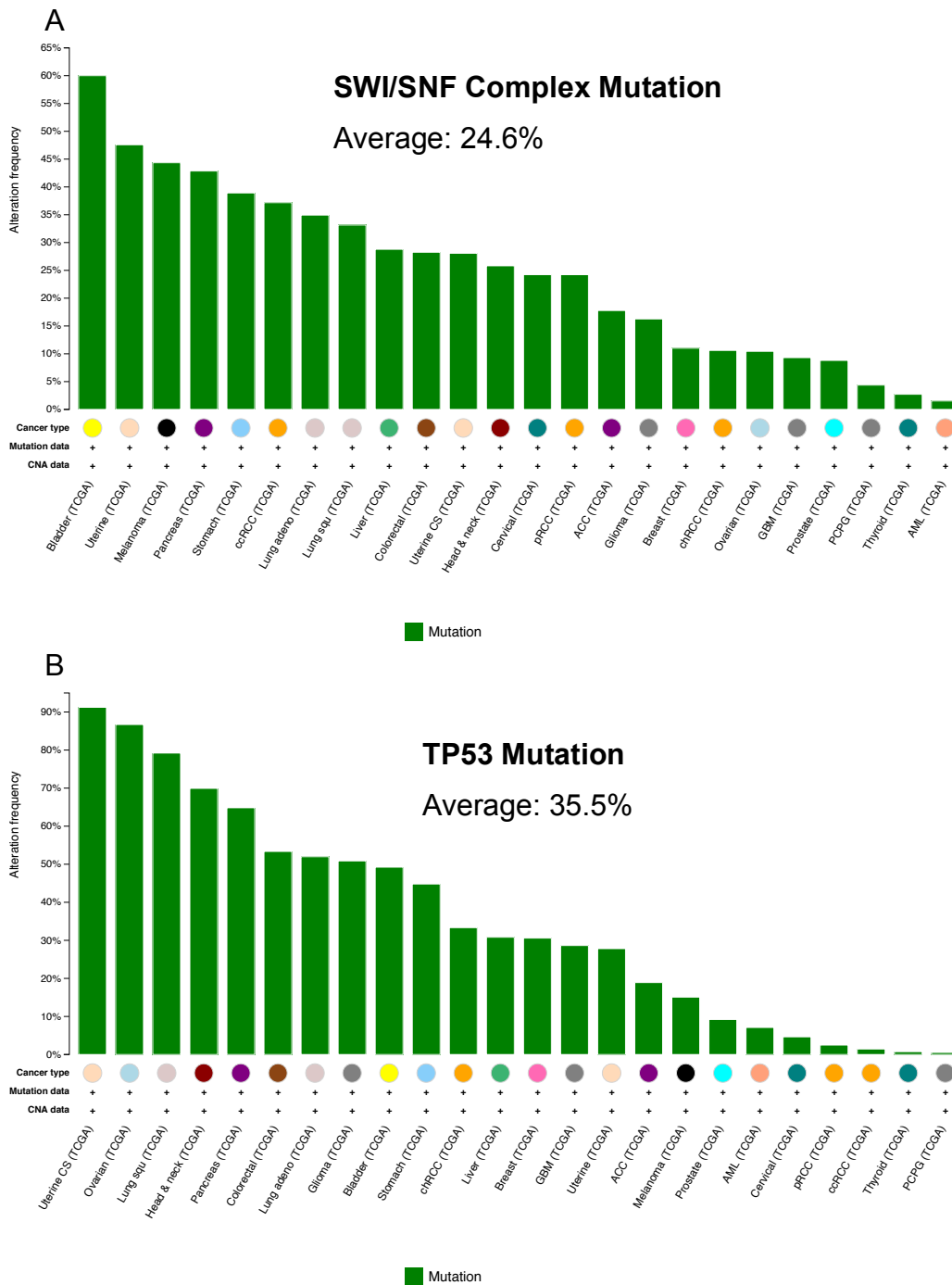


Figure 4 | SWI/SNF and TP53 mutation rates in TCGA studies

A. The mutation rates of the SWI/SNF complex members are highest in bladder cancer (60%) followed by uterine (48%) and melanomas (44%). The average mutation rate in all TCGA studies is 24.6% **B.** The mutation rates of TP53, the single most mutated gene in human cancer, are highest in uterine cancer (91%) followed by ovarian cancer (87%) and lung squamous cancer cell carcinoma (79%). The average mutation rate throughout the TCGA studies is 35.6%. Graphs acquired from cBioportal [15][16].

1.6 PBRM1

PBRM1 is composed of six bromodomains (BDs), two bromo adjacent homology (BAH) domains and one high mobility group (HMG) domain (Figure 5) [18].

Whereas the BAH domains are mediating protein-protein interactions within the SWI/SNF complex and the HMG domain binds to DNA [7], the BDs have been shown to bind acetylated histones *in vitro* in two independent studies [20][21]. Therefore the role of the BDs in PBRM1 is supposedly to bind the PBAF complex to chromatin. Whether all BDs are necessary for all functions of PBRM1 or if some BDs are redundant is currently not clear. Furthermore it remains a possibility that the BDs are also able to bind to other acetylated non-histone proteins. The latter has been demonstrated for the Rsc4 (Remodelling the structure of chromatin) protein, one of the three separate proteins which comprise PBRM1 in yeast [22].



Figure 5 | Domain architecture of PBRM1

PBRM1 is composed of six BDs, two BAHs domains and one HMG domain. Picture was acquired from [18]

As a key subunit in the SWI/SNF complex, it is not surprising that PBRM1 plays an important role in development. In mice, PBRM1 loss reduces epithelial-to-mesenchymal-transition and migration of epicardial cells, which leads to aberrant coronary development and ultimately to embryonic lethality after E14.5 [23].

PBRM1 was also reported to be important in centromeric sister chromatid cohesion in mammalian cells. This causes numerical (higher average chromosome number per cell) or dynamical chromosomal instability (higher number of chromosome breaks) and ultimately results in lower viability after induction of DNA damage in mouse embryonic stem cells lacking PBRM1 [24].

1.7 The tumour suppressive function of PBRM1

Although *PBRM1* mutation is only occurring in 2% of cases in breast cancer [15] [16], it has been indicated to have tumour suppressive function. PBRM1 cDNA overexpression was inhibiting colony formation and reducing the size of growing colonies mediated through PBRM1-dependent increased expression of the cyclin-dependent kinase inhibitor p21 [25].

Although PBRM1 is not mutated in bladder cancer, its knockdown was found to enhance proliferation and migration *in vitro* and tumour formation *in vivo* [26]. Furthermore PBRM1 knockdown has been indicated to slightly increase proliferation in human primary BJ fibroblasts [27].

Despite the high mutation rate in ccRCC, VHL inactivation alone is not sufficient to induce renal cell tumourigenesis [28]. As PBRM1 is the second most mutated gene in ccRCC, this suggests a tumour suppressive role of PBRM1. This is further underlined by a correlation between the loss of PBRM1 expression and late tumour stage, poor tumour differentiation and lower overall survival as well as a link of low PBRM1 expression with worse cancer-specific survival and progression-free survival [29] [30].

In ccRCCs PBRM1 has been indicated to have tumour suppressive function by accelerating proliferation and enhancing the migration of 786-O cells after transient knockdown with BAF180 siRNA. In the kidney cancer cell line SN12C PBRM1 transient PBRM1 knockdown was furthermore associated with an increased capability for colony formation in soft agar [10].

1.8 Objective

The tumour suppressive function of *VHL* has been heavily studied in the last two decades, but despite all the work on *VHL* no therapies have emerged.

The high mutation rate of *PBRM1* has only been discovered recently and functional studies in ccRCCs and other cancers indicated a strong tumour suppressive phenotype. However, these studies did not interrogate ccRCCs that had developed in the PBRM1 mutant background.

As the downstream pathways of *PBRM1* mutations are potential therapeutic targets in a large fraction of RCC, understanding the mechanisms of PBRM1-mediated tumour suppression is a critical open question in the field.

2. Results

2.1 Tumour suppressive phenotype of PBRM1 knockdown

2.1.1 Knockdown of PBRM1

The only study regarding the tumour suppressive function of PBRM1 in ccRCC, reported that a knockdown of PBRM1 enhanced the proliferation in the PBRM1 wild-type (WT) 786-O cell line [10]. Therefore my first experiment aimed at reproducing this phenotype in 786-O cells. Instead of transient knockdown, a previously tested, PBRM1 targeting shRNA named PBRM1 miR7 was cloned into the LT3-GEPIR vector, which allowed for a Doxycycline (Dox) inducible stable knockdown [31]. An established Renilla Luciferase targeting hairpin (Ren. 713) was used to control for general toxicity of shRNA expression [32].

The 786-O cells were grown for 6 days with the indicated Dox levels to induce stable knockdown. As expected, Dox induced expression of the Renilla control shRNA did not affect the PBRM1 protein levels. In the 786-O miR7 cells addition of 100 or 150 ng/ml Dox triggered the miR7 expression and this induced a near complete knockdown of PBRM1 with both concentrations (Figure 6).

Dox was previously indicated in affecting the proliferation of human cell lines and so the lowest possible concentration to induce a near complete knockdown was used for subsequent experiments [33].

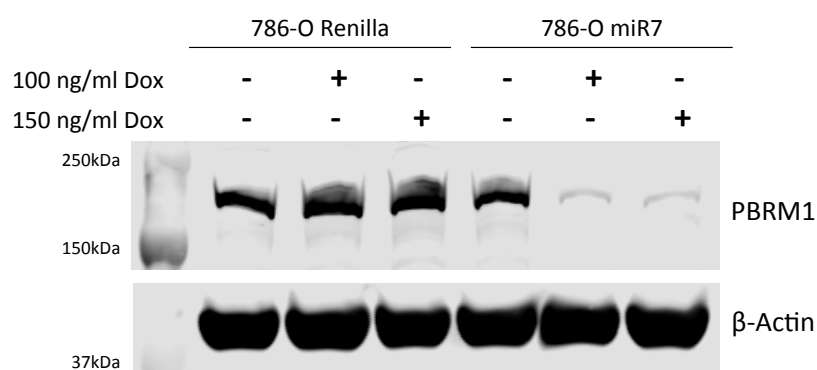


Figure 6 | Dox inducible miR7 expression results in PBRM1 knockdown

786-O cells expressing a control hairpin (Renilla) or a hairpin targeting PBRM1 (miR7) were harvested after 6 days of culture with the indicated concentrations of Dox. 40 μ g of whole cell lysate were analysed by western blot with antibodies against PBRM1 and β -Actin as loading control.

2.1.2 PBRM1 knockdown did not enhance in vitro proliferation

In a proliferation assay the knockdown of PBRM1 did not change the proliferation compared to the Renilla control, albeit the proliferation of both was slightly decreased when compared to the controls grown without Dox (Figure 7).

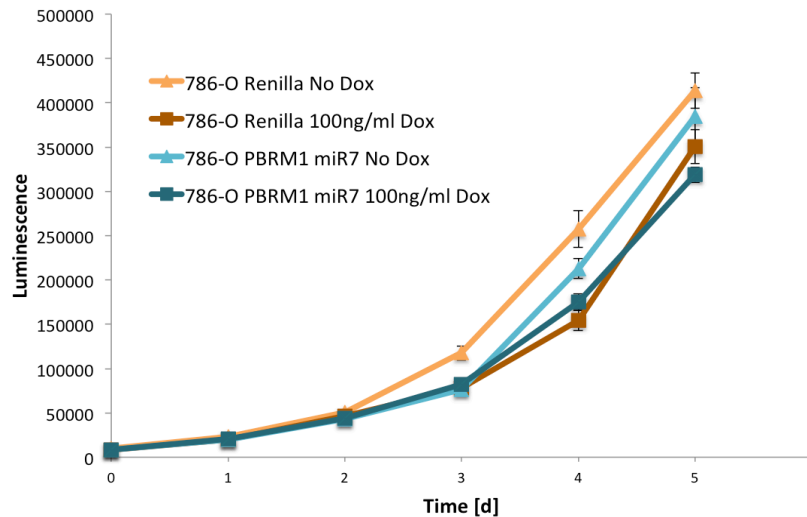


Figure 7 | PBRM1 knockdown does not affect proliferation of 786-O cells

Growth of 786-O cells containing a control Renilla shRNA or an shRNA targeting PBRM1 (miR7) was determined by measuring ATP dependent luminescence. shRNA expression was induced 6 days prior to start of experiment and maintained at 100 ng/ml. Displayed values represent means of technical replicates and standard error of mean (=SEM) (n=4).

Therefore it was concluded that the shRNA-mediated knockdown of PBRM1 had no effect on 786-O proliferation and thus the reproduction of the published phenotype was not successful. Furthermore the 786-O cells were sensitive to the used concentration of Dox as proliferation was marginally diminished upon Dox addition.

This indicated that PBRM1 WT cells might not be the ideal model system to study the tumour suppressive function of PBRM1 in ccRCC. RCC is a type of cancer that is dependent on a very unique set of mutations, which suggests that specific affected pathways force the malignant transformation. It is possible that the 786-O cells found a way to circumvent the dependency on PBRM1 loss, for instance by tackling the pathway down- or upstream of PBRM1.

2.2 Effects of PBRM1 expression in PBRM1 mutant cell lines

2.2.1 PBRM1 expression is inducible by Dox

As knockdown in PBRM1 WT cells was not a suitable model system to study the effects of PBRM1 in ccRCC, we turned to PBRM1 mutant cells. Such cell lines are the OS-RC2, OS-LM1B, RCC-MF and RCC-MF LM1C cells.

The OS-RC2 cells contain a Thymine to Cytosine point mutation on position 698, which leads to an amino acid change from Isoleucine to Threonine (1). This Isoleucine is conserved throughout many human BD containing proteins and is therefore likely to be important for protein function [34].

The OS-RC2 cells were transduced with the herpes simplex virus type 1 thymidine kinase/ green fluorescence protein (GFP)/ firefly luciferase (TGL) triple reporter plasmid to allow intravenous inoculation in mice and isolation of those rare clones that were able to colonize the lungs, which is the most frequent site of ccRCC metastasis [6]. This gave rise to a metastatic derivative of the OS-RC2 cells, the OS-LM1B cell line, which was highly enriched in the ability for lung colonization [35].

RCC-MF cells have a 1 base pair (bp) depletion of the Adenine on position 1583, which leads to a frame shift and complete loss of PBRM1 [36].

The RCC-MF LM1C cells are metastatic derivatives of the RCC-MF cell lines that were derived similar to the OS-LM1B cells by Dr Sakari Vanharanta.

In tissue culture the OS-RC2 and OS-LM1B cells formed a confluent monolayer. The OS-RC2 cells were morphologically distinguishable from the OS-LM1B cells because their shape was rather oblong as compared to the rounder shape of OS-LM1B cells. In contrast the RCC-MF and RCC-MF LM1C cells grew in very tight colonies that never filled all the available space on the tissue culture plate. There was no obvious morphological difference observable between RCC-MF and RCC-MF LM1C cells (Figure 8).

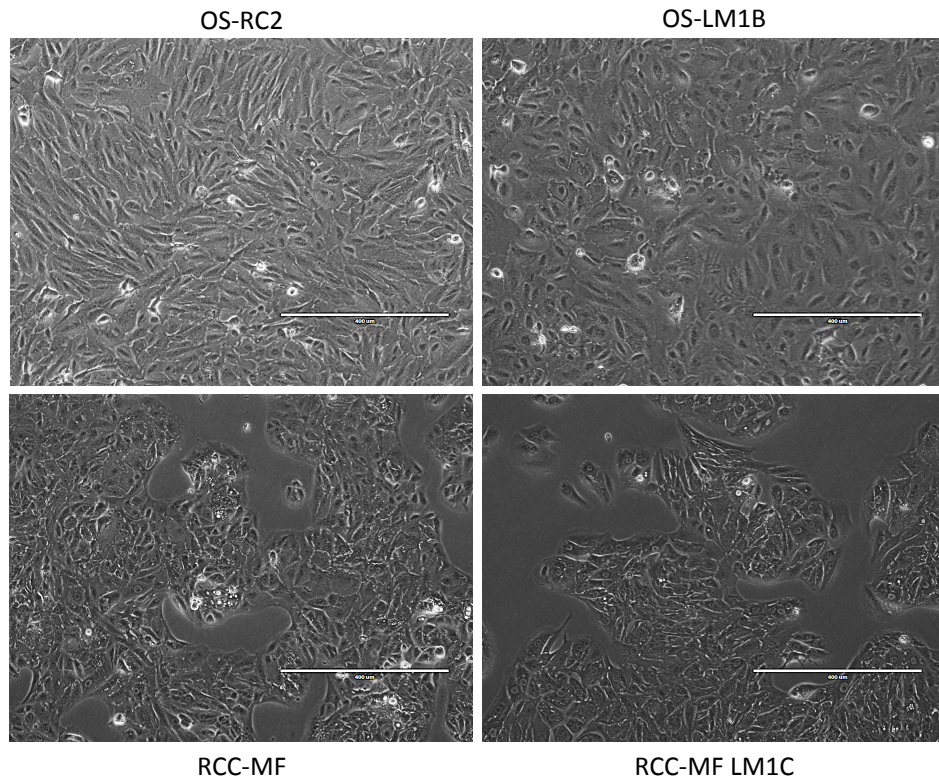


Figure 8 | Morphology of OS-RC2, OS-LM1B, RCC-MF and RCC-MF LM1C cells
 The OS-RC2 and OS-LM1B cells grow in a confluent monolayer (top). The OS-RC2 cells have a rather oblong shape (top left), whereas the shape of OS-LM1B cells is rounder (top right). The RCC-MF and RCC-MF LM1C cells grow in colonies and are morphologically not distinguishable (bottom left and right). Pictures were acquired with a 10X magnification. Scale bars represent 400μM.

PBRM1 is a protein that has multiple different isoforms that mostly differ in regions between domains. Some isoforms do miss parts of the BAH1 or HMG domains but apart from one truncated isoform that lacks everything downstream the end of BD6, the BDs are never affected (2). Isoform 2 is, with 1634 amino acids, the second longest splice variant and was already used to investigate the role of PBRM1 re-expression in breast cancer cells [25]. Therefore isoform 2 was selected in this study and its cDNA was cloned into the pLVX-Tight-Puro vector of the Lenti-X Tet-On® Advanced Inducible Expression System (Clontech). This system was used to enable Dox driven expression of PBRM1 in OS-RC2, OS-LM1B, RCC-MF and RCC-MF LM1C cells.

The inducibility of PBRM1 was examined by western blot. Induction was achieved by addition of 25 ng/ml Dox to the culture media and cells were harvested after 3 and 6 days. The 786-O cells were used as control to estimate a WT PBRM1 level.

Because the OS-RC2 cells only harbour a point mutation resulting in the change of one amino acid it is possible that they have intact PBRM1 expression. Indeed the OS-RC2 Empty Vector cells expressed low levels of PBRM1, which remained unchanged by Dox addition but was lower than the 786-O level. Without Dox the amount of PBRM1 in the OS-RC2 PBRM1 cells was similar to the Empty Vector control. The addition of Dox induced a stable expression of PBRM1 over the course of 6 days that was comparable to the 786-O control (Figure 9A).

As the OS-LM1B cells were metastatic derivatives of the OS-RC2 cells, the OS-LM1B Empty Vector cells also expressed mutant PBRM1. The OS-LM1B PBRM1 cells without Dox had a rather low level of PBRM1 as compared to the OS-LM1B Empty Vector samples. This was explainable by reduced total protein, estimated by β -Actin staining.

Addition of Dox for 3 days as well as 6 days induced expression of PBRM1, albeit the amount of PBRM1 in the 786-O cells was slightly higher. The granular appearance of the western blot was caused by problems during the transfer (Figure 9B).

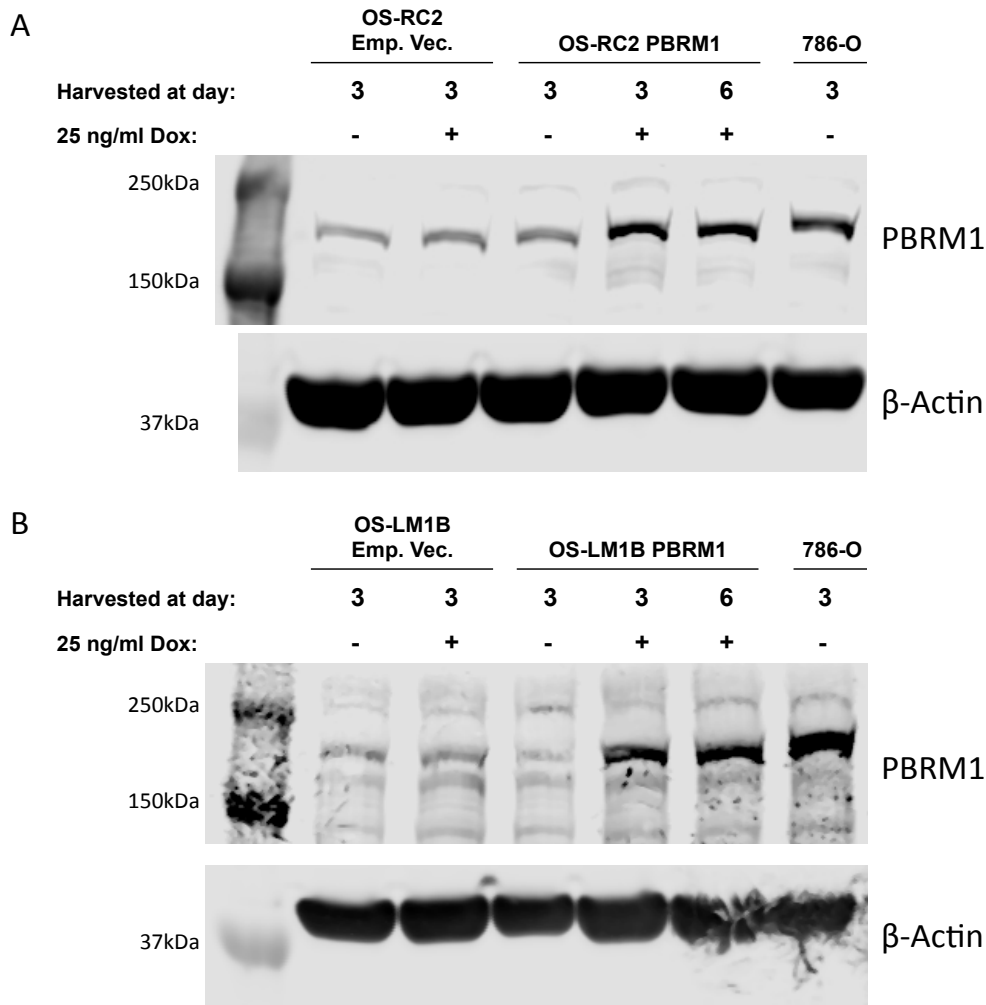


Figure 9 | Dox induces PBRM1 expression in OS-RC2 and OS-LM1B cells

OS-RC2 (**A**) and OS-LM1B (**B**) cells expressing PBRM1 induced by addition of 25ng/ml Dox or an Empty Vector control (Emp. Vec.) were harvested at the indicated time points with or without addition of Dox as indicated. 40 μ g of whole cell lysate were analysed by immunoblotting with antibodies against PBRM1 and β -Actin as loading control. The 786-O cells were used as an indication for wild type PBRM1 levels.

The RCC-MF cells harbour a PBRM1 truncating mutation and so, as expected, the Empty Vector cells did not express PBRM1. The RCC-MF PBRM1 cells leaked low levels of PBRM1 even when no Dox was added, a common problem with inducible systems. The addition of Dox led to robust PBRM1 expression, albeit it was slightly lower expressed than in 786-O cells (Figure 10A).

As the OS-LM1B cells the RCC-MF LM1C cells were metastatic derivatives of the RCC-MF cells. Comparable to the RCC-MF cells, the RCC-MF LM1C Empty Vector cells did not express PBRM1 and the RCC-MF LM1C PBRM1 cells leaked low levels of PBRM1. Dox addition led to stable expression of PBRM1 in the RCC-MF LM1C PBRM1 cells, which was lower than in the 786-O WT cells (Figure 10B).

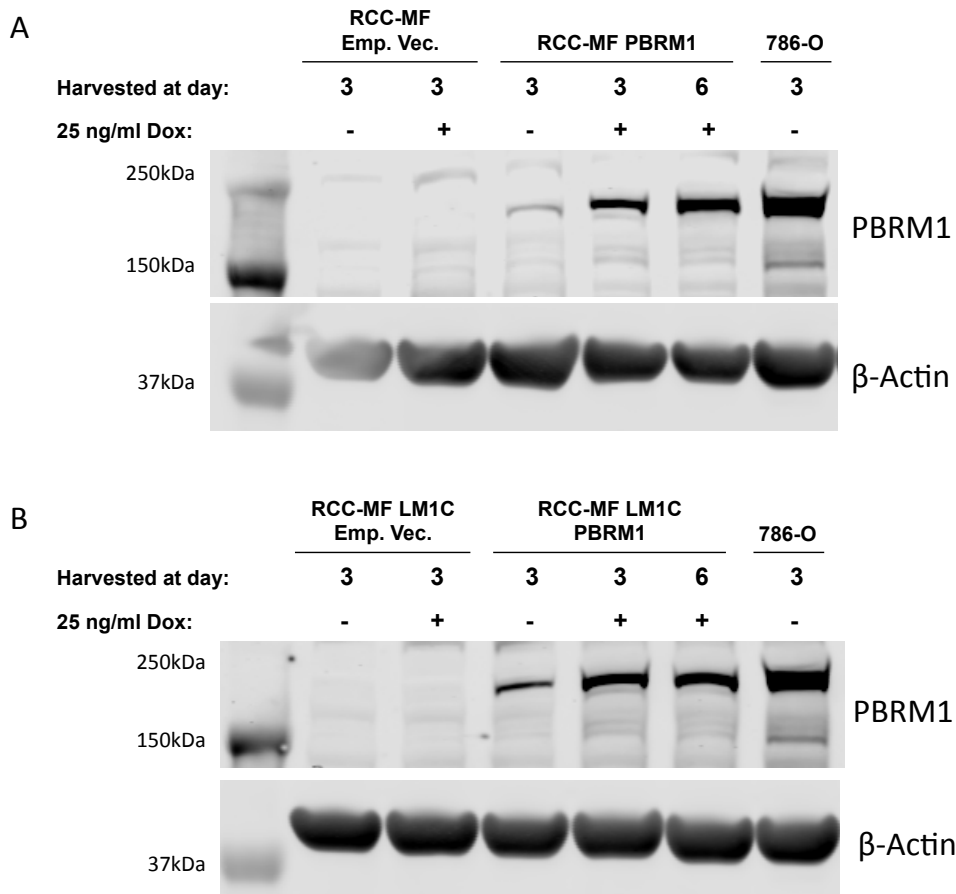


Figure 10 | Dox induces PBRM1 expression in RCC-MF and RCC-MF LM1C cells
RCC-MF (**A**) and RCC-MF LM1C (**B**) cells expressing PBRM1 induced by addition of 25 ng/ml Dox or an Emp. Vec. control were harvested at the indicated time points with or without addition of Dox as indicated. 40 μ g of whole cell lysate were analysed by western blot with antibodies against PBRM1 and β -Actin as loading control. The 786-O cells were used as an indication for wild type PBRM1 levels.

All cell lines were able to express PBRM1 dependent on induction by Dox. The RCC-MF and RCC-MF LM1C PBRM1 cells leaked low levels of PBRM1 even without Dox. Taking single cell clones from the RCC-MF PBRM1 cells revealed that only few clones did not leak low levels of PBRM1 and still retained the ability to inducibly express it (data not shown). Therefore the possibility of using single cell clones that did not leak PBRM1 was considered

for subsequent experiments. Yet, even clones from the same cell population might exhibit e.g. a different proliferation, which would complicate comparison to clones from other cell populations. Taking this into consideration I decided to proceed with the whole cell population and against using single cell clones. The OS-RC2 and OS-LM1B PBRM1 cells did not seem to leak PBRM1 expression even without Dox. Yet, this might be masked by the residual mutated PBRM1, which made it difficult to detect potential small differences in expression levels.

The PBRM1 expression levels in all cell lines, apart from the OS-RC2 PBRM1 cells, were lower than in the PBRM1 WT 786-O cells. To prevent from toxicity caused by protein overexpression and because 100 ng/ml Dox had already be shown to reduce the proliferation in 786-O cells it was decided to keep the Dox concentration as low as possible for subsequent experiments.

2.2.2 The expressed PBRM1 incorporates into the PBAF complex

Although most splice variants only differ in regions between domains, the question remained if the expressed isoform of PBRM1 was functional. To test for functionality it was verified that PBRM1 was able to assemble with the PBAF SWI/SNF complex.

This was achieved by immunoprecipitation (IP) of PBRM1 or ARID2, which is a PBAF complex member, followed by subsequent Western blotting with ARID2 or PBRM1 antibodies respectively.

For the IPs OS-RC2 PBRM1, OS-RC2 Empty Vector, RCC-MF PBRM1 and RCC-MF Empty Vector were cultivated in the presence of Dox.

The HEK293T cells were used as a positive control for SWI/SNF complex formation and an IgG antibody was utilized as a control to detect unspecific antibody binding.

As expected OS-RC2 Empty Vector cells contained only residual mutated PBRM1 and the OS-RC2 PBRM1 cells were able to express PBRM1. The expression of PBRM1 in HEK293T cells was much stronger than in the OS-

RC2 PBRM1 cells. Total protein levels were similar as demonstrated by β -Actin (Figure 11A, Input). Using the ARID2 antibody PBRM1 could be immunoprecipitated in all samples. The relative PBRM1 levels between the samples resembled the input (Figure 11A, IP: ARID2).

In the IP with the IgG negative control an unspecific band with the size of the PBRM1 protein was detectable. The strength of this unspecific band was comparable to the PBRM1 level in OS-RC2 Empty Vector (Figure 11A, IP: IgG).

The ARID2 input levels of both OS-RC2 cell lines were similar, whereas the HEK293T cells expressed more ARID2. Total protein levels were similar as demonstrated by β -Actin (Figure 11B, Input). Using the PBRM1 antibody it was able to immunoprecipitate ARID2 in all samples, with the strongest signals in HEK293T followed by OS-RC2 PBRM1 and a weaker band in OS-RC2 Empty Vector (Figure 11B, IP: PBRM1). Hardly any unspecific binding could be detected in the IP with IgG (Figure 11B, IP: IgG).

So it was concluded that the expressed PBRM1 could be immunoprecipitated with the PBAF complex member ARID2 and vice versa. This demonstrated that the expressed PBRM1 was able to incorporate into the SWI/SNF complex. Especially in the PBRM1 IP it became clear that the mutated residual PBRM1 of OS-RC2 Empty Vector cells could load into the PBAF complex as well. This was not entirely surprising, as the PBRM1 mutation occurred in a BD, which is presumably not important for the SWI/SNF complex formation. This is further underlined by a recent report that indicated the C-Terminal end, which contains the HMG domain, in being responsible for loading into the PBAF complex [37].

Yet to exclude the possibility that the immunoprecipitated protein in the OS-RC2 PBRM1 sample was exclusively mutated but not the expressed PBRM1, the RCC-MF cells were used for an IP as well, as those cells do not express mutated PBRM1.

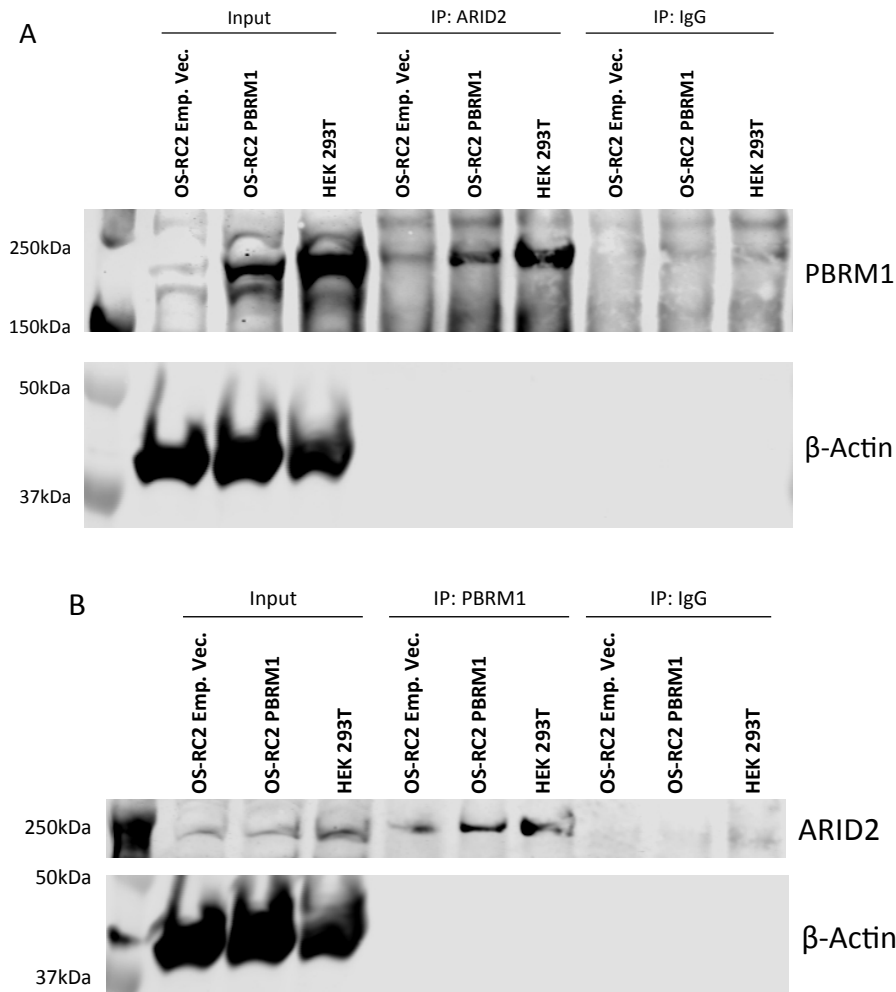


Figure 11 | Expressed PBRM1 is able to incorporate into the PBAF complex in OS-RC2 cells

OS-RC2 cells were harvested 4 days after addition of Dox. HEK 293T cells were used as WT control for SWI/SNF complex formation. IP was performed from 2.3 mg of total protein lysate with ARID2 (**A**) and PBRM1 (**B**) antibodies, followed by Western blot for PBRM1 (**A**) and ARID2 (**B**). IgG antibody was used as negative control for unspecific binding. 50µg of whole cell lysate were utilized to determine the input protein levels and β-Actin controlled for the input loading.

The RCC-MF Empty Vector and PBRM1 cells expressed similar levels of ARID2 and the RCC-MF PBRM1 cells exclusively expressed PBRM1. HEK293T cells expressed both ARID2 and PBRM1 in a higher quantity than the RCC-MF cells. Total protein levels were similar as demonstrated by β-Actin staining (Figure 12, Input).

IP with ARID2 followed by western blot with ARID2 demonstrated that ARID2 could be isolated from the whole cell lysates in comparable quantities in all samples. Considering this and the fact that PBRM1 expression in RCC-MF PBRM1 cells was relatively strong, only a small fraction of the expressed

PBRM1 was integrated into the SWI/SNF complex as shown by IP with ARID2 and Western blot for PBRM1. As expected PBRM1 could not be immunoprecipitated with ARID2 in RCC-MF Empty Vector cells. The IP of PBRM1 with ARID2 was much more efficient in HEK293T cells than in RCC-MF PBRM1 cells (Figure 12, IP: ARID2).

The IP and the Western blot with PBRM1 demonstrated again that the RCC-MF PBRM1 and HEK293T cells expressed PBRM1 but not the RCC-MF Empty Vector cells. Yet only small quantities of ARID2 were detectable in the IP of PBRM1 in RCC-MF PBRM1 cells, whereas in the HEK293T cells much more ARID2 was immunoprecipitated (Figure 12, IP: PBRM1). Neither ARID2 nor PBRM1 bound unspecifically to IgG in HEK 293T cell lysate (Figure 12, IP: IgG).

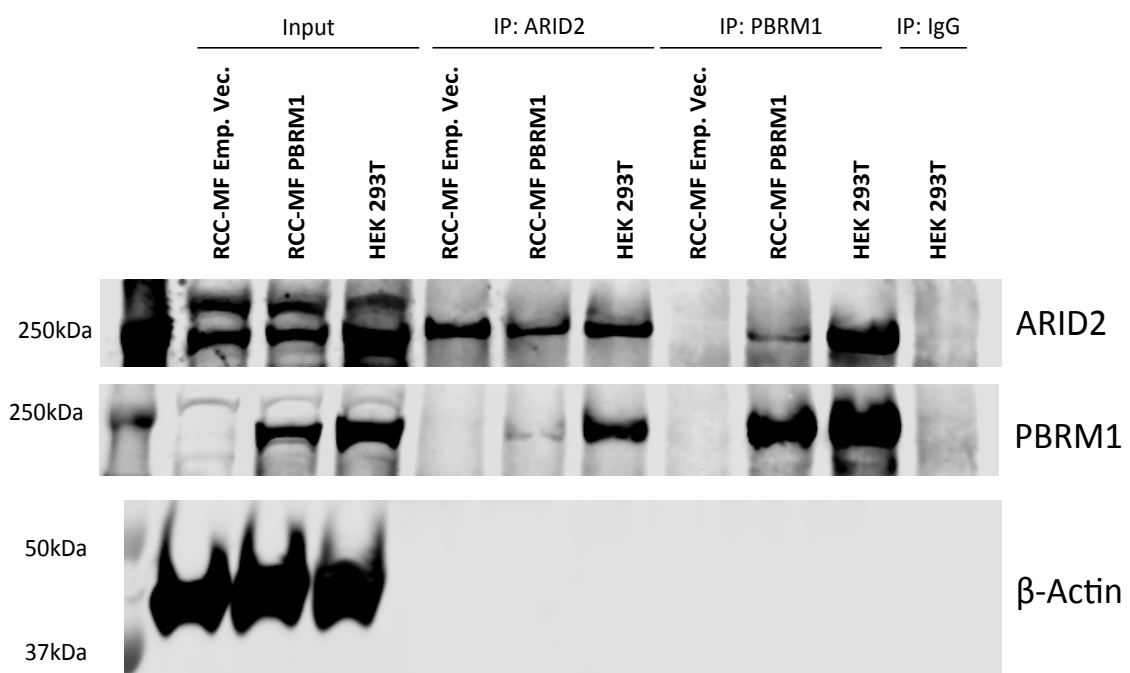


Figure 12 | Expressed PBRM1 is able to incorporate into the PBAF complex in RCC-MF cells

RCC-MF cells were harvested 3 days after addition of Dox. HEK 293T cells were used as WT control for SWI/SNF complex formation. IP was performed from 1.3 mg of total protein lysate with ARID2 and PBRM1 antibodies, followed by western blot for PBRM1 and ARID2. IgG antibody was used as negative control for unspecific binding. 50µg of whole cell lysate were loaded to compare input protein levels.

So it could be confirmed that PBRM1 was also able to incorporate into the PBAF complex in RCC-MF cells. Yet the efficiency of this process was extremely low and seemed to be better in OS-RC2 cells

It might be possible that this was caused by the expression of the wrong PBRM1 isoform. Another possibility is that the complete loss of PBRM1 destabilizes the SWI/SNF complex and in the course of tumour evolution the RCC-MF cells lost the ability to efficiently form the PBAF complex.

Nonetheless some PBRM1 containing PBAF complexes were forming and if this resulted in strong tumour suppressive phenotypes this would still become detectable in subsequent assays.

2.2.3 In vitro proliferation is not PBRM1 dependent

Changes in proliferation due to PBRM1 knockdown were frequently reported and so the influence of PBRM1 expression on growth was first assessed.

In the absence of Dox the OS-RC2 PBRM1 and the Empty Vector cells proliferated with equal speed. Addition of Dox to the growth media had a subtle inhibitory effect that was not PBRM1 dependent but affected both cell lines in the same manner (Figure 13A).

The OS-LM1B cells were more resistant to Dox as their growth was not inhibited when Dox was added. But also in these metastatic cells PBRM1 expression did not affect proliferation (Figure 13B).

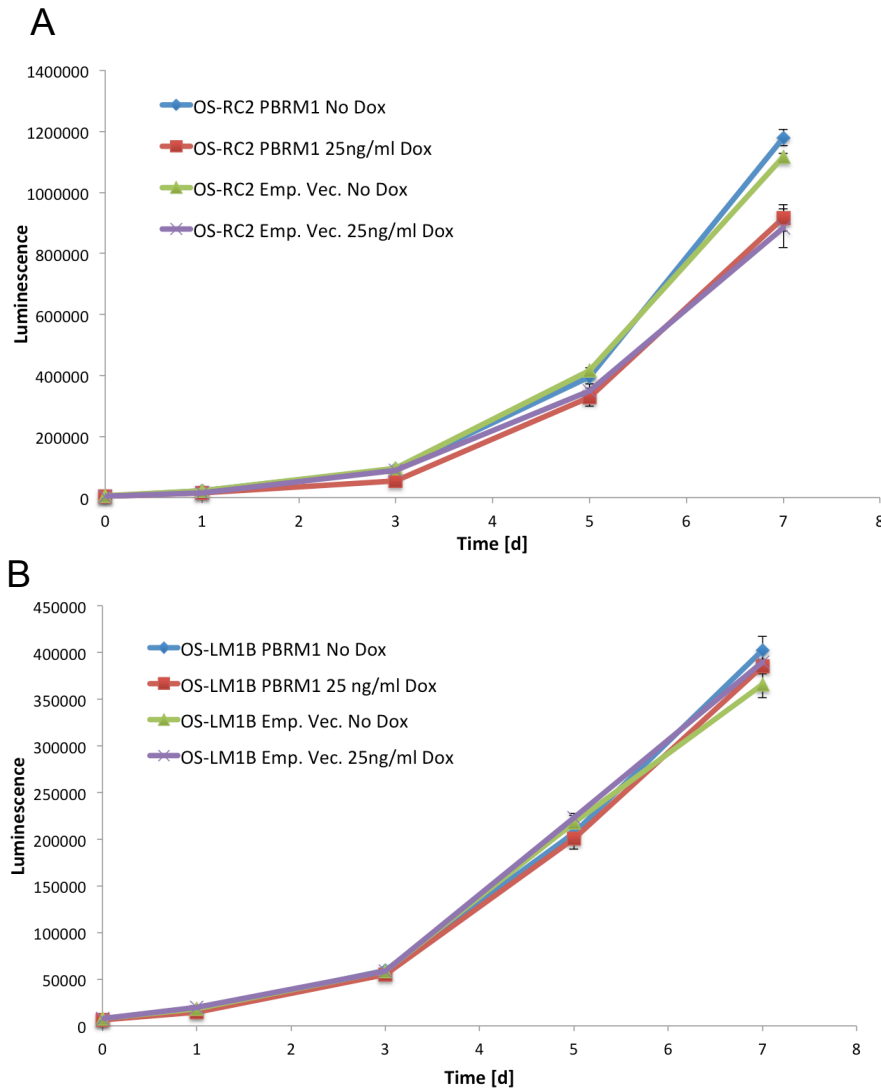


Figure 13 | PBRM1 expression does not affect proliferation of OS-RC2 or OS-LM1B cells

Growth of OS-RC2 (A) and OS-LM1B (B) cells expressing PBRM1 or Emp. Vec. was determined by measuring ATP dependent luminescence. PBRM1 expression was induced with 25 ng/ml Dox. Displayed values represent means of technical replicates and SEM (n=4).

For the RCC-MF cells the proliferation assay displayed a higher inherent variance. This could be observed via a larger SEM and the proliferation curves crossed several times during the course of the experiment (Figure 14A). RCC-MF cells tended to grow in colonies that began to merge when the cells approached confluency, but there would always remain empty batches between the colonies (Figure 8). How many empty batches remained between colonies presumably induced some randomness in the cell number and thus a bigger variance, especially in the later time points of the experiment. Nonetheless PBRM1 expression did also not affect proliferation in RCC-MF cells (Figure 14A).

The RCC-MF LM1C displayed the same growth pattern as RCC-MF cells and thus the proliferation assay was also prone to a higher variability. Dox had only minimal inhibitory effects on proliferation and due to the big error bars there was essentially no difference between RCC-MF LM1C cells that expressed PBRM1 and the Empty Vector control (Figure 14 B).

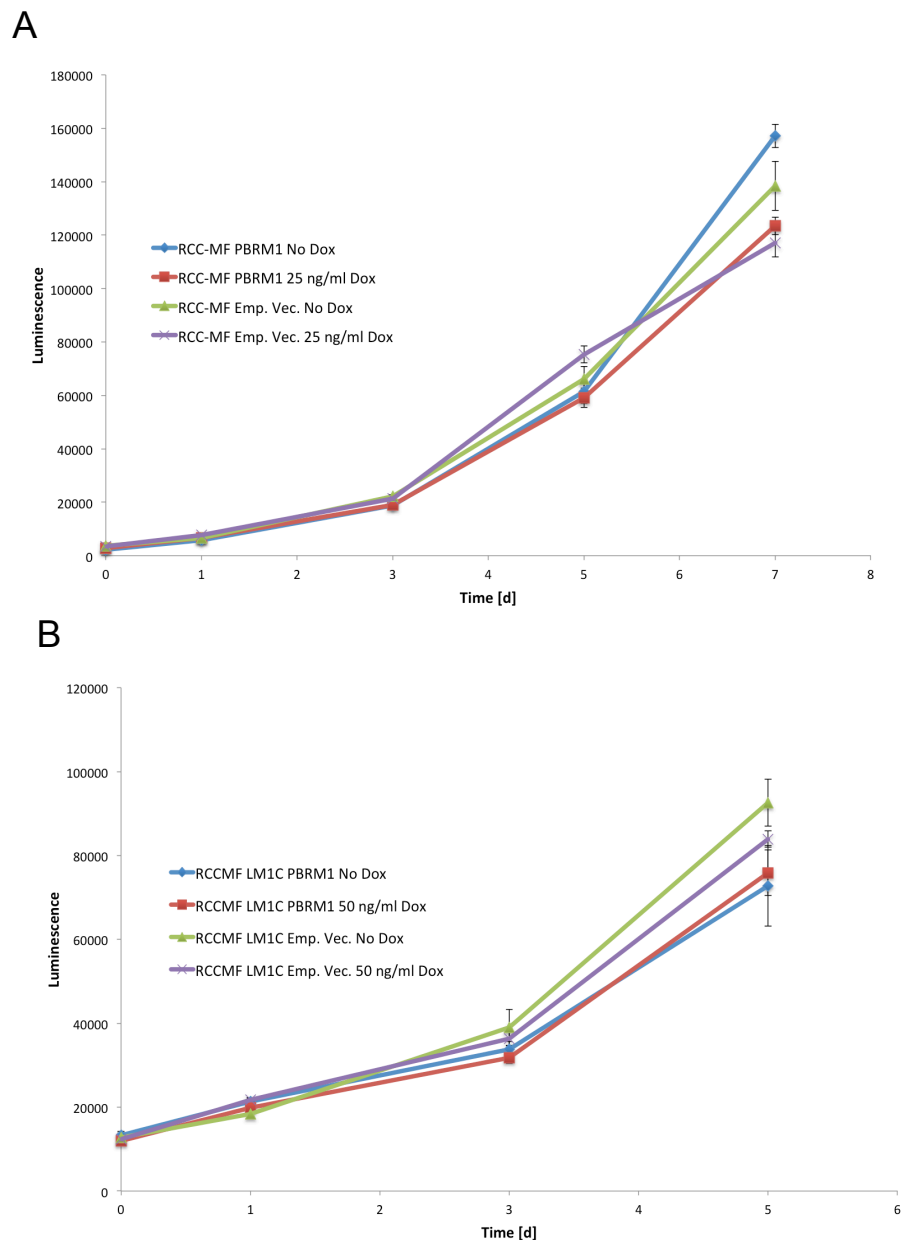


Figure 14 | PBRM1 expression does not affect proliferation of RCC-MF or RCC-MF LM1C cells

Growth of RCC-MF (A) and RCC-MF LM1C (B) cells expressing PBRM1 or Emp. Vec. was determined by measuring ATP dependent luminescence. PBRM1 expression was induced with 25 (A) or 50 (B) ng/ml Dox. Displayed values represent means of technical replicates and SEM (n=4).

Contradicting a published report [10], proliferation of ccRCC cells was not affected by PBRM1 neither in parental nor in metastatic cell lines. This was in line with results acquired by shRNA mediated PBRM1 knockdown in 786-O cells (Figure 7).

2.2.4 PBRM1 has no effect on proliferation in stress conditions

PBRM1 expression did not change proliferation in standard cell culture conditions. Yet it was reasoned that some effects might have been masked by optimal proliferation conditions. The SWI/SNF complexes are able to model the expression of a large gene numbers and it was hypothesized that cells containing WT PBRM1 and thus a WT PBAF complex would not be able to sustain growth in stress conditions.

2.2.4.1 PBRM1 expression is not critical for proliferation in high cell dilution

In normal cell culture cells are grown in a high cell density to maintain optimal growth. Therefore there are always many cells available to produce different signalling compounds. Not every cell is capable of forming a colony if grown in high cell dilution and so it was hypothesized that PBRM1 expression might influence the capability of the OS-RC2 cells to form colonies when seeded in low cell density. Nonetheless the expression of PBRM1 did not change the colony number in OS-RC2 cells (Figure 15).

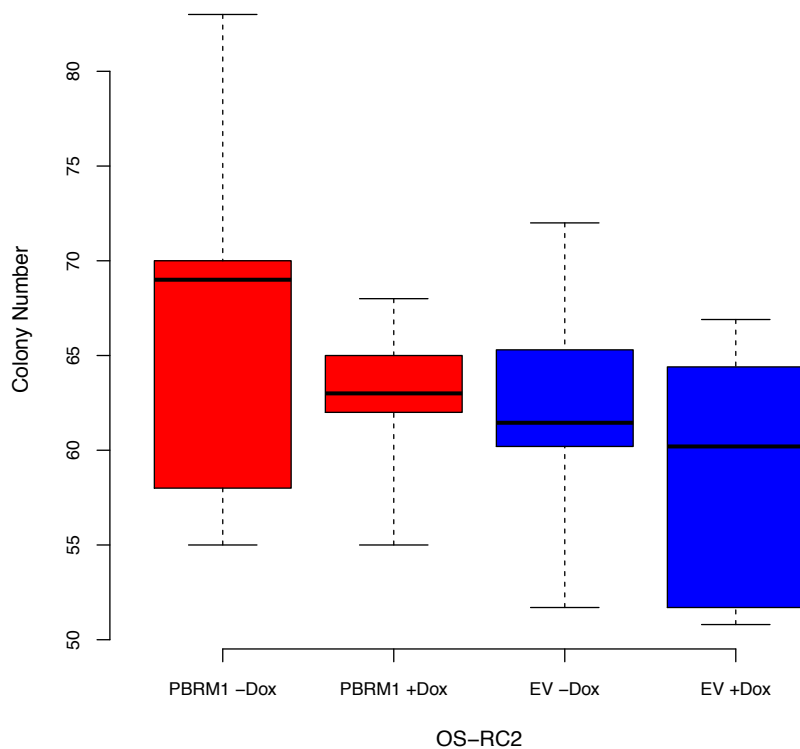


Figure 15 | PBRM1 does not alter growth in high cell dilutions

OS-RC2 PBRM1 and Empty Vector (EV) cells were grown in high cell dilution either without Dox (-Dox) or with 25 ng/ml Dox (+Dox). Colonies are counted after 9 days and results are displayed as box plots with n=6.

2.2.4.2 PBRM1 has no influence on proliferation in stress conditions

To grow cells in high cell dilution did not reveal PBRM1 dependent differences. Nonetheless it was possible that different stress conditions relevant for tumour cells would reveal a PBRM1 dependent phenotype.

To promote optimal growth in cell culture, cells are grown with an excess of growth factors provided by the addition of fetal calf serum (FCS). These growth factors were reduced 10-fold to determine the effects of PBRM1 expression in a condition with limited growth factor availability.

Due to uncontrolled growth and poor vascularization nutrient availability is limited in tumours and especially glucose concentrations are often 3- to 10-fold lower than in normal tissues, which leads to adaptations of the metabolism to low glucose levels in cancer cells [38]. To mimic this situation, glucose levels were reduced 11-fold to 1 mM in the growth media.

Tumours often acidify their microenvironment due to high glycolytic activities, lowering the extracellular pH as far as 5.6 [39]. Thus it was investigated if growth at pH=5.5 was affected by PBRM1 expression.

As previously determined, PBRM1 expression had no influence on proliferation in normal growth media after 3 days compared to Day 0 in OS-RC2 and OS-LM1B cells. The assay displayed a relative large variance indicated by the difference in the average proliferation between Empty Vector cells with and without Dox (Figure 16A and B).

In general the average proliferation was highly similar in all conditions and both cell lines (Figure 16A and B). Only when grown in media with low pH, the OS-LM1B PBRM1 No Dox sample displayed a higher relative proliferation compared to OS-LM1B PBRM1 25 ng/ml Dox (Figure 16B). This was thought to be an outlier caused by a bad measurement, as after 5 days of culture with low pH media, this difference in average proliferation was not observable any more (data not shown).

Therefore it could be concluded that PBRM1 expression did not affect the proliferative capacities of parental and metastatic OS cells neither in low FCS, low glucose nor in low pH conditions (Figure 16A and B). This was further underlined by the fact that the results were highly similar when the cells were grown for 5 days in these conditions (data not shown).

A single stress condition alone was possibly not able to unravel the effect of PBRM1 expression, therefore an additional stress condition consisting of a combination of 1 mM Glucose and pH=5.5 was included for RCC-MF and RCC-MF LM1C cells.

The RCC-MF cells displayed high proliferative variability in normal media, which was not thought to be caused by PBRM1 expression but rather induced by the growth pattern of MF cells (Figure 17A).

As discussed before the RCC-MF and RCC-MF LM1C cells grow in colonies, which is presumably the reason why in proliferation assays the variances between technical replicates were larger than in the OS cell lines.

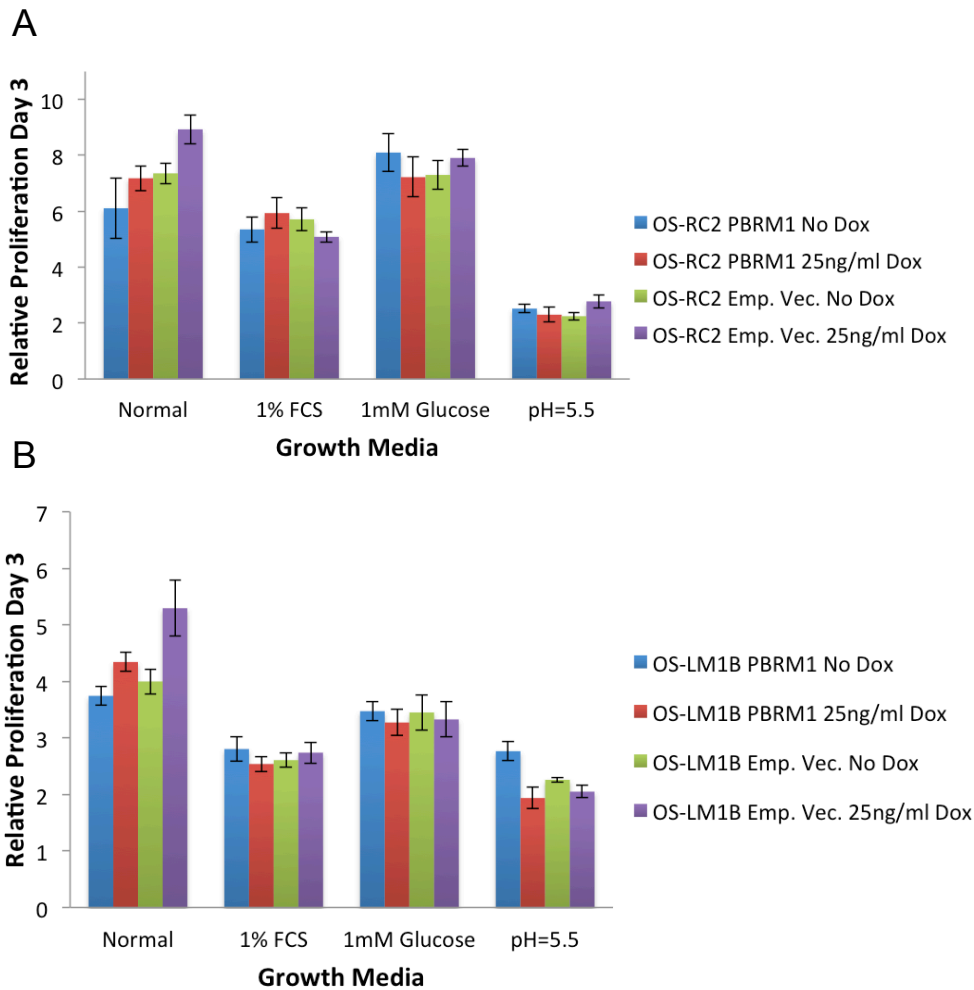


Figure 16 | Proliferation in stress conditions is not affected by PBRM1 in OS-RC2 and OS-LM1B cells

Relative proliferation after 3 days compared to Day 0 is determined under normal, low serum (1% FCS), low glucose (1 mM Glucose) and low pH (pH=5.5) conditions in OS-RC2 (A) and OS-LM1B (B) PBRM1 and Emp. Vec. cells. PBRM1 expression was induced with 25 ng/ml Dox. Data shown represent mean and SEM of n=3.

In general the RCC-MF cells were more sensitive to the stress conditions than the OS cells, as all conditions, except low glucose, inhibited proliferation. Low pH and the low pH/glucose combination completely stalled RCC-MF proliferation, whereas 1% FCS killed about half of the seeded cells by Day 3. PBRM1 expression did not alter proliferation in any condition (Figure 17A).

The RCC-MF LM1C cells behaved very similarly to the RCC-MF cells and the response to the different applied conditions was not PBRM1 dependent by Day 3 (Figure 17B).

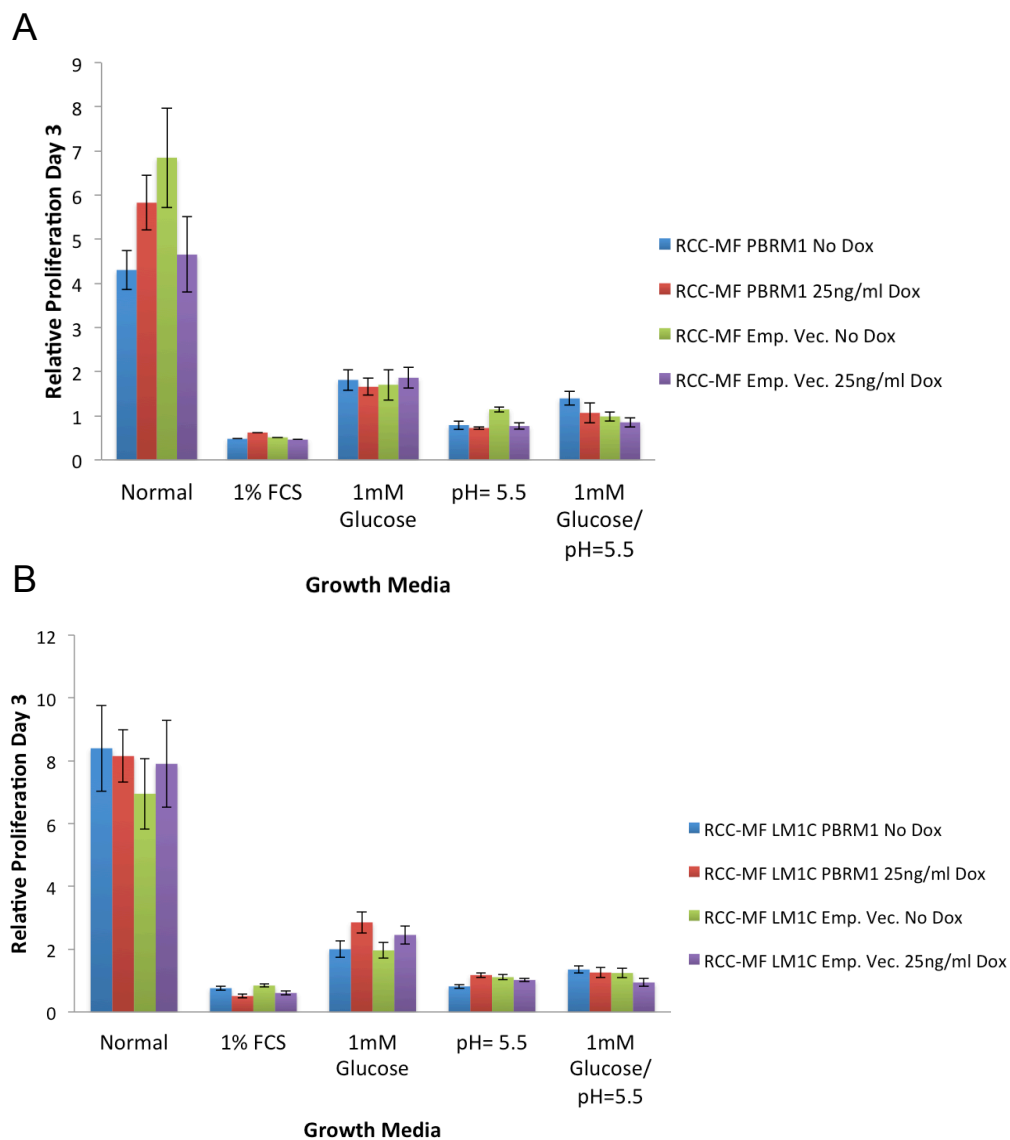


Figure 17 | Proliferation in various stress conditions is not affected by PBRM1 in RCC-MF and RCC-MF LM1C cells

Relative proliferation after 3 days compared to Day 0 is determined under normal, low serum (1% FCS), low glucose (1 mM Glucose) and low pH (pH=5.5) conditions in RCC-MF (A) and RCC-MF LM1C (B) PBRM1 and Emp. Vec. cells. PBRM1 expression was induced with 25 ng/ml Dox. Data shown represent mean and SEM of n=3.

Growth capacities of PBRM1 mutant cell lines in several challenging stress environments were not altered by PBRM1 expression. Therefore it was concluded that PBRM1 did not exert its tumourigenic function by affecting proliferation.

2.2.5 Resistance to reactive oxygen species is not PBRM1 dependent

Reactive oxygen species (ROS) such as hydrogen peroxide (H_2O_2) are produced through the metabolism of molecular oxygen. H_2O_2 is one of the major sources of endogenous ROS because it is generated as by-product of e.g. aerobic respiration in mitochondria. ROS are usually kept in control by a tight balance between ROS and biochemical antioxidants. Imbalance in this system, for instance due to down-regulation or mutation of important enzymes, can, due to the high reactivity of ROS, lead to tissue, DNA and protein damage which causes mutations, chromosomal instability and membrane or organelle failure. Especially the reactivity of ROS with DNA is widely accepted as a driver of cancer [40].

Due to the elevated proliferation of cancer cells and thus higher mitochondrial activity also more ROS are generated. Cancer cells must therefore avoid accumulation of high ROS concentrations, potentially by up regulation of antioxidant genes. As part of the SWI/SNF complex the loss of PBRM1 could influence the expression of a large number of genes and thus it was hypothesized that loss of PBRM1 would deregulate some important functions in the answer to or the production of ROS like H_2O_2 . Therefore PBRM1 loss could lead to higher resistance against induced ROS by addition of H_2O_2 .

The survival of OS-RC2 and RCC-MF cells was measured 3 days after addition of different H_2O_2 concentrations to the culture media. The survival curves of OS-RC2 PBRM1 and Empty Vector cells without Dox were slightly different, but as addition of Dox did not alter the shape of the curves, it was concluded that resistance to ROS was not conferred by PBRM1 (Figure 18A). This finding was further emphasized by the fact that the survival curves for all conditions in RCC-MF were highly similar (Figure 18B). Thus the response to H_2O_2 induced ROS was not PBRM1 dependent in OS-RC2 and RCC-MF cells.

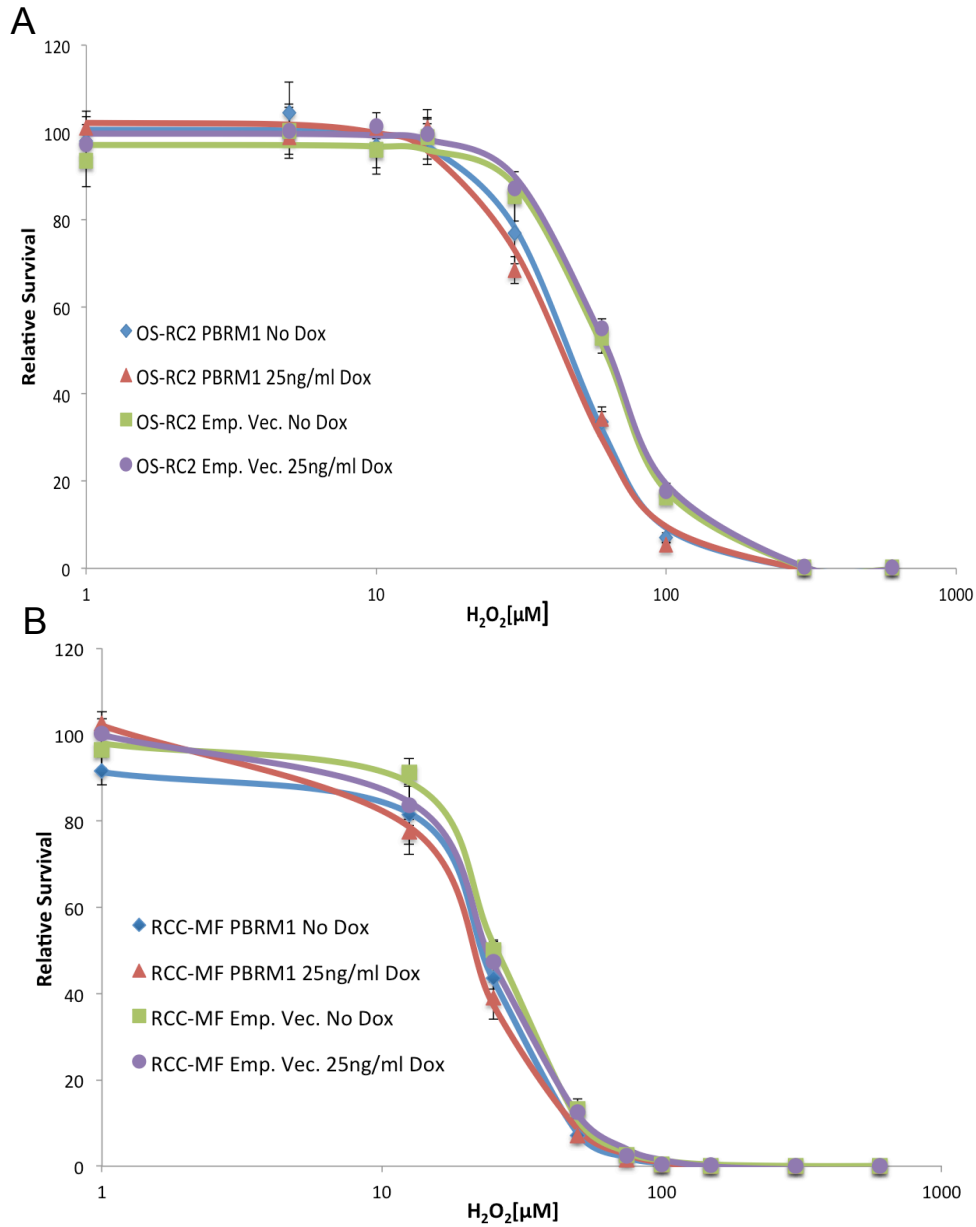


Figure 18 | Survival of OS-RC2 and RCC-MF cells after induction of ROS was not influenced by PBRM1

Relative survival of (A) OS-RC2 and RCC-MF (B) PBRM1 and Emp. Vec. cells with increasing concentrations of H₂O₂. PBRM1 expression was induced by 25 ng/ml Dox. Each value represents the mean of technical replicates and SEM (n=3).

2.2.6 Resistance to induced DNA double strand breaks is not dependent on PBRM1

Absence of PBRM1 was reported to induce defects in cohesion leading to chromosomal instability. Cells that are defective in cohesion are often hypersensitive to DNA damaging agents and consequently PBRM1 knockdown reduced the resistance to the DNA crosslinking agent mitomycin C in human fibroblasts [24].

Etoposide, a drug often used in chemotherapy, induces DNA damage due to inhibition of topoisomerase II. This prevents DNA strand re-ligation and thus causes DNA strands to break [41].

Topoisomerase II was furthermore reported to have increased function due to BRG1 binding (BRG1 is the ATPase subunit in the PBAF complex) [42].

Thus it was hypothesized that expression of PBRM1 would increase the resistance to Etoposide either because PBRM1 expressing cells are more resistant to DNA damage or because restoration of a lost SWI/SNF complex member enhances Topoisomerase II activity.

The survival of OS-RC2 and RCC-MF cells was measured 3 days after addition of different Etoposide concentrations to the culture media. The OS-RC2 Empty Vector cells exhibited similar survival curves with and without Dox. The OS-RC2 PBRM1 cells seemed to be more resistant to Etoposide when PBRM1 was expressed, because the survival with low Etoposide concentrations was higher than in OS-RC2 PBRM1 No Dox samples. Yet, if PBRM1 would enhance the resistance to Etoposide, the expected largest differences in the survival curves would occur around 50% survival and not with the lowest Etoposide concentrations as was the case. Moreover the survival curve of the PBRM1 expressing cells was very similar to both Empty Vector conditions.

Together this indicated that PBRM1 was not able to enhance resistance to Etoposide in OS-RC2 cells and that the observed difference was rather caused by an incorrect measurement of the cell viability in the 'No Etoposide' condition to which every value was relative to (Figure 19A).

The RCC-MF cells displayed highly similar survival in all conditions (Figure 19B). This further underlined the conclusion that resistance to Etoposide was not dependent on PBRM1.

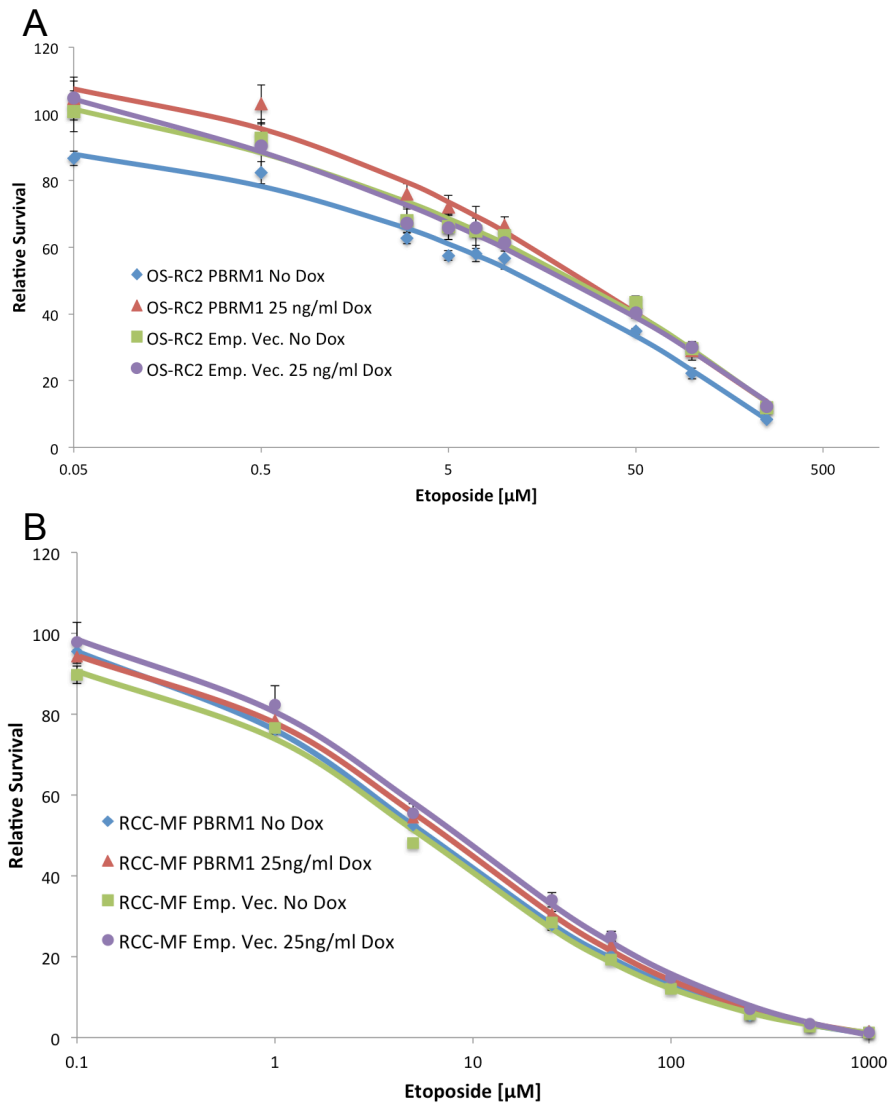


Figure 19 | Survival of OS-RC2 and RCC-MF cells after induction of DNA damage is not influenced by PBRM1

Relative survival of (A.) OS-RC2 and RCC-MF (B.) PBRM1 and Emp. Vec. cells with increasing concentrations of Etoposide. PBRM1 expression was induced with 25 ng/ml Dox. Each point represents the mean of technical replicates (n=3). The error bars display SEM.

2.2.7 Anchorage independent growth is enhanced by PBRM1

The anchorage independent growth assay displays the ability of cells to grow independently from a solid surface, which is a well-established feature of cancer cells. Transient PBRM1 knockdown indicated an increase in colony forming capability when grown in soft agar [10]. Therefore it was tested if the expression of PBRM1 could modify the ability to form colonies in this assay.

The OS-RC2 and RCC-MF cells were not able to form colonies in soft agar (data not shown). It is known that the metastatic potential is closely linked to the ability for anchorage independent growth and therefore OS-LM1B cells were also tested for their capability to form colonies in soft agar [43].

Four independent experiments were conducted in which the ability of OS-LM1B PBRM1 and Empty Vector cells to form colonies was measured when grown with and without Dox. The OS-LM1B Empty Vector cells displayed a low capability to grow in soft agar, which seemed to be enhanced when the OS-LM1B cells expressed PBRM1 (Figure 20B and C).

In order to combine all replicate experiments, the colony counts of the 'With Dox' condition were normalized to the respective average colony number of the 'No Dox' condition for PBRM1 and Empty Vector within each replicate. Subsequently each PBRM1 and Empty Vector value was normalized to the average of the Empty Vector values within each replicate (Figure 20A).

Throughout four independent experiments PBRM1 expression enhanced the colony formation capability in average 2.2-fold compared to Empty Vector. A two-tailed Mann-Whitney test showed that the increase in colony formation capability was highly significant: $U=477$, $n=24,20$, $p<0.0001$.

This result again stood in contrast with published data acquired through transient knockdown of PBRM1 [10]. Furthermore it indicated that the OS-RC2/OS-LM1B PBRM1 mutation interfered with PBRM1 WT function and that these cell lines could be considered as PBRM1 mutant although they expressed residual mutant PBRM1.

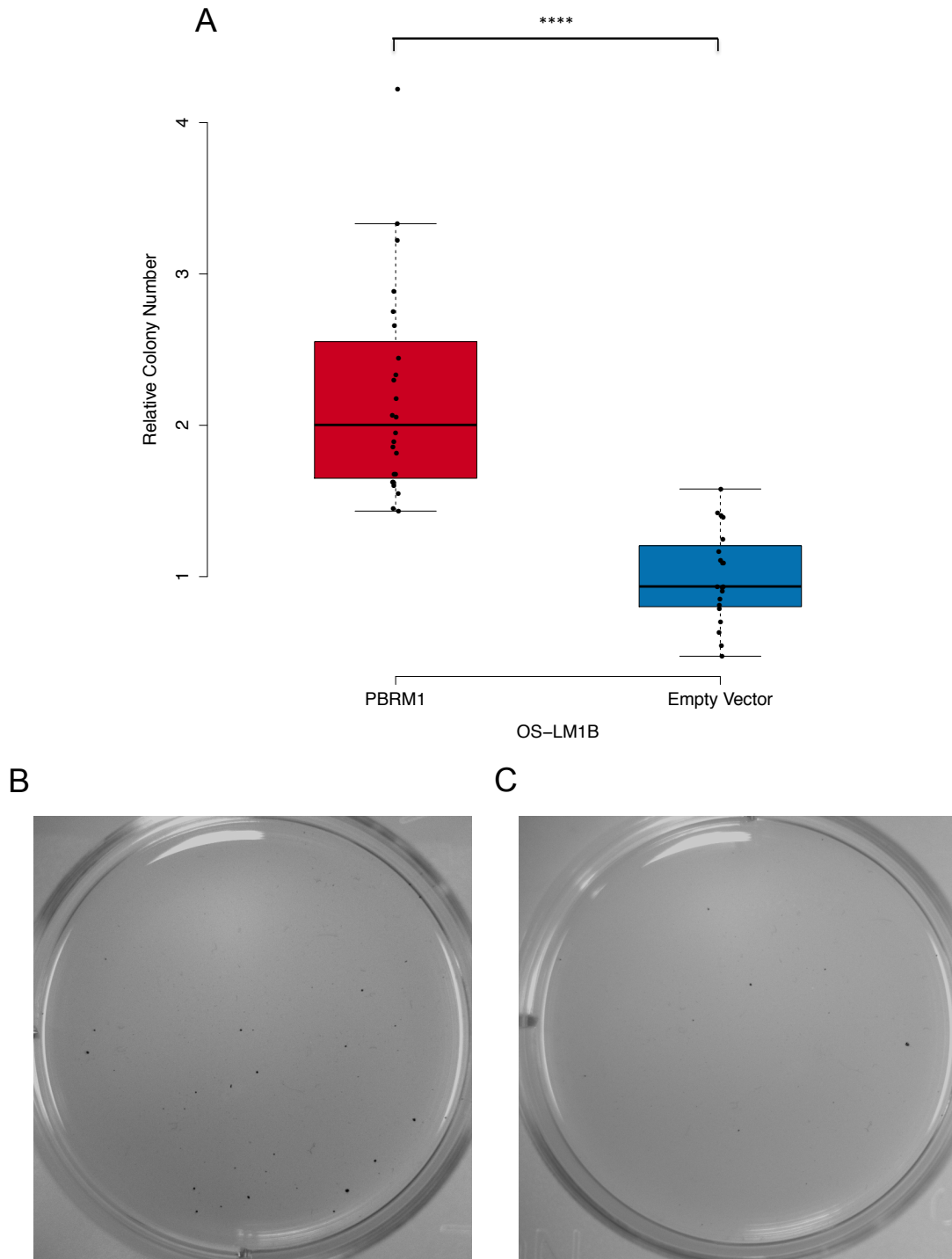


Figure 20 | PBRM1 expression is able to increase the colony number in OS-LM1B cells

A. Boxplot displaying the relative colony number normalized to Empty Vector condition. The p-value was determined with the Wilcoxon Rank Sum Test. $n = 24$ (PBRM1) and 20 (Empty Vector). ****= $p\text{-value} < 0.0001$. Representative images of OS-LM1B PBRM1 (**B**) and Empty Vector (**C**) cells cultivated with Dox.

2.3 Endogenous expression of PBRM1 in mutant cell lines by CRISPR-Cas9 mediated repair

PBRM1 is expressed in multiple isoforms. These splice variants are highly similar and differ mostly in regions between domains (2). IPs indicated that the expressed isoform 2 was able to incorporate into the SWI/SNF complex. Yet the majority of the expressed PBRM1 was not able to load into the PBAF complex (Figure 11 and 12).

This approach omitted all other isoforms and it couldn't be excluded that expression of all of them would increase the efficiency of SWI/SNF complex formation. It is also a possibility that different isoforms exert distinct functions in the PBAF complex even though all isoforms are highly similar.

Moreover it is impossible to know the true WT level of any protein in a mutated cell line. Although comparison with a similar WT cell line gives a good indication of correct protein level, over or under-expression cannot be excluded.

To circumvent these eventualities it was aimed for a repair of the small PBRM1 mutations in the OS-RC2 and RCC-MF cell lines, enabling a true WT expression of the full spectrum of PBRM1 isoforms. To achieve this goal the type II bacterial clustered, regularly interspaced, short palindromic repeats (CRISPR)-associated protein 9 (CRISPR- Cas9) system was utilized.

Cas9 is a nuclease that is guided to the target DNA by single guide (sg)RNAs and is thus able to efficiently induce DNA double strand breaks (DSBs) at the desired target sequences. The only other requirement needed by the Cas9 enzyme to cut target DNA is a protospacer adjacent motif (PAM) of the sequence 5'- NGG -3' which directly precedes the target DNA bound by the sgRNAs. The DSBs are induced 3 bp upstream of the PAM and either repaired by the non-homologous end joining (NHEJ) pathway or the homology directed repair (HDR) pathway. The NHEJ pathway re-ligates the DNA fragments, a process that is error prone and frequently leads to insertion/deletion (indel) mutations. If this takes place in the coding region of a gene, frame shift mutations are common, which effectively leads to gene knockout.

The HDR pathway is used if a repair template is present. By providing an exogenously introduced repair template it is possible to precisely modify the target sequence, which potentially could be exploited to repair mutations that occurred in tumour cells [44].

2.3.1 Strategy 1 – Using HDR for repair of small mutation

The aim was to repair the 698 T>C mutation of OS-RC2 cells and the 1583delA mutation of RCC-MF cells using HDR. The CRISPR design tool was used to design potential sgRNAs around the region of the mutation [44].

In both cell lines 2 sgRNAs were selected due to their proximity to the site of mutation (Table 4) and those sgRNAs were cloned into the px330-U6-Chimeric_BB-CBh-hSpCas9 plasmid (px330_sgRNA_Cas9) a vector, that expressed both the sgRNA and Cas9 [45].

Transient transfection was selected as a means to import DNA into the cells, because the expression of Cas9 and sgRNA was undesirable after the mutation had been reverted. The px330 plasmid was co-transfected with a single-stranded DNA oligonucleotide (ssODN) carrying the WT PBRM1 sequence as a repair template to induce HDR.

The px330_sgRNA_Cas9 plasmid did contain a marker to select for successful transfection, therefore a small plasmid expressing a fluorescent protein was added to the transfection mix as well. For this purpose pcDNA3.1 (-) was chosen, in which RFP was cloned as a selection marker. All cell lines used, had previously been transduced with the TGL triple reporter plasmid by Dr Sakari Vanharanta.

Therefore fluorescence-activated cell sorting (FACS) could be utilized to sort RFP⁺ single cells into 96-well plates. For potential downstream mouse experiments it was ensured that the cells still carried the TGL plasmid by sorting for GFP⁺/RFP⁺ double positive cells (Figure 21A).

After optimization of the transfection the fraction of double positive cells was approximately 16% for OS-RC2 and approximately 12% for OS-LM1B cells (Figure 21B, C).

Even after extensive transfection optimization the RCC-MF cells were very stressed by the transfection and so the fraction of double positive cells was usually <0.5% (data not shown).

The sorted cells were kept in culture for 2-3 weeks and DNA of growing colonies was isolated. In general the OS-LM1B cells had a higher ability to survive the stresses imposed by transfection, cell sorting and growth in high cell dilution and were able to form more colonies.

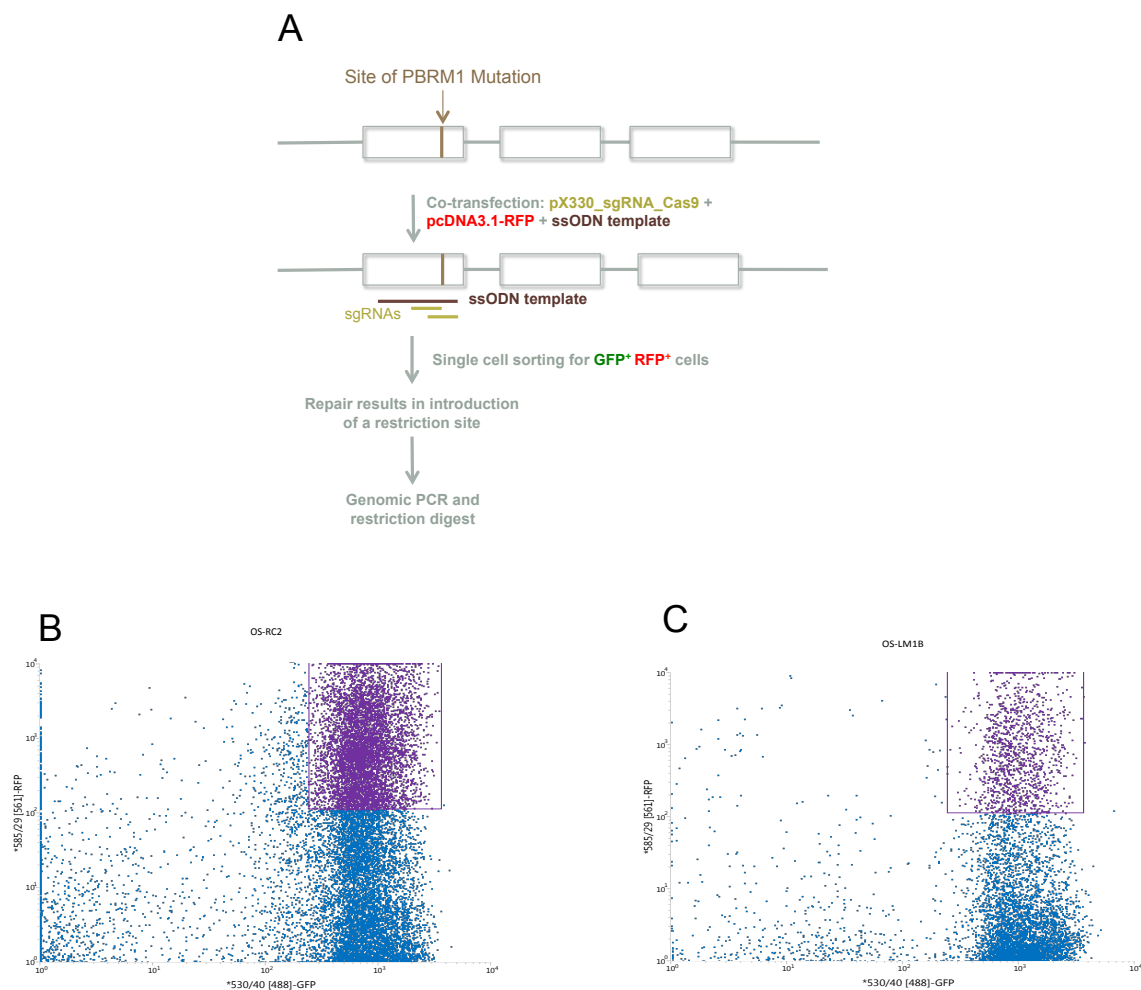


Figure 21 | Schematic of the workflow leading to CRISPR-Cas9 mediated repair of PBRM1 mutation and representative sorting for GFP⁺/RFP⁺ double positive OS-RC2 and OS-LM1B cells

A. The px330_sgRNA_Cas9 plasmid expresses the sgRNA and Cas9. Cas9 is guided to the target DNA by the sgRNA where it induces DSBs. If the DSBs are repaired using the ssODN template the PBRM1 mutation will be reverted to the WT sequence. The RFP expressed from pcDNA3.1- RFP is used as a marker indicating successful transfection for cell sorting. The growing colonies are screened by restriction digest for PBRM1 WT sequence. Representative gating for OS-RC2 (**B**) and OS-LM1B (**C**) GFP⁺ and RFP⁺ double positive cells. The gates were set using unstained and single positive GFP and RFP control cells.

Successful repair of the OS-RC2/OS-LM1B mutation would create a BsrDI restriction site at the PBRM1 Exon 6. Therefore screening of colonies could be achieved by PCR amplification of PBRM1 exon 6 and subsequent restriction digest of the PCR product. PCR amplification generated a 402 bp fragment, which could only be cut by BsrDI if the wild type sequence (CATTGC) but not the mutated sequence (CACTGC) was present, yielding in fragments of 268 bp and 134 bp.

A representative digestion from OS-RC2 and OS-LM1B cells is displayed in Figure 22A and B. All recovered OS-RC2 clones were mutant. As positive control 786-O PCR product was digested, which resulted in the expected fragments, although the digestion was not complete (Figure 22A).

The screened OS-LM1B clones were also all negative, apart from clone 25 which potentially could have been a heterozygote, carrying one mutant and one wild type PBRM1 copy. As positive control PCR from RCC-MF genomic DNA was used. Digestion resulted in the expected fragments but was not complete (Figure 22B).

The amplified PCR product of Clone 25 was further analysed by Sanger sequencing. Sanger sequencing was performed with the reverse primer of the PCR reaction. As previously mentioned, the OS-RC2/OS-LM1B cells contain a T>C mutation on PBRM1 position 698, but due to amplification with the reverse primer the complimentary bases A or G were to be expected. The position of the mutation was indicated by a red arrow in Figure 23A.

From Sanger sequencing it became clear that the OS-LM1B Clone 25 did not contain a wild type PBRM1 sequence. Yet between one of the three Guanines on positions 701-703 a one bp deletion had taken place in one allele, as a one bp shifted background sequence started from these positions (Figure 23A, indicated by the black arrow). In fact this position was 3 bp away from the PAM of one of the sgRNAs (Table 4, sg 1.1) used and thus exactly where a Cas9 directed DSB guided by sg 1.1 should take place (Figure 23B).

Of the few RCC-MF cells that were transfected even fewer survived the stress imposed by single cell sorting and were able to form a viable colony. Thus only one RCC-MF clone could be tested for a repaired PBRM1 gene, which was negative (data not shown).

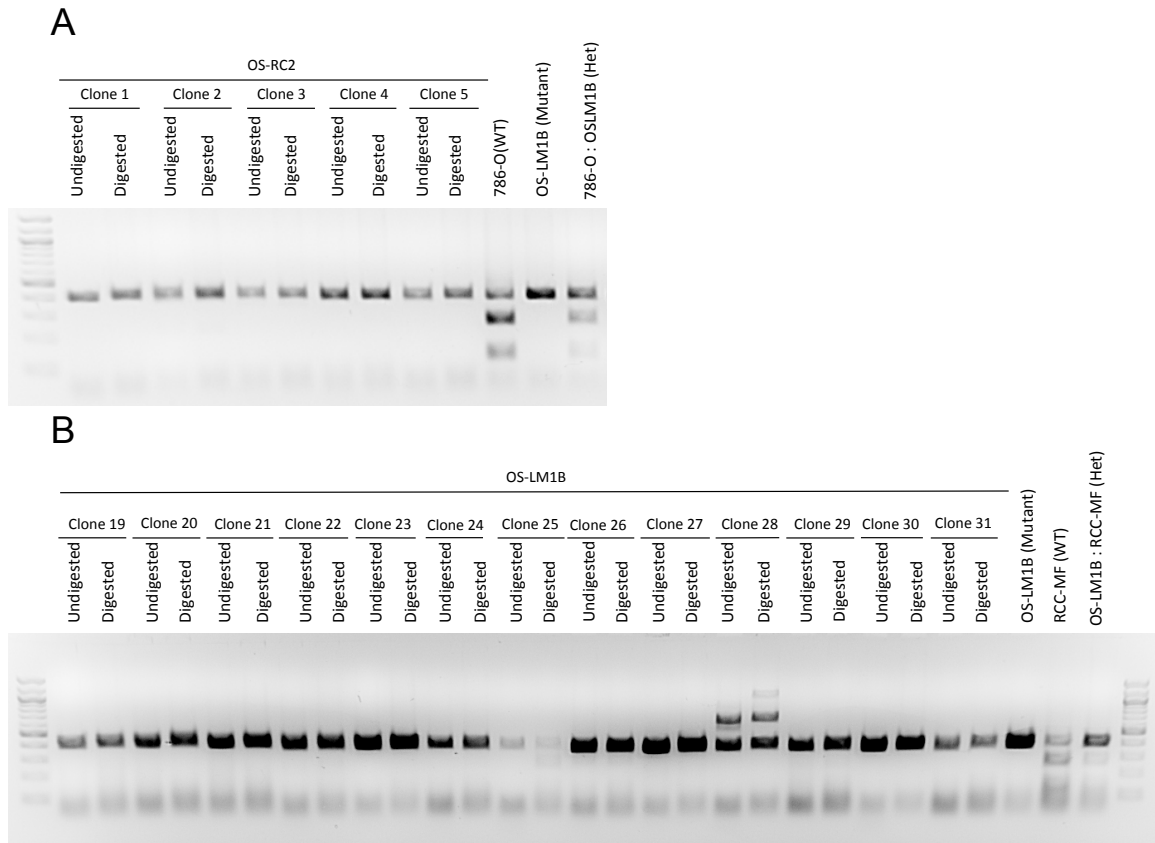


Figure 22 | CRISPR-Cas9 transfected OS-RC2 or OS-LM1B cells did not repair PBRM1 mutation

BsrDI restriction digest of PCR amplified region around PBRM1 Exon 6 in OS-RC2 (A) and OS-LM1B (B) cells. 786-O (A) or RCC-MF (B) cells were used as positive controls and OS-LM1B cells were used as negative control.

In total one RCC-MF, 33 OS-RC2 and 105 OS-LM1B clones were tested in several independent attempts but not one with a PBRM1 wild type locus could be found. However sequencing of OS-LM1B clone 25 suggested that DSBs had been induced at the correct position by the expressed Cas9 enzyme guided with sg 1.1. That by screening of >100 clones no PBRM1 WT clone could be found indicated that the efficiency of HDR was extremely low. Hence the experimental design had to be changed in a way that allowed high throughput screening of large cell numbers.

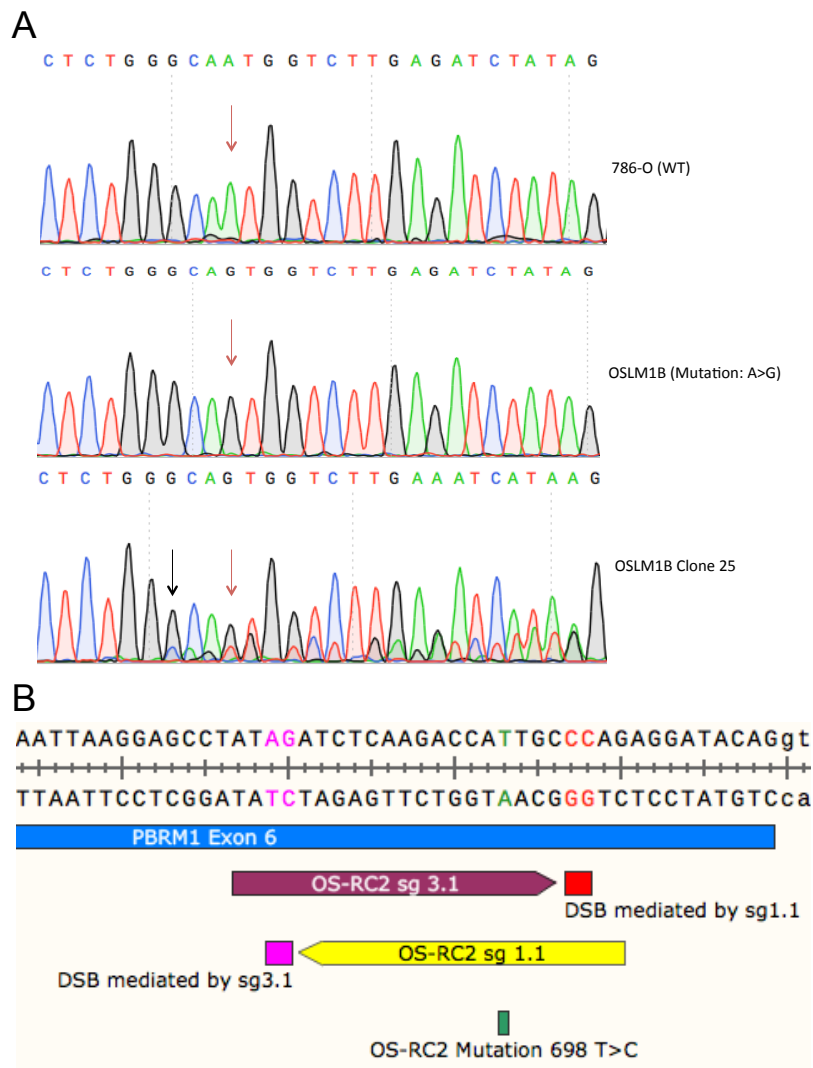


Figure 23 | The OS-LM1B Clone 25 contains the PBRM1 mutation

A. Sanger sequencing of the PBRM1 exon 6 from OS-LM1B Clone 25. 786-O and OS-LM1B DNA were used as a WT and mutant control respectively. The position of PBRM1 mutation is indicated by a red arrow. The black arrow indicates the start of a background sequence caused by a 1 bp deletion. **B.** Schematic indicating the position of Cas9 mediated DSBs in PBRM1 Exon 6 guided by sg 1.1 and sg 3.1.

2.3.2 Strategy 2 – Using HDR to repair small mutation and incorporate a Puromycin resistance gene

To achieve this it was decided on using plasmid DNA as a template rather than ssODN. The increase in template size facilitated flexibility in the experimental design, which allowed more freedom in the template design due to a size increase from ~100 bp of a ssODN to several kbp of the template plasmid.

The PBRM1 mutation of OS-RC2/OS-LM1B cells is in close proximity to the end of Exon 6 (Figure 23B). So a template plasmid was envisioned that would contain two long homology arms (>800 bp), with a Puromycin cassette inserted between the homology arms that allowed screening for Puromycin resistant cells. The Puromycin cassette was designed to be inserted 100 bp downstream of the end of Exon 6 to exclude disruption of potential splice sites (Figure 24). The Puromycin cassette was composed by a Puromycin resistance gene preceded by a phosphoglycerate kinase 1 (PGK) promoter and followed by a Woodchuck Hepatitis Virus Posttranscriptional Regulatory Element (WPRE), which is reported to enhance the stability of the Puromycin mRNA and protein yield [46]. The Puromycin cassette was furthermore flanked by LoxP sites, for the potential event that wild type PBRM1 expression would be disrupted by the presence of the Puromycin gene in the intronic region (Figure 24).

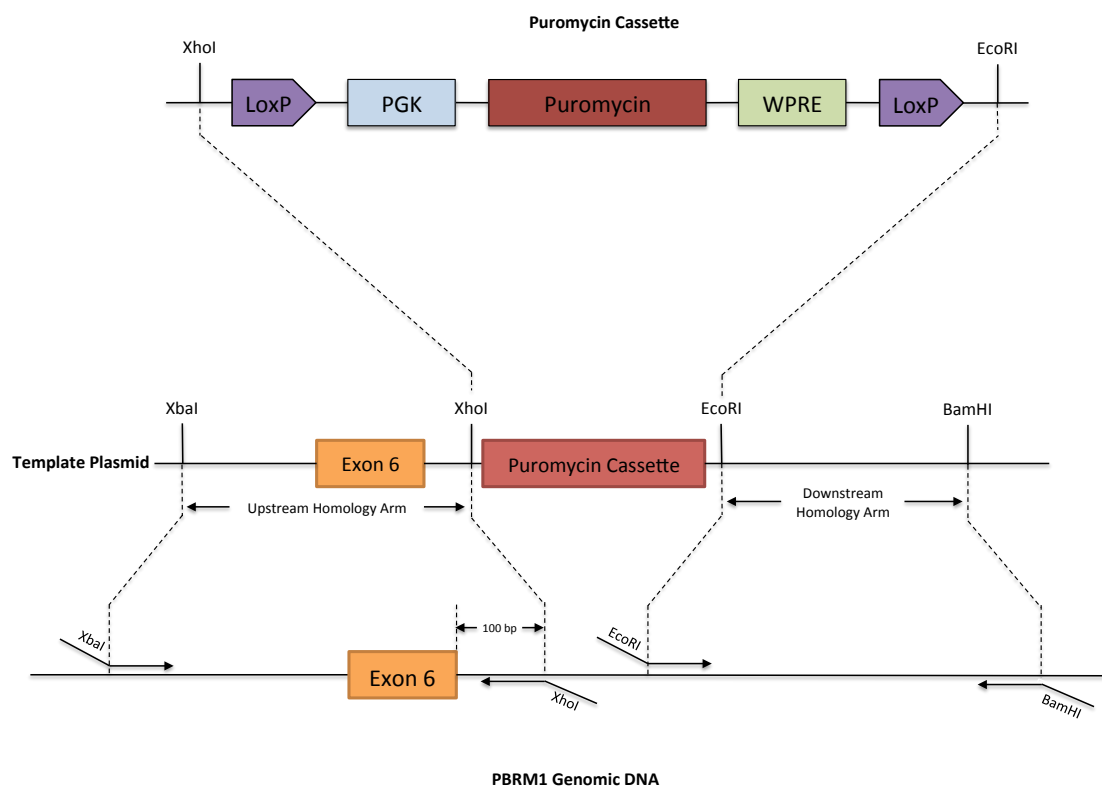


Figure 24 | Schematic of cloning the Puromycin cassette between the upstream and downstream homology arms

LoxP sites flank the Puromycin cassette composing of PGK promoter, the Puromycin resistance gene and the WPRE element. XhoI and EcoRI restriction sites are used to introduce the Puromycin cassette into the template plasmid. Upstream and Downstream Homology Arms are PCR amplified from 786-O genomic DNA and inserted by XbaI/XhoI (Upstream) and EcoRI/BamHI (Downstream) restriction sites introduced by the primer used in the PCR.

The Puromycin cassette combined with the homology arms resulted in a fragment of >3700 bp size. To keep the size of the final plasmid reasonably small it was decided on the pcDNA 3.1(-) vector as with around 5400 bp its length was already relatively short. As expression of the multiple cloning site (MCS) and a selection marker were not desired, the Cytomegalovirus (CMV) enhancer and promoter in front of the MCS, as well as the neomycin resistance with the according promoter were removed by restriction digest. The resulting vector, termed pcDNA-Template, had a size of ~3300 bp and contained only a MCS and an origin of replication plus ampicillin resistance important for replication and maintenance in *E.coli*.

The upstream homology arm, spanning from 5' to 3' of PBRM1 Exon 6, followed by the Puromycin cassette and the downstream homology arm were sequentially cloned into the MCS of the pcDNA-Template plasmid, using restriction sites that were introduced by PCR amplification at the end of each fragment (Figure 24).

Yet this template could potentially be recognized and bound by the sgRNAs, which would result in Cas9 mediated template digestion. Therefore it was necessary to introduce silent mutations in the sgRNA-binding region by site directed mutagenesis (SDM). Ideally these mutations were directed against the 5'- NGG -3' PAM of the sgRNAs, as the presence of this sequence is absolutely required for sgRNA binding [44]. Silent mutation of the PAM was only possible for the sg 1.1 where AGG was changed to AGA (Figure 25, brown arrow indicates G>A mutation). For sg 3.1 silent mutation at the PAM was impossible, therefore 2 other mutations were introduced between 8-14 bp from the 3' end of the sgRNA, as mismatches in this region are less tolerated than at the 5' end [44]. The introduced mutations were AAG to AAA (Figure 25, purple arrow indicates G>A mutation) and ACC to ACA (Figure 25, blue arrow indicates C>A mutation). These plasmids were termed sg 1.1/3.1 PBRM1 WT Template Plasmid.

On position 698, which is the position of OS-RC2 PBRM1 mutation, these templates contained the PBRM1 WT sequence. For comparison in downstream experiments, cells were required that had gone through the same

process of transfection, Cas9 expression and Puromycin selection but still contained the OS-RC2 PBRM1 mutation.

Taking this into consideration, alongside with the silent mutations to prevent sgRNA binding, the PBRM1 T>C mutation was introduced into the template vector as well and the resulting plasmids were termed sg 1.1/3.1 PBRM1 Mut Template Plasmid (Figure 25, red arrow indicates T>C mutation).

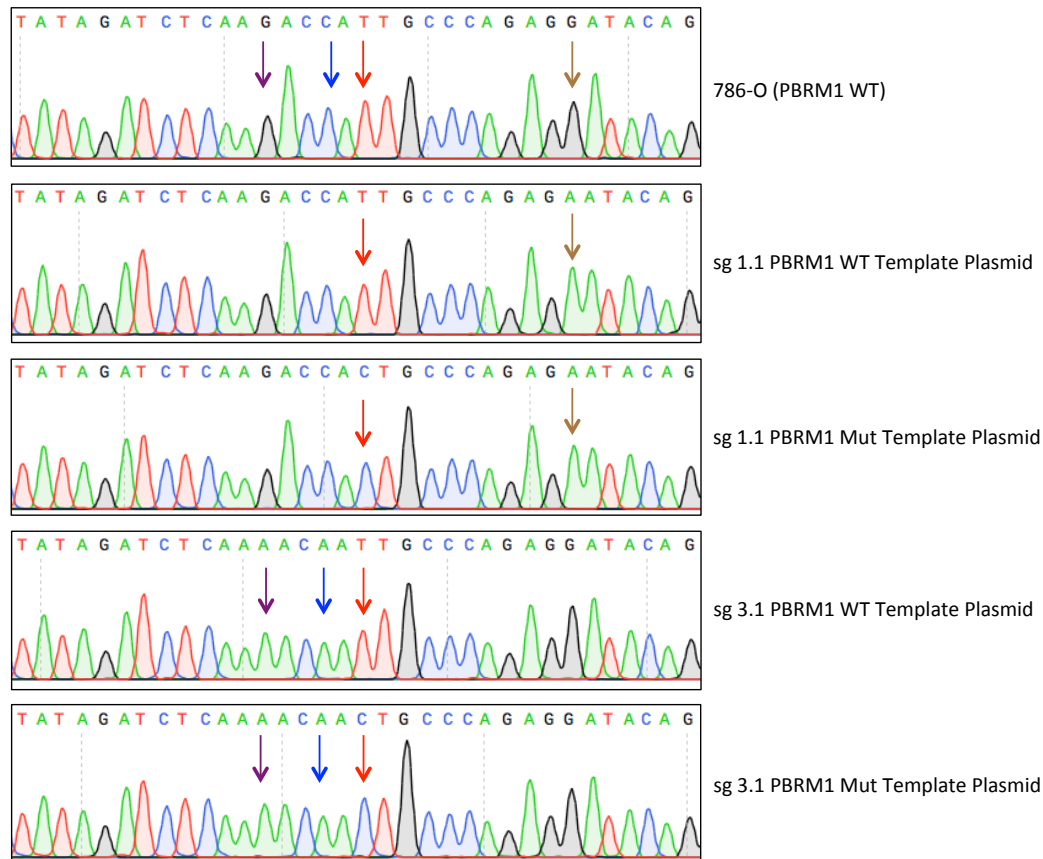


Figure 25 | PBRM1 locus modified by site directed mutagenesis to prevent sgRNA binding

Site directed mutation for sg 1.1 and sg 3.1 was confirmed by sequencing. The brown arrow indicates the position of the AGG to AGA mutation for sg 1.1. The purple arrow indicates the AAG to AAA mutation for sg 3.1. The blue arrow indicates the position of the ACC to ACA mutation for sg 3.1. The red arrow indicates the position of the PBRM1 mutation.

The px330_sgRNA_Cas9 plasmid, the template plasmid and the pcDNA3.1-RFP, as control for successful transfection, were co-transfected in OS-RC2 cells. After transfection cells were cultured in media containing 1 μ M Scr7. Scr7 is an inhibitor of the DNA ligase IV, which is a key enzyme in the NHEJ pathway. This was recently reported to dramatically increase the efficiency of HDR [48] [49].

To reduce selection for cells carrying only the transfected template plasmid with the Puromycin resistance, the cells were kept in exponential growth for 4 additional days before Puromycin selection was started, which was only survived by very few cells. After colonies emerged another round of Puromycin selection was used to kill cells that previously survived because of remaining template plasmid.

This ensured that a pool of cells was received that had integrated Puromycin in the genomic DNA. Yet this Puromycin resistance could also arise from random integration rather than from Cas9 mediated HDR and so the cell pool had to be screened.

Therefore genomic DNA of the cell pool was extracted and primer pairs were designed to screen the PBRM1 exon 6 locus for integration of the Puromycin cassette (Figure 26A). The Puromycin primer pair was designed to bind outside the upstream homology arm and within the Puromycin cassette, which effectively allows amplification only if the Puromycin cassette was integrated at the correct locus (expected fragment size: 1370 bp).

Even though several different PCR conditions were tested, only unspecific fragments were amplified, which was indicated by the presence of these fragments in the control PCR with 786-O DNA (Figure 26B).

This genomic PCR had the disadvantage that no positive control was available to optimize the conditions for amplification. The fact that unspecific fragments were amplified in each tested PCR condition indicated that the primer pair might not be optimal for genomic PCR

Thus the Exon 6 control primer pair was designed, which spanned the whole of Exon 6 and the Puromycin cassette, but was located within the homology arms. Amplification of Exon 6 without integrated Puromycin cassette would give rise to a 695 bp fragment, whereas the presence of the Puromycin cassette increased the fragment size to 2854 bp.

The genomic DNA was optimized with 786-O genomic DNA until it robustly produced the expected 695 bp fragment. Using genomic DNA from the cell pools primarily resulted in amplification of the 695 bp fragment. But in the pools derived from transfection with sg 1.1 PBRM1 Mut and WT template

plasmid and sg 3.1 PBRM1 Mut template plasmid, additionally a fragment with 2854 bp was amplified, which indicated the presence of the exon 6 with the Puromycin cassette (Figure 26C).

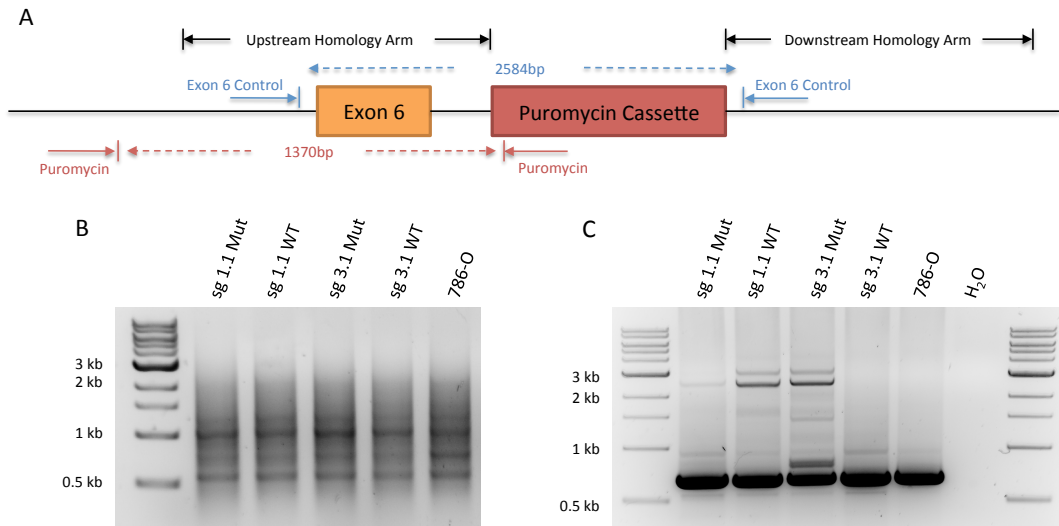


Figure 26 | Amplification of PBRM1 Exon 6 reveals no integrated Puromycin

A. Schematic displaying the binding sites of the Exon 6 and Puromycin control primer pairs
B. PCR with the Puromycin primer pair is not able to amplify the expected fragment (1370 bp)
C. PCR with the Exon 6 Control primer pair amplifies the Exon 6 locus without Puromycin (695 bp) and with Puromycin in between (2584 bp).

It is important to bear in mind that this fragment would also be amplified if the Puromycin cassette and parts of the homology arms were randomly integrated into the genomic DNA. These randomly integrated fragments are undistinguishable from correctly inserted fragments.

Nonetheless the 2584 bp fragments amplified from the 'OS-RC2 sg 1.1 PBRM1 WT pool' and 'OS-RC2 sg 3.1 PBRM1 Mut pool' samples were excised from the gel and analysed by Sanger sequencing to confirm the amplification of the Puromycin cassette.

The exon 6 sequence of the excised fragment from the 'OS-RC2 sg 1.1 PBRM1 WT pool' sample was identical with the sg 1.1 PBRM1 WT template plasmid sequence used in the transfection (Figure 27).

From this it could be concluded that the PBRM1 Exon 6 and the Puromycin cassette from the template had been integrated somewhere into the genome. But excitingly at the site of the PBRM1 mutation (Figure 27, red arrow) and at

the site of the silent mutation (Figure 27, brown arrow) there were background peaks indicating the presence of the original OS-RC2 sequence.

The same applied for the fragment excised from PCR amplification with the 'OS-RC2 sg 3.1 PBRM1 Mut Pool' sample, which contained the expected template plasmid sequence but at the sites of the silent mutations (Figure 27, purple and blue arrow) original OS-RC2 background peaks could be found.

The presence of the original OS-RC2 sequence, in a fragment that was excised at a fragment size that could only be achieved if Puromycin was inserted, indicated the existence of cells in the pool that used HDR to integrate the Puromycin cassette after exon 6 but did not exchange the sequence of exon 6 itself with the sequence presented on the template plasmid. If cells exist where this event was able to happen then it is very likely that also cells exist in the pool, which integrated the Puromycin cassette and exchanged the PBRM1 exon 6 with the template DNA.

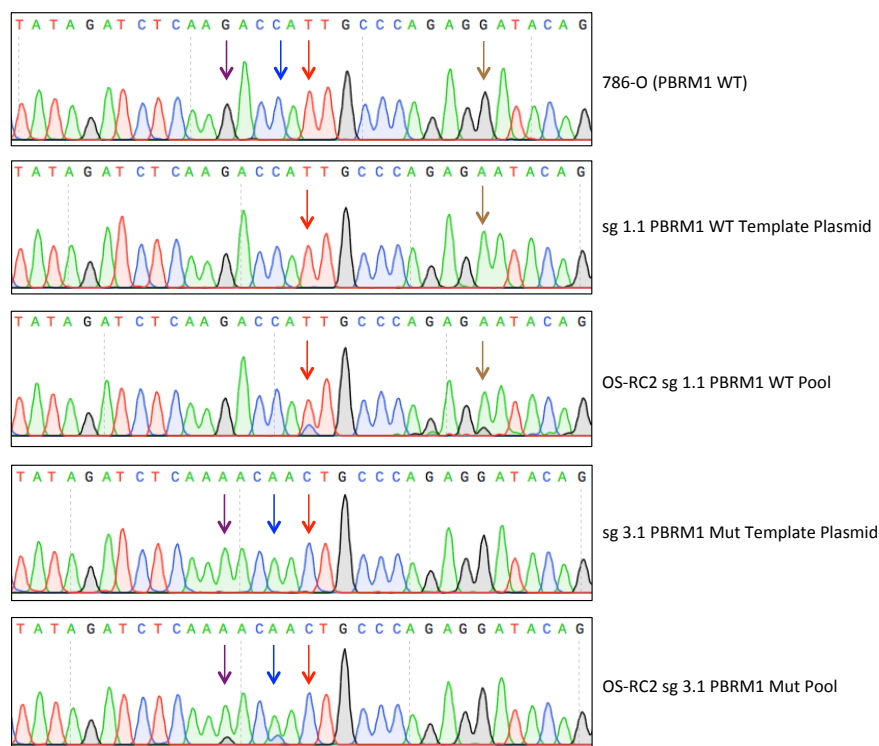


Figure 27 | Sequencing of amplified fragment reveals Puromycin integration at exon 6

The displayed sequences show the PBRM1 exon 6 around the region of the OS-RC2 PBRM1 mutation (red arrow). The silent mutation introduced into the sg 1.1 PBRM1 WT Template Plasmid is indicated by a brown arrow, whereas the silent mutations in the sg 3.1 PBRM1 Mut Template Plasmid are indicated by the purple and blue arrows. The 786-O and template plasmid sequences are used as references to which the sequences from the cell pools are compared.

2.4 Screen for components that are synthetic lethal with PBRM1

Synthetic lethality is defined as the principle that co-occurrence of two events leads to cellular or organismal death. This is mostly known in the context of two loss-of-function mutations, but can also take place due to the overexpression of genes or the action of chemical compounds [49].

Synthetic lethality is more and more recognized as a way to kill cancer cells, because in most cases they rely on very specific mutations, which often leads to secondary dependencies. As an example, ARID1A mutant tumour cells are entirely dependent on a WT ARID1B gene. ARID1A and B are core subunits of the BAF complex and loss of both impairs proliferation by destabilizing the SWI/SNF complex [17]. This indicates that complete loss of SWI/SNF complex function is lethal for cells. In line with this is the finding that SMARCA4 (BRG1) depleted cancer cells are very sensitive to loss of the second ATPase subunit SMARCA2 (BRM) [50].

PBRM1 is part of the multi-protein PBAF SWI/SNF complex and at some point in ccRCC formation its loss is advantageous for the tumour formation or progression as shown by mutation frequencies of up to 40% in ccRCC [10]. As explained above some subunits might have redundant functions to compensate for loss of one subunit. Therefore it was hypothesized that PBRM1 depletion might leave the tumour cells vulnerable to loss of another SWI/SNF complex subunit.

PBRM1 is mainly characterized by its 6 BDs that are important for binding of acetylated lysines. Apart from PBRM1 there are 45 other BD-containing proteins encoded in the human genome [34].

It is possible that depletion of one BD containing protein is accepted or even beneficial but the cancer cells do not tolerate loss of another.

The Polycomb repressive complex 2 (PRC2) catalyses trimethylation of histone H3 lysine 27 (H3K27me3) which mediates transcriptional repression.

Moreover it was reported that loss of function of PRC2 is responsible for an epigenetic switch from H3K27me3 to acetylation of H3K27 [51]. BDs can bind to acetylated H3K27 and with them transcriptional regulators are recruited [34]. Following these findings it was shown that malignant peripheral nerve sheath tumours, a type of tumour with frequent PRC2 inactivation, were sensitive to BD inhibitors [52].

Furthermore it is long known that the SWI/SNF complexes oppose genetic silencing by PRC 1 and 2. Therefore it was not surprising that loss of the SWI/SNF core subunit SNF5 enhances expression of PRC2 members, which results in transcriptional repression of PRC2 target genes. SNF5 loss leads to formation of aggressive cancers, which is completely prevented by PRC2 inactivation [53].

These findings point at a potential sensitivity to PRC2 knockdown in PBRM1 mutant context.

Therefore a screen was envisioned that aimed at finding synthetic lethal dependencies based on the hypotheses that PBRM1 loss conveys sensitivities to inactivation of BD-containing proteins, SWI/SNF complex or PRC members.

As best available model for PBRM1 presence and loss the OS-RC2 and RCC-MF cells with PBRM1 or Empty Vector were used and the hypotheses were tested by gene knockdown from a pool of shRNAs. For each of the 101 genes, 8 different shRNAs were designed following shRNA prediction rules (Table 8) [54].

As positive control the Replication Protein A was targeted. Its knockdown causes cell cycle arrest in dividing cells [55]. As negative control shRNAs targeting the Renilla Luciferase were used. Together with negative and positive control genes the pool was comprised of a total of 825 shRNA.

The shRNA pool was part of a bigger shRNA oligomer library with a size of 139 bp per fragment. From this shRNA library the desired shRNA subpool was amplified using PCR amplification. In this PCR the forward primer adds an XhoI restriction site to the shRNA oligomers resulting in a 158 bp fragment. A barcode at the reverse primer matching the barcode of the desired shRNA

subpool allowed to specifically amplify the desired shRNA library (Figure 28 A and B).

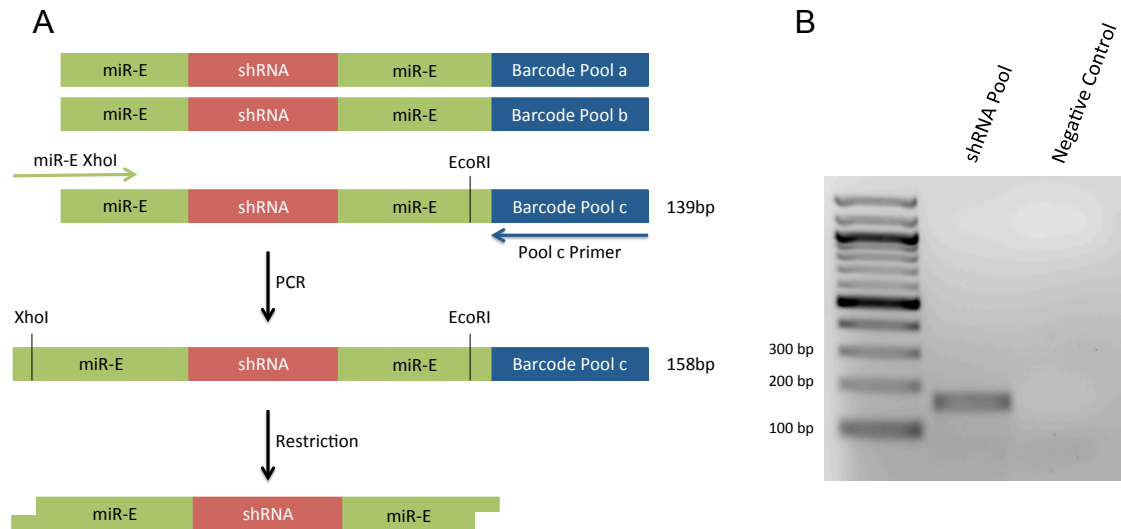


Figure 28 | Scheme of shRNA amplification and integration

A. Schematic showing the amplification of the 139bp shRNA subpool using a barcoded reverse primer. The resulting 158 bp fragment is then restricted with EcoRI and XhoI and thereafter ready for integration into the SREP plasmid **B.** The expected 158 bp fragment could be amplified from a pool of shRNA oligomers.

Utilizing the EcoRI and XhoI restriction sites the amplified shRNA backbones were cloned into the SREP plasmid (SREP is a derivative of the SGEP plasmid where GFP was substituted with dsRed). The plasmids were then transformed into *E.coli* via electroporation. After electroporation 1.08×10^6 colonies were obtained which was equivalent to a 1309-fold representation of each shRNA. From these colonies the plasmid pool was derived by maxipreparation, which was subsequently used for lentivirus production. The cloning of the shRNA plasmid library was performed in cooperation with Mercedes Vasquez from the Vanharanta Laboratory.

The OS-RC2 and RCC-MF PBRM1 and Empty Vector cells were infected with the lentivirus pool to integrate the shRNA into the genomic DNA. Once integrated, the spleen focus-forming virus (SFFV) promoter mediated constitutive expression of the dsRed fluorophore and the shRNA. To ensure that >80% of the infected cells only carried a single virus, infection at a Multiplicity of infection (MOI) of <0.43 was required. A MOI of <0.43 was equivalent to an infection efficiency of <35% positive cells (4.6.2.2). After

infection, cell sorting was used to collect all dsRed⁺ cells. All cell lines were infected at an infection efficiency of <35% which ensured that most infected cells only contained a single shRNA (Table 1).

Table 1 | Infection efficiencies and cells infected with a single virus

Cell Line	Infection efficiency [%]	Single infected cells [%]
OS-RC2 Empty Vector	19.84	89.35
OS-RC2 PBRM1	11.88	93.81
RCC-MF Empty Vector	32.43	81.68
RCC-MF PBRM1	29.72	83.40

After cell sorting each cell line was seeded into culture dishes into normal growth media or Dox containing media. It was taken care that throughout the screen a minimal 1000-fold representation of each shRNA was maintained. And thus each cell line and condition 3×10^6 cells were seeded and $>2 \times 10^6$ cells were stored as day 0 reference sample. The cells were kept in exponential growth phase for 11 days before genomic DNA was extracted. In this time the RCC-MF cells were able to go through ~5 population doublings. The OS-RC2 cells went through ~9 population doublings. This timespan was selected because strong synthetic lethal interactions will already be able to be picked up as 5 or 9 population doublings correspond to a 3- or 8-fold difference in shRNA representation if a shRNA slows down proliferation by 50% compared to a negative control shRNA (3.6.2.3).

PCR amplification was performed in 8 parallel PCR reactions from 16 μ g genomic DNA, which is equivalent to 2.6×10^6 cells [56]. The genomic PCR was able to amplify the expected 133 bp fragment in all cell lines and conditions as well as from the plasmid pool. Amplification from water controls was used to determine potential contamination (Figure 29A).

The 133 bp fragments were purified and Sanger sequencing was utilized to check if the correct locus was amplified. Thus it could be determined that in all cell lines grown with Dox a pool of shRNAs was amplified, which was

indicated by a highly variable sequence in the region of the shRNA antisense guide strand (Figure 29B).

Through the genomic PCR an index sequence was introduced in each sample and after quantification of the DNA concentration all samples were mixed equally and submitted for high throughput sequencing.

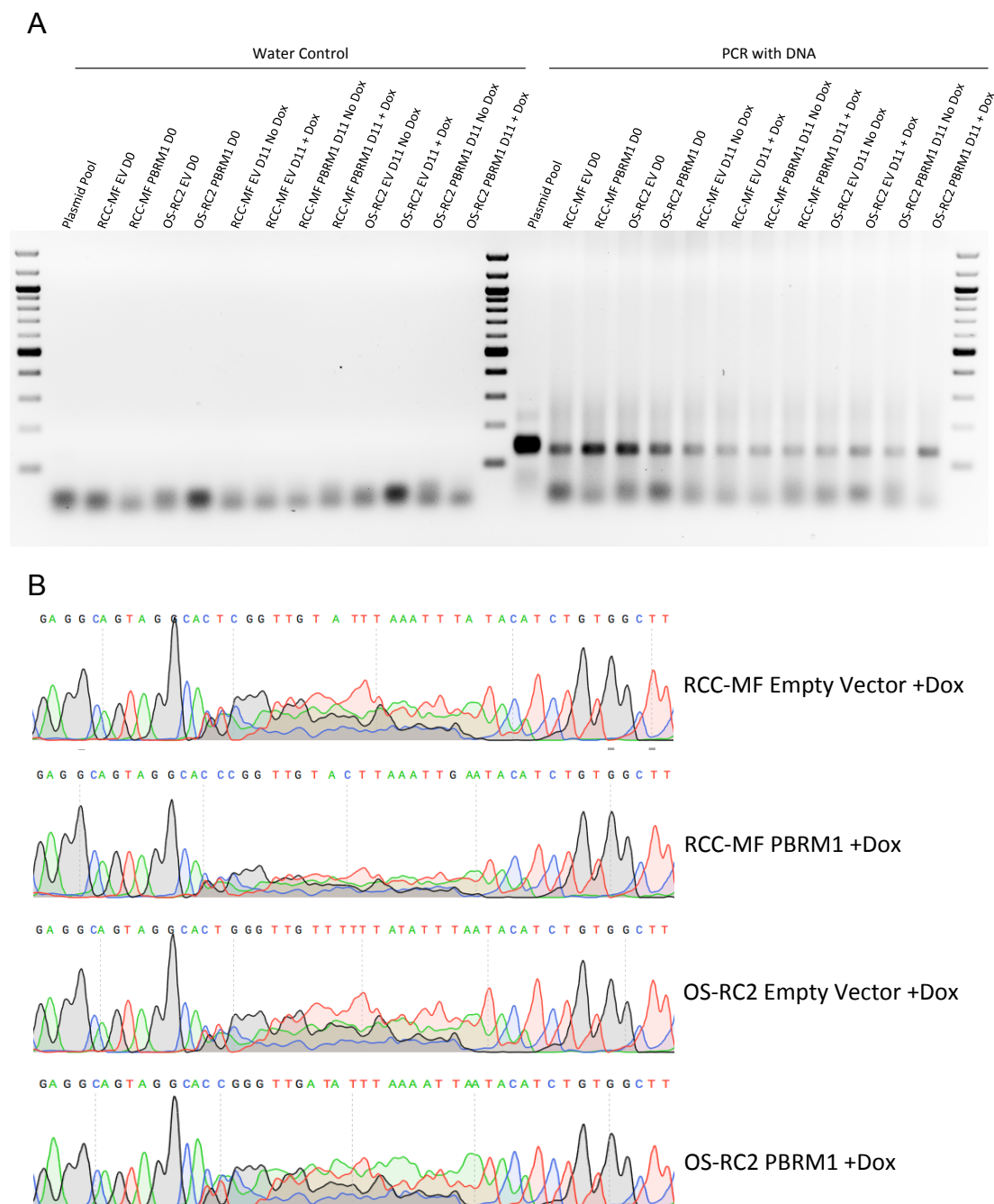


Figure 29 | Genomic PCR is able to amplify a pool of shRNA fragments.

A. Genomic PCR was able to amplify the expected 133 bp fragment in all samples and in the plasmid pool. Water controls were performed to detect potential contaminations **B.** Sanger sequencing of all +Dox samples confirmed that the amplified fragments still consisted of a pool of shRNA.

3. Discussion

ccRCC is a type of cancer that specifically requires mutation of genes located on the p-arm of chromosome 3, most dominantly VHL followed by PBRM1. Common mutations in other cancers like KRAS and TP53 are rare, which suggests that the alteration of specific pathways are required to enable tumour formation or progression in kidney cells [7]. Despite the high mutation rates, VHL inactivation is not sufficient to give rise to ccRCCs and thus a more thorough understanding of the ccRCC tumourigenesis is needed [28].

PBRM1 has recently been identified with a mutation rate of up to 40% in ccRCC, which makes understanding of its contribution to ccRCC tumourigenesis a desirable target. Published data, gained by transient PBRM1 knockdown in ccRCC cell lines, pinpoint at a strong tumoursuppressive role of PBRM1 in proliferation, migration and colony formation [10].

3.1 Tumour suppressive phenotype of PBRM1

Therefore a first attempt aimed at reproducing the published phenotype. Although a near complete knockdown could be achieved in the PBRM1 WT 786-O cell line, proliferation remained unchanged and so the published phenotype could not be reproduced (Figure 6 and 7).

It is likely that in ccRCC tumourigenesis, very specific pathways have to be affected. Therefore it was hypothesized that PBRM1 WT ccRCCs find another route to alter these, still unknown, pathways and are thus insensitive to PBRM1 knockdown. This would also present an explanation for the findings that PBRM1 knockdown is able to increase proliferation in other cancer types and human primary fibroblasts, as in those cells these pathways would not be affected [25]–[27].

Therefore the best possible model systems to study the tumour suppressive function of PBRM1 are mutant cell lines like the OS-RC2 and RCC-MF cells where PBRM1 expression can be induced.

PBRM1 mutation was indicated in causing late tumour stage, poor differentiation and lower overall survival [29] and therefore the effects of

PBRM1 expression were also studied in the metastatic OS-LM1B and RCC-MF LM1C cells.

RCC-MF and RCC-MF LM1C cells leaked low levels of PBRM1 even without addition of Dox, which is a common problem in Dox inducible systems (Figure 10). In OS-RC2 and OS-LM1B leakiness could not be detected but this could have been masked by the expression of mutant PBRM1 (Figure 9).

Subsequently it was considered to screen single cell clones for leakiness and continue working with non-leaking clones. Yet clones from the same cell population might exhibit different features like proliferation speed. This would effectively limit analysis to No Dox and +Dox conditions within the same clone but comparisons between different cell lines like PBRM1 and Empty Vector would be extremely difficult. This was unacceptable as Dox was shown to be able to affect proliferation in human cell lines and so an Empty Vector control is needed to control for effects solely caused by Dox. This is why work was continued using whole cell populations.

To test for functionality of the expressed PBRM1 its capability to immunoprecipitate with ARID2 was assessed. Both the OS-RC2 and RCC-MF cells were able to immunoprecipitate PBRM1 with ARID2 and vice versa (Figure 11 and 12). In OS-RC2 cells the mutant PBRM1 was also able to integrate into the PBAF complex, which was not unexpected as the mutation affects a BD and not the C-terminal end, which was shown to be responsible for incorporation into the SWI/SNF complex [37].

In general the complex formation seemed to be more efficient in OS-RC2 cells than in RCC-MF cells. Maybe the complete loss of PBRM1 destabilizes the PBAF complex and during tumour evolution the cancer cells loose the ability to efficiently assemble the SWI/SNF complex. This hypothesis could be tested by IP of another SWI/SNF complex member like BRG1 and western blotting for ARID2. If complex formation is disrupted the immunoprecipitation of these proteins should be severely impaired.

Nonetheless in both cell lines at least some expressed PBRM1 could be found in cooperation with the PBAF complex member ARID2, which was an indication that PBAF complexes containing WT PBRM1 were formed. So it

was concluded that those cell lines could be used to investigate a potential tumoursuppressive function of PBRM1.

Changes in proliferation due to PBRM1 knockdown were frequently reported and so the influence of PBRM1 expression on growth was first assessed. Neither the OS-RC2 or OS-LM1B nor the RCC-MF or RCC-MF LM1C altered their proliferation dependent on PBRM1 (Figure 13 and 14). The same finding held true when proliferation in different stress conditions was examined (Figures 15-17). These findings strongly indicated that the advantage of PBRM1 loss in ccRCCs was not mediated by elevated proliferation and so other avenues were explored.

The resistance to ROS and DNA damaging agents is an important feature of many cancer cells and the SWI/SNF complexes are potentially able to influence the expression of many genes. But in OS-RC2 and RCC-MF cells the resistance towards ROS induced by H₂O₂ and the DNA damaging agent Etoposide was not found to be mediated by PBRM1 (Figure 18 and 19)

The capability for anchorage independent colony formation is a well-established feature of cancer cells that increases with metastatic potential. Therefore it was not surprising that neither the parental OS-RC2 nor the RCC-MF cells were able to form colonies in soft agar.

In the metastatic OS-LM1B cells, PBRM1 expression significantly increased the ability to form colonies in soft agar by ~2-fold (Figure 20). This result directly contradicted published data acquired by transient PBRM1 knockdown in a ccRCC cell line [10].

Importantly this indicates that PBRM1 loss is not beneficial for the metastatic potential of kidney cancer cells, which suggests that the cancer cells accept a reduction in metastatic potential because they gain a bigger advantage at an earlier time-point in tumour formation. Therefore it could be hypothesized that PBRM1 loss is critical for emerging tumours and that PBRM1 plays a, yet unknown, role in tumour initiation and formation, rather than tumour progression. This is supported by a study showing that PBRM1 mutation occurs early in the phylogenetic trees of ccRCCs and in fact it is the only

mutation beside VHL that can already be present in the founding tumour cell [57]. Therefore next experiments should try to recapitulate the observed phenotype in RCC-MF LM1C cells and potentially also in a mouse experiment.

Moreover this result strongly indicated that the PBRM1 mutation of OS-RC2 and OS-LM1B cells interfered with PBRM1 WT function and that these cell lines can be treated as PBRM1 mutant cell lines regardless of the expressed mutated PBRM1.

Consistently all experiments failed to reproduce or directly opposed the published tumour suppressive phenotype of PBRM1. How PBRM1 mediates its tumour suppressive function in ccRCCs thus still remains an open question in the field.

This study indicates that PBRM1 might not be a classical tumour suppressor by direct suppression of tumour growth. Indeed its expression in metastatic cells even enhanced their ability to form colonies.

An alternative is that it administrates its tumour suppressive function by being a genetic caretaker. Mutation of genetic caretakers lead to genomic instability and this is driving tumour progression [58]. In favour of this speaks that PBRM1 is important for either establishment or maintenance of cohesion on centromeres and depletion leads to genomic instability by increasing aneuploidy [24]. Although PBRM1 expression did not change the response to DNA damage induced by Etoposide, it is well possible that mutation in a genetic caretaker does not change resistance to DNA damaging agents.

However a third option is that PBRM1 acts as an epigenetic caretaker and by its presence or absence in the SWI/SNF complex alters the expression levels of genes, in a number of pathways, which leads to tumour formation.

3.2 Repair of small PBRM1 mutation

To avoid selection of one out of several similar splice variants for expression, it would be better to be able to repair the PBRM1 mutations in the cell lines. To achieve this, components of the CRISPR-Cas9 system were co-transfected with a ssODN template. Single cell clones were tested for a

repaired PBRM1 mutation but no repaired PBRM1 mutation could be found in more than 100 OS-RC2 and OS-LM1B clones (Figure 22).

From this it was concluded that the repair of small mutations was a very inefficient process in these cell lines and a system was needed that allowed screening of large cell numbers.

Thus the ssODN template was changed with a plasmid template that contained an upstream homology arm, containing PBRM1 exon 6, followed by a Puromycin resistance cassette and a downstream homology arm. The template plasmids were modified at the site of OS-RC2 PBRM1 mutation to contain PBRM1 mutant or WT sequence and silent mutations were introduced, which prevent sgRNA binding and template digestion.

A screening PCR, designed to amplify only Puromycin integrated by HDR at the correct locus, produced only unspecific bands. Therefore another PCR was designed that could also amplify randomly integrated template plasmid. This PCR resulted in fragments that were due to their size thought to contain the Puromycin cassette (Figure 27).

Upon sequencing of these fragments the expected template sequences with all the introduced mutations were obtained.

Interestingly, background peaks at the positions of the inserted silence mutations could be observed and upon close examination those were identified as original OS-RC2 sequence. The presence of these sequence peaks followed by the Puromycin cassette was only possible if the Puromycin cassette was integrated behind exon 6 in OS-RC2 cells but exon 6 itself remained unchanged. Therefore it is highly likely that the OS-RC2 cell pool also contains cells where the respective genomic DNA was replaced by both the Puromycin cassette and the exon 6 from the template plasmid.

So in the next step these cell pools could be single cell sorted and the resulting single cell clones could be tested for correct integration of the Puromycin cassette and concurrent exchange of the PBRM1 Exon 6.

With these cells the IPs should be repeated to test for improved efficiency of PBAF complex formation as well as some of the tumoursuppressive assays to answer the question if cells expressing full WT PBRM1 would behave differently from the cells where the PBRM1 isoform 2 was expressed.

3.3 Synthetic Lethality

Synthetic lethality is more and more recognized as a possibility to selectively kill cancer cells and its relevance in the SWI/SNF complexes is underlined by several studies [17] [50]. Therefore the hypotheses were proposed that loss of PBRM1 and loss of another SWI/SNF complex member, another BD containing protein or PRC members could be synthetically lethal.

To test these hypotheses a knockdown screen was performed in OS-RC2 and RCC-MF cells. After 11 days of tissue culture, fragments containing a pool of shRNA could be amplified by genomic PCR, which were submitted to high throughput sequencing.

If a synthetic lethal interaction between PBRM1 and any of the screened genes would occur, depletion or strong reduction of the respective shRNAs from the shRNA pool would be expected in all cells without expression of a WT PBRM1. Not all of the 8 shRNA designed per gene will induce a good knockdown so it would not be unexpected if only some of those were to be depleted from the shRNA pool.

Moreover PBRM1 expression in the RCC-MF cells was displayed to be leaky even without addition of Dox. Therefore an intermediate shRNA reduction of the No Dox condition compared to Dox induced PBRM1 expression is to be expected in these cells.

In case such a gene could be identified the next steps would involve the individual knockdown with the most potent shRNAs and validation of the phenotype that mutation in PBRM1 and knockdown of the candidate gene leads to lethality or stalled proliferation, whereas the expression of WT PBRM1 enables survival and growth. If the gene could be validated the next step could involve subcutaneous injection into immunocompromised mice to assess if the observed phenotype has relevance in an *in vivo* model.

Of course it is also thinkable that some shRNAs get enriched in comparison with the control shRNA. This would happen if the knockdown of a gene leads to proliferative advantage in either PBRM1 presence or absence, which would

of course be of interest, as it could reveal something about the function of PBRM1 and affected pathways.

The ultimate goal of all cancer research is to specifically kill tumour cells but leave healthy cells untouched. If a synthetic lethal interaction with one of the screened genes could be found, inhibition of this gene would specifically target PBRM1 mutant cancer cells, but not healthy PBRM1 WT cells.

As PBRM1 is a mutation occurring early in the tumour evolution this could not only become a powerful weapon against a large fraction of primary ccRCCs but might also be able to tackle metastatic disease.

4. Materials and Methods

4.1 General methods

4.1.1 Polymerase chain reaction (PCR)

PCRs were performed on an Eppendorf Mastercycler. For PCR amplification the AccuPrime Pfx SuperMix (Life Technologies) was used and the elongation time was estimated as 1 minute per 1 kbp. The PCR mix was assembled according to the following:

15 μ l AccuPrime Pfx SuperMix
1 μ l Forward Primer (10 μ M)
1 μ l Reverse Primer (10 μ M)
5 ng Template DNA

For PCR amplification the following program was used:

95°C	5 min	x 35 cycles
95°C	15 sec	
AT°C	30 sec	
68°C	1 min/kb	
68°C	10 min	
10°C	Hold	

The annealing temperatures (AT) of the used primer pairs are indicated in table 2.

Table 2 | Primer sequences, annealing temperature and fragment sizes

Primer Name	Application	Forward Primer Sequence 5'-3'	Reverse Primer Sequence 5'-3'	AT [°C]	Fragment size
miRE-Xho_Fwd/ miRE_EcoOligo_Rev	Amplification of PBRM1 miR7 from pGIPZ_PBRM1_miR7	CTCGAGAAGGTATA TTGCTGTTGACAGT GAGCG	TCTCGAATTCTAGCC CCTTGAAGTCCGAG GCAGTAGGC	56	125 bp
PBRM1_Exon6_F/ R	Amplification of PBRM1 Exon 6 for CRISPR screening (OS-RC2/OS-LM1B)	TCCTAAGTCATGCT GTTGGATAGA	TGCTAATAACCCCTT ACAGAGACA	57.6	402 bp
pcDNA_MSC_NcoI _F2/R2	Amplification of MCS from pcDNA3.1(-)	ATGCCCATGGGAG ACCCAAGCTGGCT AGCGTT	ATGCCATATGAACTG ACACACATTCCACA GAA	63	868 bp
pcDNA_Amp_NdeI _F2/R2	Amplification of Ampicillin from pcDNA3.1(-)	ATGCCATATGTGCGA CCTCTAGCTAGAGC TTGG	ATGCCCATGGCGTA TATCTGGCCCGTAC ATCG	63	2417 bp
LT3GEP_Lox_Puro F2/R2	Addition of LoxP Sites to Puromycin amplified from LT3GEP	ATGCCTCGAGATAA CTTCGTATAATGTA TGCTATACGAAGTT ATTTGACGCGTAAT TCTACCGG	ATGCGAATTCATAAC TTCGTATAGCATAACA TTATACGAAGTTATG TCTCGACTGCAGAA TTAATTC	62	1920 bp
PB_Ex6_Up F2/R2	Amplification of PBRM1 Exon6 Upstream Homology from 786-O genomic DNA	ATCGTCTAGAAGAG TAGCTGGGACTATA GTTGTA	ATCGCTCGAGCCCC TTACAGAGACAAC TACTGCT	62.5	948 bp
PB_Ex6_Down F2/R2	Amplification of PBRM1 Exon6 Downstream Homology from 786-O genomic DNA	ATCGGAATTCACTG ATTGTAGCTTTGGA TTGCA	ATCGGGATCCACCT CTATGACTCTGCAAA GTAGT	62.5	895 bp
Mut_Primer_sg1.1_ F/R	SDM to introduce silent mutation for sg1.1	CAAGACCATTGCC AGAGAATACAGG	CCTGTATTCTCTGG GCAATGGTCTTG	58	7000 bp
Mut_Primer_sg3.1_ F/R	SDM to introduce silent mutation for sg3.1	CTCAAACAATTGC CCAGAGGATACAG	CTGTATCCTCTGGG CAATTGTTTTGAG	58	7000 bp
Mut_698T>C_sg1.1_ F/R	SDM to introduce silent mutation for sg1.1 and PBRM1 mutation	CAAGACCACTGCC CAGAGAATACAGG	CCTGTATTCTCTGG GCAGTGGTCTTG	58	7000 bp
Mut_698T>C_sg3.1_ F/R	SDM to introduce silent mutation for sg3.1 and PBRM1 mutation	CTCAAACAACTGC CCAGAGGATACAG	CTGTATCCTCTGGG CAGTTGTTTTGAG	58	7000 bp
BamHI_dsRed_F2/ EcoRI_dsRed_R	Addition of BamHI/EcoRI sites to dsRed amplified from LT3GEN	ATGCGGATCCGAG CTTGCGTTGGATCC AC	CTCGTTGGTCTTAAG CTCGT	60	826 bp
PBRM1_Exon6_fwd / PBRM1_Exon6_Con trol_Rev	Endogenous repair screen for insertion of Puromycin	TCCTAAGTCATGCT GTTGGATAGA	TCCTAAAGCTATTTG GAAGCAGAT	58	695 bp (no Puromycin) 2584 bp (Puromycin)
PBRM1_Ex6_Screen _PGK F/R	Endogenous repair screen for insertion of Puromycin	TCACTGCAACCTCC ATCTCCTG	ACCCGGTAGAATTA CGCGTCAA	64	1370 bp

4.1.2 Cloning

4.1.2.1 Restriction Digest

Restriction enzyme mediated digestion of DNA fragments or vector backbones was used for cloning steps. Purification of PCR amplified fragments was achieved with using the QIAquick PCR Purification Kit (QIAGEN). Restriction enzymes were purchased from New England Biolabs (NEB). Per μg of DNA 5 Units of restriction enzyme, the appropriate amount of 10X buffer and H_2O to fill up to a buffer concentration of 1X were used. The DNA fragments were digested for 1-2 h at the recommended temperature. After the digest the restriction enzymes were heat inactivated for 20 minutes at 65°C . The digested plasmid was treated with Antarctic Phosphatase (NEB) following the manufacturers instructions.

To separate undigested from digested fragments or digested fragments of different sizes, agarose gel electrophoresis was used. For DNA $>1\text{kbp}$ 1% agarose (w/v) and for fragments $<1\text{kbp}$ 2% agarose (w/v) respectively were dissolved in 1x TAE by boiling. After cooling down to approximately 60°C , ethidium bromide ($1\ \mu\text{g}/\text{ml}$) was added and the liquid was poured into a gel tray for polymerization. The DNA samples were mixed 5:1 with 6x TriTrack DNA Loading Dye (Thermo Scientific) and loaded onto the polymerized gel. According to the expected size ranges 200 ng of TriDye 100 bp DNA Ladder (NEB) or TriDye 1 kb DNA Ladder (NEB) were used as size markers. Gels were run in 1x TAE and DNA fragments were visualized and cut out using UV light. Gel purification of the DNA fragments was accomplished using the QIAquick Gel Extraction Kit (QIAGEN) following the manufacturers instructions.

1x TAE

40 mM Tris (pH 8.0)

20 mM Acetic Acid

1 mM EDTA

4.1.2.2 Ligation and transformation

For ligation 50 ng of vector backbone were mixed 1:3 with the insert DNA fragment. To the vector and insert 1/10 of 10X T4 DNA Ligase Buffer and 400 Units of T4 DNA Ligase (NEB) were added and filled up to a total volume of 10 µl with H₂O. Ligation was achieved through incubation at 16°C overnight or 1h at room temperature. The ligation mix was used to transform NEB 5-alpha Competent *E. coli* (High Efficiency) (NEB) following the manufacturers instructions. After transformation the bacteria were plated on LB Agar plates with Ampicillin (100 µg/ml) and grown overnight at 37°C. The following day colonies were picked and inoculated in LB Ampicillin (100 µg/ml) overnight.

4.1.3 Miniprep and maxiprep

For plasmid preparation 2 ml or 100-200ml overnight culture were used for a miniprep or a maxiprep respectively. The miniprep was performed using the QIAprep Spin Miniprep Kit (QIAGEN). The maxiprep was performed using the PureYield Plasmid Maxiprep System (Promega) following the manufacturers instructions.

4.1.4 Protein extraction

For protein extraction cells were harvested by trypsinization, pelleted at 200 g for 5 min and the cell pellet was washed with PBS followed by centrifugation. The cell pellet was either used directly for protein extraction or stored at -80°C until use.

One volume of cell pellet was resuspended in 3 volumes of RIPA Buffer (Sigma) completed with 1:100 Protease Inhibitor Cocktail (Sigma) and lysed under constant rotation for 45 min at 4°C. Subsequently samples were centrifuged at 21000 g for 20 min, 4°C. The supernatant was transferred to a new tube and the protein concentration was quantified using the Pierce BCA Protein Assay Kit (Thermo Scientific) following the manufacturer instructions. The samples were then either used directly in a western blot or stored at -80°C.

PBS

137 mM NaCl

2.7 mM KCl

10 mM Na₂HPO₄

2 mM KH₂PO₄

4.1.5 Western Blot

4.1.5.1 SDS-Page

For a western blot 40 µg protein were mixed with 4X Bolt LDS Sample Buffer (Life Technologies) and filled up with H₂O for a 1X Sample Buffer concentration. The samples were then boiled for 5 minutes at 95°C and loaded onto a Bolt 4-12% Bis-Tris Plus Gel (Life Technologies). Additionally 8 µl of Precision Plus Protein Kaleidoscope Standard (BioRad) were loaded as size indicator. For optimal protein separation 165 V were applied for 40 minutes in 1X Bolt MES SDS Running Buffer (Life Technologies).

4.1.5.2 Transfer

For the transfer the western blot sandwich had to be assembled in the Mini Blot Module (Life Technologies). All components were soaked in and the western blot tank was filled with 1X Bolt Transfer Buffer (Life Technologies). The proteins were transferred for 4h with a constant current of 200mA at room temperature. After the transfer the nitrocellulose membrane was stained with Ponceau S solution (Sigma), cut in slices according to the experimental design and destained with dH₂O

4.1.5.3 Antibody Binding

To prevent unspecific antibody binding the membrane was blocked using Odyssey Blocking Buffer (LI-COR) for 30 minutes at room temperature. The primary antibody was prepared in Odyssey Blocking Buffer as indicated in table 3 and incubated overnight at 4°C with constant mixing. The following day the membrane was washed 3 times for 10 minutes with PBS-T. The secondary antibody was prepared in Odyssey Blocking Buffer as indicated in table 3 and incubated with the membrane for 1h at room temperature with constant mixing. Thereafter the membranes were washed 3 times for 10

minutes with PBS-T again and then fluorescence was measured on a LI-COR Odyssey.

Table 3 | Primary and secondary antibodies

Primary Antibody	Dilution	Species	Distributor
PB1/BAF180	1:1000	Rabbit	Bethyl, A301-591
ARID2	1:500	Rabbit	Bethyl, A302-230A1
β -Actin	1:5000	Mouse	Sigma, A1978
Secondary Antibody	Dilution	Species	Distributor
Anti-Mouse IgG H&L (Alexa Fluor® 680)	1:10 000	Donkey	Abcam
Anti-Rabbit IgG H&L (Alexa Fluor® 790)	1:10 000	Donkey	Abcam

PBS-T

137 mM NaCl
 2.7 mM KCl
 10 mM Na₂HPO₄
 2 mM KH₂PO₄
 0.1% Tween-20 (v/v) (Sigma)

4.1.6 Cell culture

786-O, OS-RC2, OS-LM1B, RCC-MF and RCC-MF LM1C cells were cultured in RPMI-1640 with 10% FCS (Gibco), penicillin (100 U/ml, Sigma) and streptomycin (100 U/ml, Sigma) (Pen/Strep). HEK-293T cells were cultured in DMEM with 10% FCS, L-glutamine (2mM) and Pen/Strep. Cells were maintained at 37°C and 5% CO₂.

4.1.6.1 Passaging

When approaching confluency the cells were washed using PBS and detached from the culture plate using Trypsin-EDTA (0.05%, Sigma). After detaching Trypsin-EDTA was inactivated with media and the desired amount of cells was reseeded onto a fresh culture dish.

PBS

137 mM NaCl

2.7 mM KCl

10 mM Na₂HPO₄

2 mM KH₂PO₄

4.1.7 Lentiviral transduction

4.1.7.1 Lentivirus generation

For lentivirus generation 3×10^5 HEK 293T cells were seeded into one well of a 6-well plate the day prior to transfection. 10 μ l Lipofectamine 2000 (Life Technologies) were mixed with 160 μ l Optimem media (Life Technologies) and 1.5 μ g of the plasmid of interest was mixed with 0.5 μ g and 1.3 μ g of the packaging vectors pMD2.G and psPAX2 respectively in 160 μ l Optimem media. After a 5-minute incubation period these components were mixed drop-wise, gently flicked and incubated for 30 min at room temperature. Subsequently this mixture was added to the HEK-293T cells in 1 ml fresh media. Following an overnight incubation, the culture media was renewed and the virus supernatant was collected 48h – 72 h after the media change. The lentiviral supernatant was centrifuged at 200 g to pellet cellular debris and subsequently passed through a 45 μ m filter. The viral supernatant was then directly used for infection of target cells or stored at -80°C until use.

4.1.7.2 Infection of target cells

The day prior to infection, target cells were seeded at 70 – 80% confluency on a 6-well plate. Infection was achieved by adding lentivirus supernatant to media supplemented with 8 μ g/ml polybrene (Millipore) overnight respectively. The media was replaced in the morning of the next day to selection media. For selection, culture media was supplemented with 3 μ g/ml Puromycin or 800 μ g/ml G418 for OS-RC2 and OS-LM1B cells. RCC-MF cells were selected in 5 μ g/ml Puromycin or 800 μ g/ml G418 and 786-O cells were selected in 4 μ g/ml Puromycin. The selection was stopped when all cells on an uninfected control plate were dead.

4.2 Knockdown of PBRM1

For PBRM1 knockdown a previously tested PBRM1 targeting shRNA termed PBRM1 miR7 (Mature Antisense: TTAATTGAATTTGCATCCT) was amplified from the vector pGIPZ_PBRM1_miR7 and cloned into the LT3-GEPIR plasmid using EcoRI and XhoI restriction sites (4.1.2). A Renilla targeting shRNA was used as control. The LT3GEPIR vector was a kind gift of the Zuber Laboratory. From this plasmid a lentivirus was produced that was used to infect 786-O cells (4.1.7). Dox was added at the indicated concentrations for 6 days to induce shRNA expression.

4.3 PBRM1 expression and assays

4.3.1 PBRM1 expression

PBRM1 was cloned from the already available pLVX_PBRM1_Puro plasmid into pLVX_Tight_Puro purchased as part of the Lenti-XTM Tet-On® Advanced Inducible Expression System (Clontech) using EcoRI restriction (4.1.2).

To achieve Dox inducible expression of PBRM1, the OS-RC2, OS-LM1B, RCC-MF and RCC-MF LM1C cell lines were transduced with a lentivirus containing the pLVX-Tet-On-Advanced plasmid and selected with G418. These cells were subsequently transduced with pLVX-Tight-Puro PBRM1 or Empty Vector and selected with Puromycin (4.1.7).

4.3.2 Immunoprecipitation

The OS-RC2 PBRM1 and Empty Vector cells were cultured for 5 days with 50 ng/ml Dox and the RCC-MF PBRM1 and Empty vector cells were cultured for 5 days with 100 ng/ml Dox. The whole cell lysate was derived as described in 4.1.4, with the only exception that the protease inhibitor concentration was increased to 1:50.

To 2.3 mg (OS-RC2) or 1.8 mg (RCC-MF) whole cell lysate 5 µg PBRM1 antibody (Bethyl, A301-591A), 10 µg ARID2 antibody (Bethyl, A302-230 for OS-RC2 IP and A302-229 for RCC-MF IP) or 5 µg anti-IgG (Abcam, ab46540) were added. The cell lysate/antibody mixture was incubated overnight at 4°C. 0.25 mg Pierce Protein A/G Magnetic Beads per sample were washed twice

with IP Wash Buffer and then collected with a magnetic stand. The lysate/antibody mixture was added to the magnetic beads and incubated for 1 h at room temperature with constant rotation. Subsequently the beads were washed 3 times with IP Wash Buffer and once with purified water. Elution was achieved by incubating the beads for 10 minutes in 100 μ l 4X Bolt LDS Sample Buffer (Life Technologies) at room temperature with rotation. 30 μ l of the eluate and 50 μ g of the input sample were analysed in a western blot (4.1.5).

IP Wash Buffer:

1X TBS

0.5M NaCl

0.05% Tween- 20

4.3.3 In vitro proliferation assay

Exponentially growing cells were harvested by trypsinization and counted using the Vi-Cell XR cell viability analyser (Beckman Coulter). From these counts a 2000 cells/ml cell suspension was prepared and 200 cells were seeded into 96-well white assay plates with clear bottom (Tissue culture treated, Costar). Addition of the indicated Dox concentrations to the cell suspensions induced the expression or maintained the knockdown of PBRM1. The knockdown of PBRM1 was established by culturing the cells for 6 days with Dox prior to seeding.

At the indicated time points Cell Titer Glo Luminescent Cell Viability Assay (Promega) was used to determine the ATP concentration in each well, which was proportional to the cell number. A 1:1 mixture of the Cell Titer Glo Reagent with H₂O was used to lyse the cells. Subsequent steps were followed as indicated by the manufacturers instructions.

4.3.4 High cell dilution assay

The cell suspensions were prepared as described in 4.3.3 and 200 cells were seeded into each well of a 6-well plate. Dox was added at 25 ng/ml and refreshed every 3 days. After 9 days the culture media was removed and staining solution was added for 20 minutes. Thereafter, the staining solution

was removed and stained colonies were washed with dH₂O. The plates were air-dried and pictures of colonies were taken.

Staining solution:

0.05% Crystal Violet (w/v)
1% Formaldehyde (v/v)
PBS
1% Methanol (v/v)
H₂O up to 1L

PBS

137 mM NaCl
2.7 mM KCl
10 mM Na₂HPO₄
2 mM KH₂PO₄

4.3.5 Proliferation in stress conditions

The cells were seeded as described in 4.3.3, with the only difference that 400 cells were seeded per well of a 96-well plate. The media was aspirated the morning after seeding and replaced by stress media. To maintain the stress conditions throughout the experiment, the media was replaced every 2 days. The cell number was determined as described in 4.3.3.

<i>Low Serum</i>	RPMI, 1% FCS, L-glutamine (2 mM) and Pen/Strep
<i>Low Glucose</i>	DMEM (without any supplements), 2 mM L-Glutamine (Gibco), 1 mM D-Glucose (Life Technologies), 10% FCS and Pen/Strep
<i>Low pH</i>	RPMI, 10% FCS, L-glutamine (2 mM), Pen/Strep, pH=5.5 (adjusted with HCl)
<i>Low Glucose/pH</i>	Combination of low glucose and low pH

4.3.6 Cell survival

To assess cell survival with Etoposide and H₂O₂, a 2x10⁴ (OS-RC2) and 2.5x10⁴ (RCC-MF) cells/ml cell suspension was prepared as described in 4.3.3. From these cell suspensions 2000 (OS-RC2) or 2500 (RCC-MF) cells were seeded per 96-well plate with 25 ng/ml or without Dox. The day after

seeding the media was mixed 1:1 with media containing 2X the desired drug concentration. Cell viability was determined 3 days after the drug addition. To assess survival with H₂O₂, the OS-RC2 cells were treated with the following final concentrations: 0, 1, 5, 10, 15, 30, 60, 100, 300 and 600 μM H₂O₂ and the RCC-MF cells were treated with 0, 1, 12.5, 25, 50, 75, 100, 150, 300 and 600 μM H₂O₂.

To assess survival with Etoposide the OS-RC2 cells were treated with 0, 0.05, 0.5, 3, 5, 7, 10, 50, 100 and 250 μM Etoposide, whereas the RCC-MF cells were treated with 0, 0.1, 1, 5, 25, 50, 100, 250, 500 and 1000 μM Etoposide.

4.3.7 Soft agar assay

To plate the bottom agar layer a 1% noble agar was heated until it was completely dissolved. This was then cooled down to 42°C and mixed 1:1 with 2X culture media pre-warmed to 42°C to a final agar concentration of 0.5% and 1.5ml are pipetted in each well of a 6-well plate. The agar was cooled at room temperature until solidification had occurred. To plate the upper, cell containing, agar layer, 0.6% agar was heated until it dissolved and cooled down to 42°C. 3X RPMI media was heated to 42°C. The trypsinized and counted cells were pelleted at 180 g for 5 min and resuspended in the appropriate amount of 42°C 3X RPMI for a final concentration of 20 000 cells/ml. The 0.6% agar was mixed 2:1 with 3X RPMI media containing the cells to reach a final agar concentration of 0.4%. Subsequently 1.5ml of this mixture was plated in each well of a 6-well plate on top of the bottom agar layer. After agar hardening 400 μl 1X RPMI with 2 μg/ml or no Dox were added. Twice a week 100 μl 1X RPMI with 2 μg/ml or no Dox were added to prevent the agar from drying. After 30 days 200 μl 1 mg/ml Nitro Blue Tetrazolium chloride (Sigma) in PBS were added overnight to stain the colonies.

1% / 0.6% agar:

1 g / 0.6 g Noble Agar (Sigma, A5431)

Distilled H₂O to 100ml

Sterilization by Autoclaving

2X / 3X RPMI

2% / 3% RPMI Powder (Sigma) (w/v)
0.4% / 0.6% Sodium Bicarbonate (Sigma) (w/v)
20% / 30% (v/v) FCS
2% / 3% Pen/Strep (v/v)
2µg/ml / 3µg/ml Fungizone (Life Technologies)
Distilled H₂O to 100ml

PBS

137 mM NaCl
2.7 mM KCl
10 mM Na₂HPO₄
2 mM KH₂PO₄

4.4 Endogenous Reintroduction – Strategy 1

4.4.1 sgRNA design and cloning

The sgRNAs were designed using the CRISPR Design Tool and ordered as ssDNA oligonucleotides (Table 4). To achieve phosphorylation and annealing of the sgRNAs the following mixture was assembled, incubated for 30 min at 37°C and heat inactivated at 95°C for 5 min:

1 µl sgRNA top (100 µM)
1 µl sgRNA bottom (100 µM)
1 µl T4 ligation buffer (10X)
1 µl T4 Polynucleotide Kinase (NEB)
6 µl ddH₂O

After annealing the sgRNAs were cloned into the pX330-U6-Chimeric_BB-CBh-hSpCas9 using the BbsI restriction site followed by ligation and transformation (4.1.2.2). The pcDNA3.1-RFP vector was assembled by cloning RFP from the pTRIPZ-RFP into pcDNA3.1(-) vector using restriction digest with XbaI and XhoI (3.1.2).

Table 4 | sgRNA sequences

Name	Sequence
RCC-MF sg1	GTTCTTGAAGCTCGAGAGCC
RCC-MF sg3	GAAGCTCGAGAGCCAGGTTC
OS-RC2 sg1.1	ATCTCAAGACCACTGCCAG
OS-RC2 sg3.1	GCAGTGGTCTTGAGATCTAT

4.4.2 Transfection and cell sorting

For transfection, the pcDNA3.1-RFP and the px330-sgRNA plasmids were mixed with a molar ration of 1:2. 1 µg of plasmid DNA was co-transfected with 1 µl of ssODN template (10 µM) using Lipofectamine 2000. Per µg plasmid DNA 3 µl (OS-RC2/OS-LM1B) or 10 µl (RCC-MF) of Lipofectamine 2000 were used. Lipofectamine 2000 as well as plasmid DNA + ssODN were mixed with 160 µl Optimem per µg DNA and incubated 5 min at room temperature. Thereafter the DNA/Optimem mixture was added to the Lipofectamine/Optimem mixture and incubated another 30 min before it was added to 1.5×10^5 (OS-RC2/OS-LM1B) or 2×10^5 (RCC-MF) cells in a 6-well plate seeded the day before. The following day the Lipofectamine/DNA containing media was replaced by normal growth media and 48h post-transfection successfully transfected cells were sorted into 96-well plates due to GFP/RFP fluorescence (Table 5).

Table 5 | Specifications used for GFP/RFP sorting

Instrument: BD Influx Cell Sorter		
Laser Lines	488 nm	561 nm
Emission Filters	530/40	585/29
Fluorophore	GFP	RFP

4.4.3 Screening

The cells were grown in a 1:1 mix of fresh media with conditioned media until the colonies reached confluency. Then the cells were trypsinized and one half

was used for maintenance of the colony, whereas the other half of cells was lysed by boiling 10 min at 99°C. 3 µl of this boiled sample were used for genomic PCR as indicated in 3.1.1. Afterwards half of the PCR mix was directly used for restriction digest with BsRDI (OS-RC2/OS-LM1B) or NlaIII (RCC-MF). Subsequently the digested and the non-digested PCR mixes were analysed on a 2% agarose gel.

4.5 Endogenous Reintroduction – Strategy 2

4.5.1 Cloning of template plasmid

First the pcDNA_Template plasmid was assembled by PCR amplification of the MCS and the ampicillin resistance (4.1.1 and Table 2). Through PCR NdeI and NcoI restriction sites were added at the ends of the amplified DNA sequences, which were subsequently used for cloning (4.1.2). The PGK-Puromycin-WPRE sequence was PCR amplified from the LT3GEP plasmid with primer that introduced LoxP sites and XhoI and EcoRI restriction sites (4.1.1 and Table 2). The LT3GEP plasmid was a kind gift from the Zuber laboratory. The upstream and downstream homology arms were PCR amplified from 786-O genomic DNA. XbaI/XhoI (Upstream) and BamHI/EcoRI (Downstream) restriction sites were introduced via PCR (4.1.1 and Table 2). Using the restriction sites of the MCS both homology arms and the Puromycin resistance were sequentially cloned into the pcDNA_Template plasmid in the following order: 5'-Upstream-Puromycin-Downstream-3'.

4.5.2 Site directed mutagenesis

SDM was used to introduce specific mutations in the template plasmid. This was achieved by designing a reverse complement primer pair carrying the desired mutations. PCR amplification was followed by digestion of the methylated input plasmids (mediated by DpnI) and transformation (4.1.1, Table 2 and 4.1.2).

4.5.3 Transfection

6×10^5 OS-RC2 cells were seeded on a 15 cm dish 3 days prior to transfection. A total of 8 µg plasmid DNA were used for transfection. 95% of the total DNA consisted of a 1:1 (molar ratio) mixture of px330-sgRNA and repair template.

The remaining 5% consisted of pcDNA3.1-RFP. The transfection was executed as described in 4.4.2. The day after transfection, the media was replaced with media containing 1 μ M Scr7 (Selleckchem). 5 days after transfection the Puromycin selection (5 μ g/ml) was started and finished when all cells on a non-transfected control plate were dead. After formation of colonies the cells were selected for another 2 days with Puromycin (4 μ g/ml).

4.5.4 Genomic DNA extraction and PCR

After colonies grew out the cells were trypsinized and half of the cells were used to extract genomic DNA with the QIAamp DNA Mini Kit (QIAGEN) whereas the other half was used for maintenance.

From the extracted genomic DNA PCR was performed. After genomic PCR and analysis on an agarose gel the desired DNA fragments were excised and purified (4.1).

4.6 Synthetic Lethality Screen

4.6.1 shRNA plasmid library cloning

The shRNA oligomer library pool was ordered from Custom Array Inc. From this pool the subpool 7 was amplified using the mirE_XhoI_fwd 5'-CTCGAGAAGGTATATTGCTGTTGACAGTGAGCG -3' and Pool7_rev 5'-CTCAACTCTGTCTAAGGCACAGG -3' in 8 parallel PCR reaction as described in the following:

43 μ l AccuPrime Pfx SuperMix
4 μ l miRE_Xho_fwd (10 μ M)
2 μ l Pool7_rev (10 μ M)
7 pg Oligomer Library Pool

95°C	5 min	x 35 cycles
95°C	15 sec	
61°C	30 sec	
69°C	30 sec	
68°C	8 min	
10°C	Hold	

All PCRs were pooled and purified using the MinElute PCR Purification Kit (QIAGEN) following the manufacturers instructions. Elution from the columns was achieved with dH₂O incubation for 10 min.

For the assembly of the SREP vector, dsRed was amplified from the LT3REV vector using primer that added a BamHI restriction site during PCR amplification whereas the EcoRI restriction site was already available (4.1.1). The dsRed fragment and the SGEP vector were cloned using the BamHI and EcoRI restriction sites (4.1.2). LT3REV and SGEP were a kind gift of the Zuber laboratory.

The purified oligomers were cloned into the SREP plasmid using the EcoRI and XhoI restriction sites of the miRE backbone.

15 µl/5 µg	Purified Oligos/SREP
3.5 µl	EcoRI buffer
0.35 µl	BSA
40 Units	XhoI
100 Units	EcoRI
To 35 µl	H ₂ O

Digestion was performed for 4h at 37°C. This was followed by antarctic phosphatase treatment (NEB) following manufacturers instructions.

Thereafter the digested fragments were purified with the QIAquick Gel Extraction Kit (QIAGEN) following manufacturers instructions. Elution from the columns was achieved with dH₂O incubation for 10 min.

In each of 10 parallel ligation 300ng of digested SREP vector and 17ng of digested oligonucleotides, which corresponds to a molar ration of 1:4 respectively, were ligated with 1000 U of T4 DNA Ligase overnight at 16°C.

The parallel ligations were pooled and mixed 1:1 with Phenol (pH=8.0, Equilibrated; Affymetrix). This mixture was then loaded onto pre-spun phase lock tubes (Prime) and spun for 5 min at 16 000 g. The aqueous phase was transferred to a new tube and precipitated by adding 1/10 volume sodium acetate (3 M, pH=5.2) and 2.5 volumes 100% ethanol. Additionally 1 µl pellet paint (Novagen) was added. This was then precipitated at -80°C for 1h and spun at 16 000g for 30min at 4°C. The supernatant was aspirated, the DNA pellet was washed with 200 µl 70% Ethanol and pelleted at 16 000 g for 5 min

at 4°C. Thereafter the DNA pellet was air-dried and resuspended in 10 µl ddH₂O.

To transform the ligated plasmids 3 parallel electroporation with MegaX DH10B T1 Electrocomp *E.coli* (Invitrogen) were. The bacteria were thawed on ice and to 20 µl bacteria on 1 µl ligated plasmid was added. This was placed in a cold cuvette (Gene Pulser/Micro Pulser Electroporation Cuvettes, 0.1cm gap, Biorad) and electroporated (2kV, 200 Ω, 25 µF). Immediately afterwards 1ml recovery medium (Invitrogen) was added and the bacteria were incubated for 1h at 37°C with shaking. Then the bacteria were plated on dried LB Agar plates with Ampicillin (100 µg/ml) and grown overnight at 37°C. The colonies were scraped into 200 ml LB with ampicillin (100 µg/ml) and incubated at 37°C for 3h with shaking at 250 rpm. Thereafter the plasmids were maxiprepped (4.1.3).

4.6.2 shRNA library lentivirus generation and infection

4.6.2.1 Lentivirus generation

The generation of the lentivirus library was achieved by two parallel co-transfections of HEK 293T cells with the plasmid library, pPAX2 and pMD2.G. 15x10⁶ cells were seeded per 15cm dish and transfected as described in 4.4.2. All reagents were up-scaled by a factor of 16.6 to match the 15cm dishes.

4.6.2.2 Determination of the multiplicity of infection

1.5x10⁵ RCC-MF and OS-RC2 cells were seeded in wells of a 6-well plate the day prior to infection. To determine the MOI the cells were infected with 50, 25, 10, 5 and 1 µl of frozen virus supernatant media containing 8 µg/ml Polybrene. The media was exchanged the next morning and 48h later the fraction of cells expressing dsRed was determined in the flow cytometer (Table 6).

Table 6 | Specifications of the flow cytometer used for analysis of dsRed⁺ cells

Instrument: BD LSR Fortessa Analyser		
Laser Lines	640 nm	561 nm
Emission Filters	670/14	582/15
Fluorophore	Autofluorescence	dsRed

The following formulas enabled to calculate the MOI and the percentage of cells that were infected with a single virus from the infection efficiency:

$$m = -\ln(P(n > 0) - 1)$$

$$P(n) = \frac{m^n \times e^{-m}}{n!}$$

m...Multiplicity of Infection (MOI)

n...Number of virus that enter a cell

P(n>0)...Infection efficiency

P(n)...Probability that a cell is entered by n viruses

4.6.2.3 Infection and cultivation

The amount of virus supernatant needed to yield in 20% infection efficiency was up-scaled by a factor of 16.6 to fit for 15cm dishes. Infection was performed on 9 parallel 15 cm dishes seeded with 2.7x10⁶ OS-RC2 or RCC-MF PBRM1 and Empty Vector cells. 48h after media change the dsRed⁺ cells were sorted (Table 7).

Table 7 | Specifications of the cell sorter used to sort dsRed⁺ cells

Instrument: BD Influx Cell Sorter		
Laser Lines	405 nm	561 nm
Emission Filters	460/50	585/29
Fluorophore	Autofluorescence	RFP

After sorting 3x10⁶ cells were seeded with 100 ng/ml or without Dox. Additionally cell pellets stored at -80°C as Day 0 reference.

The cells were maintained in exponential growth for 11 days by splitting them 1:7 (OS-RC2) and 1:4 (RCC-MF) as soon as they were approaching confluency. This resulted in ~5 (RCC-MF) and ~9 (OS-RC2) population doublings.

Fold change in cell number (=shRNA representation) if a slower proliferation compared to a control shRNA is assumed:

$$\frac{y_c}{y_s} = \frac{P \times 2^{\frac{t}{T}}}{P \times 2^{\frac{t}{xT}}}$$

$$\frac{y_c}{y_s} = 2^{\left(\frac{t}{T} - \frac{t}{xT}\right)}$$

$$\frac{y_c}{y_s} = 2^{\left(\frac{xt-t}{xT}\right)}$$

$$\frac{y_c}{y_s} = 2^{\left(\frac{t}{T}\right)^{\frac{x-1}{x}}}$$

y_c ... Cell number control shRNA

y_s ... Cell number of growth slowing shRNA

P ... Cell number of starting population

t ... Total time in cell culture [h]

T ... Doubling time [h]

t/T ... Number of population doublings

x ... Factor by which the doubling time is increased

After the experiment was stopped the genomic DNA was extracted using the QIAamp DNA mini kit (QIAGEN) following the manufacturers instructions.

4.6.2.4 shRNA amplification

The shRNAs were PCR amplified using the P7_miRE_Fwd (5'-CAAGCAGAAGACGGCATACGAGATNNNNNNNTAGTGAAGCCACAGATGTA-3') and the P5_miRE_Rev (5'-AATGATACGGCGACCACCGAGATCTGAATTCTAGCCCCTTGAAGTC-3') primer pair. The P7_miRE_Fwd primer contains a variable index sequence indicated by N. For each sample 8 parallel PCRs were performed as indicated in the following:

5 μ l	10X PCR Buffer Gold
1 μ l	dNTP (10 mM each)
0.75 μ l	MgSO ₄ (100 mM)
3 μ l	Forward Primer (10 μ M)
3 μ l	Reverse Primer (10 μ M)
0.5 μ l	Amplitaq Gold

2 μ g	Genomic DNA
H ₂ O to 50 μ l	

95°C	10 min	
95°C	15 sec	x30 cycles
58°C	30 sec	
72°C	60 sec	
72°C	5 min	
10°C	Hold	

5 μ l of the PCR were checked on a 2% agarose gel and then the remaining parallel PCRs were pooled and precipitated as described in 3.6.1, with the only difference that the shRNA fragments were resuspended in 30 μ l dH₂O. The samples were run on a 2% agarose gel and the 133 bp band was cut out and purified with the QIAquick Gel Extraction Kit, following the manufacturers instructions.

The concentration of the gel purified DNA fragments was determined by quantification with the KAPA Library Quantification Kit Illumina Platforms (KAPA Biosystems). After quantification the shRNA samples were diluted to 20 nM and mixed in equal proportions. This was submitted for high throughput sequencing.

Table 8 | Genes used for the synthetic lethality screen

Bromodomain containing protein	Polycomb Repressive Complex	SWI/SNF Complex
ASH1L	EED	ACTB
ATAD2	EZH1	ACTL6A
ATAD2B	EZH2	ACTL6B
BAZ1A	SUZ12	ARID1A
BAZ1B	RBBP7	ARID1B
BAZ2A	RBBP4	ARID2
BAZ2B	BMI1	BCL11A
BPTF	PCGF2	BCL11B
BRD1	PCGF1	BCL7A
BRD2	RING1	BCL7B
BRD3	RNF2	BCL7C
BRD4	CBX2	DPF1
BRD7	CBX4	DPF2
BRD8	CBX6	DPF3
BRD9	CBX7	PHF10
BRDT	CBX8	SMARCB1
BRPF1	PHC1	SMARCC1
BRPF3	PHC2	SMARCC2
BRWD1	JARID2	SMARCD1
BRWD3	AEBP2	SMARCD2
CECR2	PHF1	SMARCD3
CREBBP	PHF2	SMARCE1
EP300	PHF3	SS18
KAT2A	PHC3	
KAT2B	RYBP	
KMT2A	TOP2A	
PBRM1	TOP2B	
PHIP	DNMT1	
SMARCA2	DNMT3A	
SMARCA4	DNMT3B	
SP100	DNMT3L	
SP110	MBD1	
SP140	MBD2	
SP140L	MBD3	
TAF1	MBD4	
TAF1L	MECP2	
TRIM24		
TRIM28		
TRIM33		
TRIM66		
ZMYND8		
ZMYND11		

5. References

- [1] D. Hanahan and R. a. Weinberg, "Hallmarks of cancer: The next generation," *Cell*, vol. 144, no. 5, pp. 646–674, 2011.
- [2] American Cancer Society, "Cancer Facts & Figures 2015," 2015.
- [3] S. R. Prasad, P. A. Humphrey, J. R. Catena, V. R. Narra, J. R. Srigley, A. D. Cortez, N. C. Dalrymple, and K. N. Chintapalli, "Common and uncommon histologic subtypes of renal cell carcinoma: imaging spectrum with pathologic correlation.," *Radiographics*, vol. 26, no. 6, pp. 1795–1806; discussion 1806–1810, 2006.
- [4] B. I. Rini, W. K. Rathmell, and P. Godley, "Renal cell carcinoma.," *Curr. Opin. Oncol.*, vol. 20, no. 3, pp. 300–306, 2008.
- [5] A. Kornakiewicz, W. Solarek, Z. F. Bielecka, F. Lian, C. Szczylik, and A. M. Czarnecka, "Mammalian Target of Rapamycin Inhibitors Resistance Mechanisms in Clear Cell Renal Cell Carcinoma," *Curr. Signal Transduct. Ther.*, vol. 8, pp. 210–218, 2013.
- [6] A. Schlesinger-Raab, U. Treiber, D. Zaak, D. Hölzel, and J. Engel, "Metastatic renal cell carcinoma: Results of a population-based study with 25 years follow-up," *Eur. J. Cancer*, vol. 44, no. 16, pp. 2485–2495, 2008.
- [7] E. Jonasch, P. A. Futreal, I. J. Davis, S. T. Bailey, W. Y. Kim, J. Brugarolas, A. J. Giaccia, G. Kurban, A. Pause, J. Frydman, A. J. Zurita, B. I. Rini, P. Sharma, M. B. Atkins, C. L. Walker, and W. K. Rathmell, "State of the Science: An Update on Renal Cell Carcinoma," *Mol. Cancer Res.*, vol. 10, no. 7, pp. 859–880, Jul. 2012.
- [8] Y. Sato, T. Yoshizato, Y. Shiraishi, S. Maekawa, Y. Okuno, T. Kamura, T. Shimamura, A. Sato-Otsubo, G. Nagae, H. Suzuki, Y. Nagata, K. Yoshida, A. Kon, Y. Suzuki, K. Chiba, H. Tanaka, A. Niida, A. Fujimoto, T. Tsunoda, T.

- Morikawa, D. Maeda, H. Kume, S. Sugano, M. Fukayama, H. Aburatani, M. Sanada, S. Miyano, Y. Homma, and S. Ogawa, "Integrated molecular analysis of clear-cell renal cell carcinoma," *Nat. Genet.*, vol. 45, no. 8, pp. 860–7, 2013.
- [9] P. R. Benusiglio, S. Couve, B. Gilbert-Dussardier, S. Deveaux, H. Le Jeune, M. Da Costa, G. Fromont, F. Memeteau, M. Yacoub, I. Coupier, D. Leroux, a. Mejean, B. Escudier, S. Giraud, a.-P. Gimenez-Roqueplo, C. Blondel, E. Frouin, B. T. Teh, S. Ferlicot, B. Bressac-de Paillerets, S. Richard, and S. Gad, "A germline mutation in PBRM1 predisposes to renal cell carcinoma," *J. Med. Genet.*, pp. 1–5, 2015.
- [10] I. Varela, P. Tarpey, K. Raine, D. Huang, C. K. Ong, P. Stephens, H. Davies, D. Jones, M. L. Lin, J. Teague, G. Bignell, A. Butler, J. Cho, G. L. Dalglish, D. Galappaththige, C. Greenman, C. Hardy, M. Jia, C. Latimer, K. W. Lau, J. Marshall, S. McLaren, A. Menzies, L. Mudie, L. Stebbings, D. a. Largaespada, L. F. Wessels, S. Richard, R. J. Kahnoski, J. Anema, D. a. Tuveson, P. a. Perez-Mancera, V. Mustonen, A. Fischer, D. J. Adams, A. Rust, W. Chan-On, C. Subimerb, K. Dykema, K. Furge, P. J. Campbell, B. T. Teh, M. R. Stratton, and P. a. Futreal, "Exome sequencing identifies frequent mutation of the SWI/SNF Complex Gene PBRM1 in renal carcinoma," *Nature*, vol. 469, pp. 539–542, Jan. 2011.
- [11] J. Brugarolas, "Molecular Genetics of Clear-Cell Renal Cell Carcinoma," *J. Clin. Oncol.*, vol. 32, no. 18, 2014.
- [12] S. Peña-Llopis, A. Christie, X. J. Xie, and J. Brugarolas, "Cooperation and antagonism among cancer genes: The renal cancer paradigm," *Cancer Res.*, vol. 73, no. 14, pp. 4173–4179, 2013.
- [13] L. Tang, E. Nogales, and C. Ciferri, "Structure and function of SWI/SNF chromatin remodeling complexes and mechanistic implications for transcription," *Prog. Biophys. Mol. Biol.*, vol. 102, no. 2–3, pp. 122–128, 2010.

- [14] J. Masliah-Planchon, I. Bièche, J.-M. Guinebretière, F. Bourdeaut, and O. Delattre, "SWI/SNF Chromatin Remodeling and Human Malignancies," *Annu. Rev. Pathol. Mech. Dis.*, vol. 10, no. 1, pp. 145–171, Jan. 2015.
- [15] J. Gao, B. A. Aksoy, U. Dogrusoz, G. Dresdner, B. Gross, S. O. Sumer, Y. Sun, A. Jacobsen, R. Sinha, E. Larsson, E. Cerami, C. Sander, and N. Schultz, "Integrative analysis of complex cancer genomics and clinical profiles using the cBioPortal," *Sci. Signal.*, vol. 6, no. 269, p. p11, 2013.
- [16] E. Cerami, J. Gao, U. Dogrusoz, B. E. Gross, S. O. Sumer, B. A. Aksoy, A. Jacobsen, C. J. Byrne, M. L. Heuer, E. Larsson, Y. Antipin, B. Reva, A. P. Goldberg, C. Sander, and N. Schultz, "The cBio Cancer Genomics Portal: An open platform for exploring multidimensional cancer genomics data," *Cancer Discov.*, vol. 2, no. 5, pp. 401–404, 2012.
- [17] K. C. Helming, X. Wang, B. G. Wilson, F. Vazquez, J. R. Haswell, H. E. Manchester, Y. Kim, G. V Kryukov, M. Ghandi, A. J. Aguirre, Z. Jagani, Z. Wang, L. a Garraway, W. C. Hahn, and C. W. M. Roberts, "ARID1B is a specific vulnerability in ARID1A-mutant cancers.," *Nat. Med.*, vol. 20, no. 3, pp. 251–4, Mar. 2014.
- [18] P. M. Brownlee, A. L. Chambers, A. W. Oliver, and J. a Downs, "Cancer and the bromodomains of BAF180.," *Biochem. Soc. Trans.*, vol. 40, no. 2, pp. 364–9, Apr. 2012.
- [19] M. Thompson, "Polybromo-1: the chromatin targeting subunit of the PBAF complex," *Biochimie*, vol. 91, no. 3, pp. 309–319, 2010.
- [20] M. Thompson and R. Chandrasekaran, "Thermodynamic analysis of acetylation-dependent Pb1 bromodomain-histone H3 interactions.," *Anal. Biochem.*, vol. 374, no. 2, pp. 304–12, Mar. 2008.
- [21] Z. Charlop-Powers, L. Zeng, Q. Zhang, and M.-M. Zhou, "Structural insights into selective histone H3 recognition by the human Polybromo bromodomain 2.," *Cell Res.*, vol. 20, no. 5, pp. 529–538, 2010.

- [22] A. P. VanDemark, M. M. Kasten, E. Ferris, A. Heroux, C. P. Hill, and B. R. Cairns, "Autoregulation of the Rsc4 Tandem Bromodomain by Gcn5 Acetylation," *Mol. Cell*, vol. 27, no. 5, pp. 817–828, 2007.
- [23] X. Huang, X. Gao, R. Diaz-Trelles, P. Ruiz-Lozano, and Z. Wang, "Coronary development is regulated by ATP-dependent SWI/SNF chromatin remodeling component BAF180," *Dev. Biol.*, vol. 319, pp. 258–266, 2008.
- [24] P. M. Brownlee, A. L. Chambers, R. Cloney, A. Bianchi, and J. a Downs, "BAF180 promotes cohesion and prevents genome instability and aneuploidy," *Cell Rep.*, vol. 6, no. 6, pp. 973–81, Mar. 2014.
- [25] W. Xia, S. Nagase, A. G. Montia, S. M. Kalachikov, M. Keniry, T. Su, L. Memeo, H. Hibshoosh, and R. Parsons, "BAF180 is a critical regulator of p21 induction and a tumor suppressor mutated in breast cancer.," *Cancer Res.*, vol. 68, no. 6, pp. 1667–74, Mar. 2008.
- [26] L. Huang, Y. Peng, G. Zhong, W. Xie, and W. Dong, "PBRM1 suppresses bladder cancer by cyclin B1 induced cell cycle arrest," 2015.
- [27] A. E. Burrows, A. Smogorzewska, and S. J. Elledge, "Polybromo-associated BRG1-associated factor components BRD7 and BAF180 are critical regulators of p53 required for induction of replicative senescence.," *Proc. Natl. Acad. Sci. U. S. A.*, vol. 107, no. 32, pp. 14280–5, Aug. 2010.
- [28] W. Y. Kim and W. G. Kaelin, "Role of VHL gene mutation in human cancer.," *J. Clin. Oncol.*, vol. 22, no. 24, pp. 4991–5004, 2004.
- [29] R. Pawłowski, S. M. Mühl, T. Sulser, W. Krek, H. Moch, and P. Schraml, "Loss of PBRM1 expression is associated with renal cell carcinoma progression.," *Int. J. Cancer*, vol. 132, no. 2, pp. E11–7, Jan. 2013.
- [30] S. J. Nam, C. Lee, J. H. Park, and K. C. Moon, "Decreased PBRM1 expression predicts unfavorable prognosis in patients with clear cell renal cell carcinoma," *Urol. Oncol. Semin. Orig. Investig.*, pp. 1–8, 2015.

- [31] C. Fellmann, T. Hoffmann, V. Sridhar, B. Hopfgartner, M. Muhar, M. Roth, D. Y. Lai, I. a M. Barbosa, J. S. Kwon, Y. Guan, N. Sinha, and J. Zuber, "An optimized microRNA backbone for effective single-copy RNAi," *Cell Rep.*, vol. 5, no. 6, pp. 1704–1713, Dec. 2013.
- [32] J. Zuber, K. McJunkin, C. Fellmann, L. E. Dow, M. J. Taylor, G. J. Hannon, and S. W. Lowe, "Toolkit for evaluating genes required for proliferation and survival using tetracycline-regulated RNAi," *Nat. Biotechnol.*, vol. 29, no. 1, pp. 79–83, 2011.
- [33] E. Ahler, W. J. Sullivan, A. Cass, D. Braas, A. G. York, S. J. Bensinger, T. G. Graeber, and H. R. Christofk, "Doxycycline alters metabolism and proliferation of human cell lines.," *PLoS One*, vol. 8, no. 5, p. e64561, Jan. 2013.
- [34] P. Filippakopoulos, S. Picaud, M. Mangos, T. Keates, J.-P. Lambert, D. Barsyte-Lovejoy, I. Felletar, R. Volkmer, S. Müller, T. Pawson, A.-C. Gingras, C. H. Arrowsmith, and S. Knapp, "Histone recognition and large-scale structural analysis of the human bromodomain family.," *Cell*, vol. 149, no. 1, pp. 214–31, Mar. 2012.
- [35] S. Vanharanta, W. Shu, F. Brenet, a A. Hakimi, A. Heguy, A. Viale, V. E. Reuter, J. J.-D. Hsieh, J. M. Scandura, and J. Massagué, "Epigenetic expansion of VHL-HIF signal output drives multiorgan metastasis in renal cancer.," *Nat. Med.*, vol. 19, no. 1, pp. 50–6, Jan. 2013.
- [36] G. Duns, R. M. W. Hofstra, J. G. Sietzema, H. Hollema, I. van Duivenbode, A. Kuik, C. Giezen, O. Jan, J. J. Bergsma, H. Bijnen, P. van der Vlies, E. van den Berg, and K. Kok, "Targeted exome sequencing in clear cell renal cell carcinoma tumors suggests aberrant chromatin regulation as a crucial step in ccRCC development.," *Hum. Mutat.*, vol. 33, no. 7, pp. 1059–62, Jul. 2012.
- [37] A. Niimi, S. R. Hopkins, J. a Downs, and C. Masutani, "The BAH domain of BAF180 is required for PCNA ubiquitination," *Mutat. Res. Mol. Mech. Mutagen.*, vol. 779, pp. 16–23, 2015.

- [38] K. Birsoy, R. Possemato, F. K. Lorbeer, E. C. Bayraktar, P. Thiru, B. Yucel, T. Wang, W. W. Chen, C. B. Clish, and D. M. Sabatini, "Metabolic determinants of cancer cell sensitivity to glucose limitation and biguanides.," *Nature*, vol. 508, no. 7494, pp. 108–12, 2014.
- [39] H. J. Park, J. C. Lyons, T. Ohtsubo, and C. W. Song, "Acidic environment causes apoptosis by increasing caspase activity.," *Br. J. Cancer*, vol. 80, no. 12, pp. 1892–1897, 1999.
- [40] G. Waris and H. Ahsan, "Reactive oxygen species: role in the development of cancer and various chronic conditions.," *J. Carcinog.*, vol. 5, p. 14, 2006.
- [41] Y. Pommier, E. Leo, H. Zhang, and C. Marchand, "DNA topoisomerases and their poisoning by anticancer and antibacterial drugs," *Chem. Biol.*, vol. 17, no. 5, pp. 421–433, 2010.
- [42] E. C. Dykhuizen, D. C. Hargreaves, E. L. Miller, K. Cui, A. Korshunov, M. Kool, S. Pfister, Y.-J. Cho, K. Zhao, and G. R. Crabtree, "BAF complexes facilitate decatenation of DNA by topoisomerase II α .," *Nature*, vol. 497, no. 7451, pp. 624–7, 2013.
- [43] M. a Cifone and I. J. Fidler, "Correlation of patterns of anchorage-independent growth with in vivo behavior of cells from a murine fibrosarcoma.," *Proc. Natl. Acad. Sci. U. S. A.*, vol. 77, no. 2, pp. 1039–1043, 1980.
- [44] F. Ran, P. Hsu, J. Wright, V. Agarwala, D. Scott, and F. Zhang, "Genome engineering using the CRISPR-Cas9 system.," *Nat. Protoc.*, vol. 8, no. 11, pp. 2281–2308, Nov. 2013.
- [45] L. Cong, F. A. Ran, D. Cox, S. Lin, R. Barretto, N. Habib, P. D. Hsu, X. Wu, W. Jiang, L. A. Marraffini, and F. Zhang, "Multiplex Genome Engineering Using CRISPR/Cas Systems," *Science (80-.)*, vol. 339, no. 6121, pp. 819–823, Feb. 2013.

- [46] J. E. Donello, J. E. Loeb, and T. J. Hope, "Woodchuck hepatitis virus contains a tripartite posttranscriptional regulatory element," *J. Virol.*, vol. 72, no. 6, pp. 5085–5092, 1998.
- [47] V. T. Chu, T. Weber, B. Wefers, W. Wurst, S. Sander, K. Rajewsky, and R. Kühn, "Increasing the efficiency of homology-directed repair for CRISPR-Cas9-induced precise gene editing in mammalian cells," *Nat. Biotechnol.*, vol. 33, no. 5, 2015.
- [48] T. Maruyama, S. K. Dougan, M. C. Truttmann, A. M. Bilate, J. R. Ingram, and H. L. Ploegh, "Increasing the efficiency of precise genome editing with CRISPR-Cas9 by inhibition of nonhomologous end joining," *Nat. Biotechnol.*, vol. 33, no. 5, pp. 538–542, Mar. 2015.
- [49] S. M. B. Nijman, "Synthetic lethality: General principles, utility and detection using genetic screens in human cells," *FEBS Lett.*, vol. 585, no. 1, pp. 1–6, 2011.
- [50] G. R. Hoffman, R. Rahal, F. Buxton, K. Xiang, G. McAllister, E. Frias, L. Bagdasarian, J. Huber, A. Lindeman, D. Chen, R. Romero, N. Ramadan, T. Phadke, K. Haas, M. Jaskelioff, B. G. Wilson, M. J. Meyer, V. Saenz-Vash, H. Zhai, V. E. Myer, J. a Porter, N. Keen, M. E. McLaughlin, C. Mickanin, C. W. M. Roberts, F. Stegmeier, and Z. Jagani, "Functional epigenetics approach identifies BRM/SMARCA2 as a critical synthetic lethal target in BRG1-deficient cancers," *Proc. Natl. Acad. Sci. U. S. A.*, vol. 111, no. 8, pp. 3128–33, 2014.
- [51] D. Pasini, M. Malatesta, H. R. Jung, J. Walfridsson, A. Willer, L. Olsson, J. Skotte, A. Wutz, B. Porse, O. N. Jensen, and K. Helin, "Characterization of an antagonistic switch between histone H3 lysine 27 methylation and acetylation in the transcriptional regulation of Polycomb group target genes," *Nucleic Acids Res.*, vol. 38, no. 15, pp. 4958–4969, 2010.
- [52] T. De Raedt, E. Beert, E. Pasmant, A. Luscan, H. Brems, N. Ortonne, K. Helin, J. L. Hornick, V. Mautner, H. Kehrer-Sawatzki, W. Clapp, J. Bradner, M.

- Vidaud, M. Upadhyaya, E. Legius, and K. Cichowski, "PRC2 loss amplifies Ras-driven transcription and confers sensitivity to BRD4-based therapies," *Nature*, vol. 514, no. 7521, pp. 247–251, 2014.
- [53] B. G. Wilson, X. Wang, X. Shen, E. S. McKenna, M. E. Lemieux, Y. J. Cho, E. C. Koellhoffer, S. L. Pomeroy, S. H. Orkin, and C. W. M. Roberts, "Epigenetic antagonism between polycomb and SWI/SNF complexes during oncogenic transformation," *Cancer Cell*, vol. 18, no. 4, pp. 316–328, 2010.
- [54] C. Fellmann, J. Zuber, K. McJunkin, K. Chang, C. D. Malone, R. a. Dickins, Q. Xu, M. O. Hengartner, S. J. Elledge, G. J. Hannon, and S. W. Lowe, "Functional Identification of Optimized RNAi Triggers Using a Massively Parallel Sensor Assay," *Mol. Cell*, vol. 41, no. 6, pp. 733–746, 2011.
- [55] M. S. Wold, "Replication protein A: a heterotrimeric, single-stranded DNA-binding protein required for eukaryotic DNA metabolism.," *Annu. Rev. Biochem.*, vol. 66, pp. 61–92, 1997.
- [56] D. Sims, A. Mendes-Pereira, J. Frankum, D. Burgess, M. Cerone, C. Lombardelli, C. Mitsopoulos, J. Hakas, N. Murugaesu, C. Isacke, K. Fenwick, I. Assiotis, I. Kozarewa, M. Zvelebil, a Ashworth, and C. Lord, "High-throughput RNA interference screening using pooled shRNA libraries and next generation sequencing," *Genome Biol.*, vol. 12, no. 10, p. R104, 2011.
- [57] M. Gerlinger, S. Horswell, J. Larkin, A. J. Rowan, M. P. Salm, I. Varela, R. Fisher, N. McGranahan, N. Matthews, C. R. Santos, P. Martinez, B. Phillimore, S. Begum, A. Rabinowitz, B. Spencer-Dene, S. Gulati, P. a Bates, G. Stamp, L. Pickering, M. Gore, D. L. Nicol, S. Hazell, P. A. Futreal, A. Stewart, and C. Swanton, "Genomic architecture and evolution of clear cell renal cell carcinomas defined by multiregion sequencing.," *Nat. Genet.*, vol. 46, no. 3, pp. 225–33, Mar. 2014.
- [58] K. W. Kinzler and B. Vogelstein, "Landscaping the Cancer Terrain," *Sci.*, vol. 280, no. 5366, pp. 1036–1037, May 1998.

6. Internet References

(1) <https://cansar.icr.ac.uk/cansar/cell-lines/OS-RC-2/mutations/>

(2) www.uniprot.org/uniprot/Q86U86

7. Appendix

7.1 Zusammenfassung

Klarzellkarzinom ist ein eine Tumorart, die spezifische Mutationen von Genen benötigt, die alle am 3p Chromosom lokalisiert sind. Am dominantesten ist die Mutation von VHL, doch trotz der hohen Mutationsrate ist der Verlust von VHL nicht genug um Klarzellkarzinom auszulösen. Deshalb wird ein tieferes Verständnis der Tumorbildung dringend benötigt. PBRM1 ist mit 40% das Gen mit der zweithöchsten Mutationsrate in Klarzellkarzinomen. Bereits veröffentlichte Arbeiten, die durch transienten PBRM1 knockdown in Klarzellkarzinomzelllinien generiert wurden, deuten auf eine starke tumorsuppressive Wirkung des Verlusts von PBRM1 hin. Jedoch hatte die Expression von PBRM1 in Zelllinien die eine PBRM1 Mutation tragen weder eine Wirkung auf normales Wachstum noch auf Wachstum in Stresssituationen. Außerdem konnte PBRM1 Expression die Resistenz zu reaktiven Sauerstoffmolekülen und induzierten DNA Schaden nicht erhöhen. Die Kapazität metastatischer Zellen Kolonien in Weichagar zu bilden erhöhte sich durch Expression von PBRM1 sogar, was im Gegensatz zu bereits publizierten Daten steht.

Weiters wurde das CRISPR-Cas9 System verwendet um die PBRM1 Mutation in den OS-RC2 Zellen zu reparieren und es konnte ein indirekter Hinweis auf geglückte Reparatur gefunden werden. Es könnte sein dass eine synthetisch letale Verbindung zwischen PBRM1 und Verlust eines zweiten Genes besteht. Deshalb wurden die Hypothesen aufgestellt, dass Verlust von Proteinen die Bromodomänen, die Mitglieder des SWI/SNF Komplexes oder des PRC Komplexes sind zu synthetischer Letalität führt. Getestet wurden diese Hypothesen durch einen shRNA Screen. Es konnte gezeigt werden dass sich, auch nach Durchführung des Experimentes, die shRNA Fragmente aus der genomischen DNA amplifizieren lassen und dass alle experimentellen Konditionen immer noch aus einem shRNA Mix bestehen.

7.2 Curriculum vitae

Contact Details

Name: David Hoffmann
Phone: +43650 5015035
E-mail: hoffmandavid@gmx.at

Education

Since 10/2013 MSc in Molecular Biology with focus on Cell Biology
University of Vienna, Austria

10/2010 – 08/2013 BSc in Biology with emphasis on Molecular Biology; graduated with honours
University of Vienna, Austria

09/2001 – 06/2009 BG/BRG Gmunden, Austria; “Matura” passed with honours

09/1997 – 06/2001 Primary school in Ohlsdorf, Austria

Research Experience

09/2014 – 08/2015 MSc Thesis in the laboratory of Sakari Vanharanta
“Dissecting the role of PBRM1 in ccRCC tumourigenesis and the search for synthetic lethal interactions”
MRC Cancer Unit, Cambridge, United Kingdom

02/2014 – 03/2014 Internship in the laboratory of Josef M. Penninger
“The role of Apelin in tumour angiogenesis”
Institute of Molecular Biotechnology (IMBA), Vienna, Austria

10/2013 Internship in the laboratory of Luisa Cochella “The importance of miRNAs in cell type specification in *C. elegans*”
Institute of Molecular Pathology (IMP), Vienna, Austria

10/2013 – 01/2013 Technical Assistant (Part-Time)
Arsanis Biosciences GmbH, Vienna, Austria

06/2013 – 07/2013 Internship in the department *mAb and Antigen Production & Analytics* guided by Adriana Badarau
Arsanis Biosciences GmbH, Vienna, Austria

02/2013 – 03/2013 BSc Thesis in the laboratory of Peter Fuchs “The role of epiplakin during Fas-induced apoptosis and the classical heat shock response in primary hepatocytes and epiplakin’s binding to keratins”
Max F. Perutz Laboratories (MFPL), Vienna, Austria

Awards

10/2013 – 09/2014 Performance scholarship awarded by the University of Vienna for exceptional curricular achievements

10/2012 – 09/2013 Performance scholarship awarded by the University of Vienna for exceptional curricular achievements

10/2011 – 09/2012 Performance scholarship awarded by the University of Vienna for exceptional curricular achievements

10/2010 – 09/2011 Performance scholarship awarded by the University of Vienna for exceptional curricular achievements

Publications

Structure-Function Analysis of Heterodimer Formation, Oligomerization and Receptor Binding of the Staphylococcus aureus Bi-component Toxin LukGH. Adriana Badarau, Harald Rouha, Stefan Malafa, Derek T. Logan, Maria Håkansson, Lukas Stulik, Ivana Dolezilkoval, Astrid Teubenbacher, Karin Gross, Barbara Maierhofer, Susanne Weber, Michaela Jägerhofer, **David Hoffmann** and Eszter Nagy. J. Biol. Chem. 2014 Nov 3.
